

**CATALYTIC UPGRADING OF PYROLYTIC OIL USING
CeO₂-ZrO₂ MIXED OXIDE CATALYSTS**

Somsak Thaicharoensutcharittham

A Dissertation Submitted in Partial Fulfilment of the Requirements
for the Degree of Doctor of Philosophy
The Petroleum and Petrochemical College, Chulalongkorn University
in Academic Partnership with
The University of Michigan, The University of Oklahoma,
and Case Western Reserve University

2011

บทคัดย่อและแฟ้มข้อมูลฉบับเต็มของวิทยานิพนธ์ตั้งแต่ปีการศึกษา 2554 ที่ให้บริการในคลังปัญญาจุฬาฯ (CUIR)
เป็นแฟ้มข้อมูลของนิสิตเจ้าของวิทยานิพนธ์ที่ส่งผ่านทางบัณฑิตวิทยาลัย

The abstract and full text of theses from the academic year 2011 in Chulalongkorn University Intellectual Repository (CUIR)
are the thesis authors' files submitted through the Graduate School.

Thesis Title: Catalytic Upgrading of Pyrolytic Oil Using CeO₂-ZrO₂ Mixed Oxide Catalysts
By: Somsak Thaicharoensutcharittham
Program: Petrochemical Technology
Thesis Advisors: Asst. Prof. Boonyarach Kitiyanan
Assoc. Prof. Thirasak Rirksomboon
Assoc. Prof. Vissanu Meeyoo
Assoc. Prof. Pramoch Rangsunvigit

Accepted by The Petroleum and Petrochemical College, Chulalongkorn University, in partial fulfilment of the requirements for the Degree of Doctor of Philosophy.

..... College Dean
(Asst. Prof. Pomthong Malakul)

Thesis Committee:

| | |
|---|--|
| (Prof. Somchai Osuwan) | (Asst. Prof. Boonyarach Kitiyanan) |
| (Assoc. Prof. Thirasak Rirksomboon) | (Assoc. Prof. Pramoch Rangsunvigit) |
| (Assoc. Prof. Vissanu Meeyoo) | (Assoc. Prof. Apanee Luengnaruemitchai) |
| (Asst. Prof. Suparin Chaiklangmuang) | |

ABSTRACT

4781002063: Petrochemical Technology Program
Somsak Thaicharoensutcharittham: Catalytic Upgrading of Pyrolytic Oil Using CeO₂-ZrO₂ Mixed Oxide Catalysts.
Thesis Advisors: Asst. Prof. Boonyarach Kitiyanan, Assoc. Prof. Pramoch Rangsunvigit, Assoc. Prof. Thirasak Rirksomboon, Assoc. Prof. Vissanu Meeyoo 113 pp.
Keywords: Methane/ Acetic acid/ Ethanol/ Acetone/ Hydrogen production/ Nickel/ Ceria-Zirconia/ Cobalt/ Potassium

Bio-oil produced from biomass is a mixture of oxygenated compounds including acids, alcohols, ketones, esters, ethers, aldehydes, phenols, and derivatives, as well as carbohydrates, and a large proportion (20–30 wt.%) of lignin-derived oligomers. One possible application of bio-oil being considered is converted to hydrogen by steam reforming. This thesis is to reports the development of catalyst for hydrogen production of steam reforming reaction over Ni supported on CeO₂-ZrO₂. Acetic acid, ethanol and acetone are used as a model of bio-oil. It was found that the Ni/Ce_{0.75}Zr_{0.25}O₂ exhibits an excellent activity for an acetic acid steam reforming comparing to Ni/MgO and Ni/Al₂O₃. This is due to good redox properties of Ce_{0.75}Zr_{0.25}O₂. Moreover, by adding potassium over Ni/Ce_{0.75}Zr_{0.25}O₂ catalyst is able to modify NiO phase from a rhombohedral to a cubic phase, resulting in the improvement of catalytic properties of the Ni/Ce_{0.75}Zr_{0.25}O₂ catalyst. The presence of K species, can also suppress carbon deposition. For the Co/Ce_{1-x}Zr_xO₂ catalysts exhibit excellent activity for steam reforming of acetone. The catalytic steam reforming of acetone occurs on both mixed oxides supports and metal phases.

บทคัดย่อ

สมศักดิ์ ไทยเจริญสุจริตทำ : การเพิ่มมูลค่าน้ำมันชีวภาพที่ได้จากกระบวนการไพโรไลซิสโดยใช้ตัวเร่งปฏิกิริยาซีเรีย-เซอร์โคเนีย (Catalytic Upgrading of Pyrolytic Oil Using CeO₂-ZrO₂ Mixed Oxide Catalysts) อ. ที่ปรึกษา : ผศ. ดร. บุญยรัชต์ กิตยานันท์ รศ.ดร. ชีรศักดิ์ ฤกษ์สมบูรณ์ รศ.ดร. ปราโมช รังสรรค์วิจิตร และ รศ.ดร. วิษณุ มีอยู่ 113 หน้า

น้ำมันชีวภาพที่ได้จากกระบวนการไพโรไลซิสประกอบด้วยสารประกอบที่มีออกซิเจนเป็นองค์ประกอบ ได้แก่ กรด แอลกอฮอล์ คีโตน เอสเทอร์ อีเทอร์ แอลดีไฮด์ ฟีนอล คาร์โบไฮเดรต และลิกนิน เป็นต้น ซึ่งสารประกอบเหล่านี้สามารถนำไปผลิตไฮโดรเจนได้โดยปฏิกิริยารีฟอร์มมิ่งด้วยน้ำ ในงานวิจัยนี้ได้ศึกษาและปรับปรุงตัวเร่งปฏิกิริยาที่สามารถให้กัมมันตภาพสูงเพื่อใช้ในการผลิตไฮโดรเจนโดยปฏิกิริยารีฟอร์มมิ่งด้วยน้ำบนตัวเร่งปฏิกิริยาโลหะนิกเกิลที่มีโลหะออกไซด์ผสมของซีเรีย-เซอร์โคเนียเป็นตัวรองรับ โดยใช้ กรดอะซิติก เอทานอล และอะซิโตนเป็นตัวอย่างของน้ำมันชีวภาพที่ศึกษา จากผลการศึกษาพบว่าตัวเร่งปฏิกิริยานิกเกิลบนตัวรองรับซีเรีย-เซอร์โคเนีย แสดงกัมมันตภาพสูงที่สุดสำหรับปฏิกิริยารีฟอร์มมิ่งกรดอะซิติกด้วยน้ำ เมื่อเทียบกับนิกเกิลบนตัวรองรับแมกนีเซียมและอลูมินา จึงอธิบายได้ว่ากัมมันตภาพของตัวเร่งปฏิกิริยาดังกล่าวสัมพันธ์กับคุณสมบัติทางรีดอกซ์ ยิ่งไปกว่านั้นจากการศึกษาตัวเร่งปฏิกิริยานิกเกิลบนตัวรองรับซีเรีย-เซอร์โคเนียที่มีโพแทสเซียมเป็นตัวปรับปรุงคุณสมบัติพบว่าสามารถเพิ่มกัมมันตภาพและเสถียรภาพ สำหรับปฏิกิริยารีฟอร์มมิ่งเอทานอลด้วยน้ำ เนื่องจากโพแทสเซียมสามารถแปลงวัฏภาคของนิกเกิลจากโรมาโบฮีดรอลไปเป็นคิวบิกซึ่งเป็นวัฏภาคที่เพิ่มกัมมันตภาพให้ตัวเร่งปฏิกิริยาและยังพบอีกว่าโพแทสเซียมสามารถลดการสะสมของคาร์บอนบนตัวเร่งปฏิกิริยาได้อีกด้วย สำหรับปฏิกิริยารีฟอร์มมิ่งอะซิโตนด้วยน้ำโดยใช้โลหะโคบอลต์บนตัวรองรับซีเรีย-เซอร์โคเนียพบว่า ปฏิกิริยาเกิดขึ้นทั้งบนโคบอลต์และบนซีเรีย-เซอร์โคเนีย

ACKNOWLEDGEMENTS

I have realized the experience gained at PPC and CEIC-UNSW as great opportunity and this dissertation might not become realistic without the assistance of the following individuals.

First of all, I deeply indebted to Assoc. Prof. Vissanu Meeyoo, Assoc. Prof. Thirasak Rirksomboon, Assoc. Prof. Pramoch Rangsunvigit, Asst. Prof. Boonyarach Kitiyanan, Prof. David Trimm and Dr. Kondo-Francois Aguey-Zinsou, my thesis supervisors, for their useful recommendations, creative comments and encouragement, in an entire period of degree preparation. I was in a happy time working with all of them. An appreciable gratitude is also conveyed to the thesis committee, Prof. Somchai Osuwan, Assoc. Prof. Apanee Luengnaruemitchai and Asst. Prof. Suparin Chaiklangmuang.

I would like to take this opportunity to thank other unmentioned faculty members and all staff of both PPC and UNSW, the owners of friendliness and valuable help.

This thesis work is funded by the Petroleum and Petrochemical College; and the National Center of Excellence for Petroleum, Petrochemicals, and Advanced Materials, Thailand. The supports are also from the Thailand Research Fund through the RGJ-PHD program (Grant 0061/45) and Waste-to-Energy project and Ratchadapiseksomphot Endowment of Chulalongkorn University. I also thank the School of Chemical Engineering and Industrial Chemistry of UNSW where part of this research was carried out.

A special thank is directed toward PPC friends, inside and outside the pyrolysis group, for their friendly assistance, cheerfulness, and encouragement. Also, I am greatly indebted to my lovely parents and family for their support, love and understanding.

TABLE OF CONTENTS

| | PAGE |
|---|---------------|
| Title Page | i |
| Abstract (in English) | iii |
| Abstract (in Thai) | iv |
| Acknowledgements | v |
| Table of Contents | vi |
| List of Tables | ix |
| List of Figures | xi |
| CHAPTER | |
| I INTRODUCTION | 1 |
| II LITERATURE REVIEW | 4 |
| III EXPERIMENTAL | 21 |
| IV HYDROGEN PRODUCTION BY STEAM REFORMING OF ACETIC ACID OVER Ni-BASED CATALYSTS | 28 |
| 4.1 Abstract | 28 |
| 4.2 Introduction | 28 |
| 4.3 Experimental | 29 |
| 4.4 Results and Discussion | 31 |
| 4.5 Conclusions | 34 |
| 4.6 Acknowledgements | 34 |
| 4.7 References | 35 |

| CHAPTER | | PAGE |
|----------------|--|-------------|
| V | STEAM REFORMING OF ETHANOL OVER Ni/Ce_{0.75}Zr_{0.25}O₂ AND Ni-K/Ce_{0.75}Zr_{0.25}O₂ CATALYSTS | 46 |
| | 5.1 Abstract | 46 |
| | 5.2 Introduction | 46 |
| | 5.3 Experimental | 47 |
| | 5.4 Results and Discussion | 50 |
| | 5.5 Conclusions | 61 |
| | 5.6 Acknowledgements | 61 |
| | 5.7 References | 61 |
| VI | CATALYTIC STEAM REFORMING OF ACETONE OVER Co/Ce_{1-x}Zr_xO₂ CATALYSTS | 65 |
| | 6.1 Abstract | 65 |
| | 6.2 Introduction | 65 |
| | 6.3 Experimental | 66 |
| | 6.4 Results and Discussion | 69 |
| | 6.5 Conclusions | 83 |
| | 6.6 Acknowledgements | 83 |
| | 6.7 References | 83 |
| VII | CATALYTIC COMBUSTION OF METHANE OVER NiO/Ce_{0.75}Zr_{0.25}O₂ CATALYST | 87 |
| | 7.1 Abstract | 87 |
| | 7.2 Introduction | 87 |
| | 7.3 Experimental | 88 |
| | 7.4 Results and Discussion | 89 |
| | 7.5 Conclusions | 92 |

| CHAPTER | PAGE |
|---|-------------|
| 7.6 Acknowledgements | 92 |
| 7.7 References | 92 |
| VIII CONCLUSIONS AND RECOMMENDATIONS | 102 |
| REFERENCES | 104 |
| CURRICULUM VITAE | 112 |

LIST OF TABLES

| TABLE | | PAGE |
|-------------------|---|-------------|
| CHAPTER II | | |
| 2.1 | Typical properties and characteristics of Wood Derived Crude Pyrolysis Oil. | 5 |
| 2.2 | An overview compound classes and some representative in pyrolytic liquid. | 6 |
| 2.3 | Chemicals from biomass bio-oil by fast pyrolysis. | 7 |
| CHAPTER IV | | |
| 4.1 | BET surface area, degree of metal dispersion and mean size diameter of the catalysts. | 38 |
| 4.2 | Acetic acid steam reforming on 0.1 g of 5%Ni/Ce _{0.75} Zr _{0.25} O ₂ , 15%Ni/Ce _{0.75} Zr _{0.25} O ₂ and 25%Ni/Ce _{0.75} Zr _{0.25} O ₂ catalysts at T= 650 °C and WHSV (HAc) = 22 h ⁻¹ . | 39 |
| CHAPTER V | | |
| 5.1 | Textural properties of Ni/Ce _{0.75} Zr _{0.25} O ₂ and Ni-K/Ce _{0.75} Zr _{0.25} O ₂ catalysts. | 51 |
| 5.2 | C-C breakage conversion (%), products distribution (%), temperature and time on stream for the steam reforming of ethanol over the Ni/Ce _{0.75} Zr _{0.25} O ₂ and Ni-K/Ce _{0.75} Zr _{0.25} O ₂ , steam-to-carbon ratio = 6, GHSV = 20 000 h ⁻¹ . | 55 |
| CHAPTER VI | | |
| 6.1 | BET surface areas and metal dispersion of the catalysts. | 70 |

| TABLE | | PAGE |
|--------------|--|-------------|
| 6.2 | Conversion (%) and products yields (%) for the steam reforming of acetone over $\text{Ce}_{1-x}\text{Zr}_x\text{O}_2$ ($x = 0, 0.25, 0.5, 0.75$ and 1), steam-to-carbon ratio = 6, LHSV of 15.3 h^{-1} , time on stream = 2 h, temperature range of 550-700 °C. | 75 |

CHAPTER VII

| | | |
|-----|---|----|
| 7.1 | Kinetic models tested in fitting the methane combustion for $\text{NiO}/\text{Ce}_{0.75}\text{Zr}_{0.25}\text{O}_2$ catalyst. | 95 |
| 7.2 | Summary of kinetic parameters over $\text{NiO}/\text{Ce}_{0.75}\text{Zr}_{0.25}\text{O}_2$ catalyst. | 96 |

LIST OF FIGURES

| FIGURE | PAGE |
|--------------------|--|
| CHAPTER II | |
| 2.1 | Processes and products from pyrolysis of biomass. 10 |
| CHAPTER III | |
| 3.1 | Schematic diagram of the experimental setup for model oxygenate hydrocarbon steam reforming. 26 |
| 3.2 | Schematic diagram of the experimental setup for methane oxidation. 27 |
| CHAPTER IV | |
| 4.1 | XRD patterns for the catalysts investigated (a) 5%Ni/Ce _{0.75} Zr _{0.25} O ₂ , (b) 15%Ni/Ce _{0.75} Zr _{0.25} O ₂ , (c) 25%Ni/Ce _{0.75} Zr _{0.25} O ₂ , (d) 15%Ni/MgO, and (e) 15%Ni/ α -Al ₂ O ₃ . 40 |
| 4.2 | H ₂ -TPR profiles for the catalysts with a heating rate of 10 °C/min, a reducing gas containing 5% H ₂ in N ₂ with a flow rate of 30 ml/min: (a) 15%Ni/MgO, (b) 5%Ni/Ce _{0.75} Zr _{0.25} O ₂ , (c) 15%Ni/Ce _{0.75} Zr _{0.25} O ₂ , (d) 25%Ni/Ce _{0.75} Zr _{0.25} O ₂ , and (e) 15%Ni/ α -Al ₂ O ₃ . 41 |
| 4.3 | Effect of S/C ratio on the C-C breakage conversion, the yields of carbon containing products and hydrogen yield over: 15%Ni/Ce _{0.75} Zr _{0.25} O ₂ , 15%Ni/MgO and 15%Ni/ α -Al ₂ O ₃ at 650°C and s/c ratio: (a) 1, (b) 3 and (c) 6. 42 |

| FIGURE | PAGE |
|---|-------------|
| 4.4 Catalytic activity for acetic acid steam reforming over 15%Ni/Ce _{0.75} Zr _{0.25} O ₂ , 15%Ni/ α -Al ₂ O ₃ , and 15%Ni/MgO catalysts: T = 650°C and S/C ratio = 1. | 43 |
| 4.5 Total amount of carbon deposited on catalysts via acetic acid steam reforming over 15%Ni/Ce _{0.75} Zr _{0.25} O ₂ , 15%Ni/MgO and 15%Ni/ α -Al ₂ O ₃ catalysts; after 320 min on stream, at 650°C, S/C ratios of 1 – 6. | 44 |
| 4.6 TEM images of the spent catalysts: (a) 15%Ni/ α -Al ₂ O ₃ , (b) 15%Ni/Ce _{0.75} Zr _{0.25} O ₂ , (c) 15%Ni/MgO. | 45 |
| CHAPTER V | |
| 5.1 SEM images of Ni/Ce _{0.75} Zr _{0.25} O ₂ (a) and Ni-K/Ce _{0.75} Zr _{0.25} O ₂ (b) catalysts. | 51 |
| 5.2 XRD patterns of Ni/Ce _{0.75} Zr _{0.25} O ₂ and Ni-K/Ce _{0.75} Zr _{0.25} O ₂ catalysts. | 52 |
| 5.3 TPR profiles of the Ni/Ce _{0.75} Zr _{0.25} O ₂ and Ni-K/Ce _{0.75} Zr _{0.25} O ₂ catalysts. The reducing gas contains 5% H ₂ in N ₂ with a flow rate of 30 ml/min and a heating rate of 10°C/min. | 53 |
| 5.4 C-C breakage conversion (%) and products distribution (%) vs. GHSV for the steam reforming of ethanol over (a) Ni/Ce _{0.75} Zr _{0.25} O ₂ and (b) Ni-K/Ce _{0.75} Zr _{0.25} O ₂ catalysts; steam-to-carbon ratio = 6, temperature = 600°C. | 56 |
| 5.5 C-C breakage conversion (%) and products distribution (%) vs. steam-to-carbon ratio (S/C) for the steam reforming of ethanol over (a) Ni/Ce _{0.75} Zr _{0.25} O ₂ and (b) Ni-K/Ce _{0.75} Zr _{0.25} O ₂ ; GHSV = 20 000, temperature = 600°C. | 58 |

| FIGURE | PAGE |
|--|-------------|
| 5.6 Carbon deposited (%) vs. temperature for the steam reforming of ethanol over the Ni/Ce _{0.75} Zr _{0.25} O ₂ and Ni/Ce _{0.75} Zr _{0.25} O ₂ steam-to-carbon ratio = 3, GHSV = 20000 h ⁻¹ . | 59 |
| 5.7 TEM images of (a) Ni/Ce _{0.75} Zr _{0.25} O ₂ and (b) Ni-K/Ce _{0.75} Zr _{0.25} O ₂ catalysts after steam reforming of ethanol steam-to-carbon ratio = 3, GHSV = 20000 h ⁻¹ for 6 h. | 60 |

CHAPTER VI

| | |
|---|----|
| 6.1 SEM images of (a) Co/CeO ₂ and (b) Co/ZrO ₂ catalysts. | 71 |
| 6.2 XRD patterns of Co/Ce _{1-x} Zr _x O ₂ catalysts (x = 0, 0.25, 0.5, 0.75 and 1). | 72 |
| 6.3 TPR profiles of the Co/Ce _{1-x} Zr _x O ₂ catalysts (x = 0, 0.25, 0.5, 0.75 and 1) and cobalt oxide. The reducing gas contains 5% H ₂ in N ₂ with a flow rate of 30 ml/min and a heating rate of 10 °C/min. | 73 |
| 6.4 Conversion (%) for the steam reforming of acetone over Ce _{1-x} Zr _x O ₂ (x = 0, 0.25, 0.5, 0.75 and 1), steam-to-carbon ratio = 6, LHSV of 15.3 h ⁻¹ , time on stream = 2 h, temperature range of 550-700 °C. | 76 |
| 6.5 Diagram for the possible reaction of acetone over Ce _{1-x} Zr _x O ₂ mixed oxide. | 76 |
| 6.6 Conversion (%) and products yields (%) for the steam reforming of acetone over Co/Ce _{1-x} Zr _x O ₂ (x = 0, 0.25, 0.5, 0.75 and 1) and Ni/Ce _{0.75} Zr _{0.25} O ₂ catalysts, steam-to-carbon ratio = 6, LHSV of 15.3 h ⁻¹ , time on stream = 2 h, temperature range of 550-700 °C. | 78 |

| FIGURE | PAGE |
|--|-------------|
| 6.7 Conversion (%) vs. time on stream for the steam reforming of acetone over Co/Ce _{1-x} Zr _x O ₂ (x = 0, 0.25, 0.5, 0.75 and 1) and Ni/Ce _{0.75} Zr _{0.25} O ₂ catalysts, steam-to-carbon ratio = 6, LHSV of 15.3 h ⁻¹ at temperature 600°C (a), 700°C (b). | 80 |
| 6.8 Carbon deposition for the steam reforming of acetone over Co/Ce _{1-x} Zr _x O ₂ (x = 0, 0.25, 0.5, 0.75 and 1) and Ni/Ce _{0.75} Zr _{0.25} O ₂ catalysts, steam-to-carbon ratio = 6, LHSV of 15.3 h ⁻¹ at temperature 600 °C and 700°C time on stream 6 h. | 81 |
| 6.9 SEM images of (a) Co/CeO ₂ , (b) Co/Ce _{0.75} Zr _{0.25} O ₂ , (c) Co/Ce _{0.50} Zr _{0.50} O ₂ , (d) Co/Ce _{0.25} Zr _{0.75} O ₂ , (e) Co/ZrO ₂ after 3 h of steam reforming of acetone reaction at 700°C. | 82 |

CHAPTER VII

| | |
|--|-----|
| 7.1 TPR profiles of Ce _{0.75} Zr _{0.25} O ₂ and NiO/Ce _{0.75} Zr _{0.25} O ₂ catalysts. The reducing gas contains 5.32% H ₂ in N ₂ with a flow rate of 30 ml/min and a heating rate of 10 °C/min. | 97 |
| 7.2 Light-off curves for Ce _{0.75} Zr _{0.25} O ₂ and NiO/Ce _{0.75} Zr _{0.25} O ₂ catalysts. The gas mixture contains 3.0%CH ₄ , 10.0%O ₂ in balanced He with a total flow rate of 100 ml/min. | 98 |
| 7.3 Experimental reaction rate (r_{CH_4}) vs. methane partial pressure (P_{CH_4}) with different oxygen partial pressures (P_{O_2}) for NiO/Ce _{0.75} Zr _{0.25} O ₂ catalyst at 450°C. | 99 |
| 7.4 The comparison between experimental reaction rates and calculated reaction rates based on the two-term model for methane combustion over NiO/Ce _{0.75} Zr _{0.25} O ₂ catalyst. | 100 |

| FIGURE | | PAGE |
|---------------|--|-------------|
| 7.5 | Arrhenius plots for the methane combustion over NiO/Ce _{0.75} Zr _{0.25} O ₂ catalyst. | 101 |

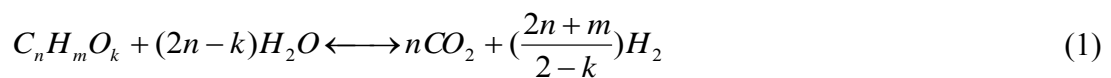
CHAPTER I

INTRODUCTION

1.1 Significance of Research

Biomass has been recognized as a major renewable energy source due to three main reasons. First, it is renewable and sustainable. Second, it appears to have positive effect to environment since there is no net release of carbon dioxide (CO₂) and very low sulfur content. Third, it appears to have significant economic potential comparing to increasing cost of fossil fuel (Ozcimen *et al.*, 2004; Jefferson *et al.*, 2006; Cadenas *et al.*, 1998).

Pyrolysis is one of the alternatives to be considered for conversion of biomass to fuels and other chemicals. Pyrolysis processes of biomass at moderate temperatures (380-600°C) yield gas, liquid, and solid fractions. The liquid or pyrolytic oil is a mixture of organic chemicals with water. The process conditions can be optimized to maximize the production of this product depending on a specific application (Inguanzo *et al.*, 2002). Pyrolytic oil, frequently called bio-oil, is a complex mixture, whose major components are oxygenated compounds such as alcohols, acids, aldehydes and ketones, as well as more complex carbohydrates and lignin derived materials (Zhang *et al.*, 2005). This bio-oil can be reformed as a whole or separated by water extraction in two fractions: an organic fraction with lignin derived materials that can be used for the production of more valuable products (Garcia *et al.*, 2000; Jindarom *et al.*, 2007), and a water soluble fraction that can be catalytically steam reformed. The steam reforming of bio-oil presents significant difficulties, especially in terms of carbonaceous deposits (i.e., coke formation). Complete steam reforming is described by the following reaction:



Note that the yield is also influenced by the water gas shift reaction (Eq. (2)) depending on the conditions of the reaction:



Due to the high temperature of this reaction, it is likely that partial thermal decomposition (Eq. (3)) and Boudard reaction (Eq. (4)) can occur simultaneously:



Carbon formation is one of the major problems in the reforming reaction. Fundamentals of carbon formation as well as strategies for its minimization have been thoroughly discussed in the literature (Trimm, 1997 and Jens, 1997). The most significant factor is the ratio of carbon in the feedstock to steam. It is also known that carbon formation increases with unsaturation, molecular weight, and aromaticity of the feed. Two strategies can be employed to decrease carbon deposits on the catalyst. The first one is based on enhancing steam adsorption on the catalyst with the objective of gasifying any carbon or carbon precursors formed on the catalyst surface. The second strategy aims at modifying the surface reaction is due to the effect of altering the crystallite size when several metals are present in the catalyst formulation or to the formation of alloys that interfere with the process of carbon dissolution in the metal.

Many catalysts containing mainly Ni, Cu, Co and noble metals, such as Rh, Ru, Re, Pd and Pt were employed in investigations of steam reforming reaction (Breen *et al.*, 2002; Liguras *et al.*, 2003; Salge *et al.*, 2005). Among those, Ni- and Co-based catalyst shows an excellent catalytic activity in hydrocarbon steam reforming performance due to its low cost and their high activity for C-C bond cleavage (Llorca *et al.*, 2002; 2003). Various metal oxides have been used to support in order to provide large surface area as well as good thermal stability, leading to high cobalt dispersion even at high temperatures (Llorca *et al.*, 2002). Recently, Ce-ZrO₂ widely use in support its highly oxygen storage capacity and redox property which show good resistance to coke formation (Pengpanich *et al.*, 2004).

From the above reason, the search for more active and cost-effective catalysts based on metal oxides for steam reforming reaction and resistance towards carbon formation remains essential. Therefore, the present proposed research study aims at a better understanding of the activities of Ni and Co supported on $\text{Ce}_{1-x}\text{Zr}_x\text{O}_2$ mixed oxide catalysts toward the steam reforming reaction.

1.2 Objective and Outline of Thesis

The main objective of this thesis is to reports the development of catalyst for hydrogen production from acetic acid, ethanol and acetone (model oxygenate hydrocarbon for water soluble fraction of bio-oil). The catalysts used in this dissertation are based on Ni and Co supported on $\text{CeO}_2\text{-ZrO}_2$. The following chapter gives a very brief background of processes for hydrogen production and a review of related literature.

The general overview of bio-oil (pyrolysis liquid product, application of liquid products and the catalysts used for upgrade liquid product are provided in Chapter 2. Chapter 3 describes the various experimental techniques utilized in the catalyst preparation, characterization, and reaction studies. Details of the catalytic activity test system are also given. The steam reforming of acetic acid over $\text{Ni/Ce}_{0.75}\text{Zr}_{0.25}\text{O}_2$ catalyst is described in Chapter 4. This chapter includes the activity, selectivity and stability of $\text{Ni/Ce}_{0.75}\text{Zr}_{0.25}\text{O}_2$ catalyst compared with $\text{Ni/Al}_2\text{O}_3$ and Ni/MgO catalysts for this reaction. The role of reducible support on decrease of coke formation is discussed. In an attempt to lower carbon deposition, the effect of addition of K into Ni supported $\text{Ce}_{0.75}\text{Zr}_{0.25}\text{O}_2$ catalyst on ethanol steam reforming was investigated and described in Chapter 5. The alternative Co catalyst investigated on the steam reforming of acetone are examined in Chapter 6 and compared to the results on $\text{Ni/Ce}_{0.75}\text{Zr}_{0.25}\text{O}_2$ catalyst. Furthermore, methane oxidation over $\text{Ni/CeO}_2\text{-ZrO}_2$ catalyst and reaction kinetic expressions is also purposed in Chapter 7. Finally, in Chapter 8, the overall conclusions of this thesis are discussed along with some recommendations for future research.

CHAPTER II

LITERATURE REVIEW

2.1 Pyrolysis

Pyrolysis is the process in which the organic materials are heated up in the absence of oxygen, resulting in breaking of organic molecules, to useful gases, liquids (bio-oil) and solid residues. Relatively low temperature, 300-600°C, are generally employed in pyrolysis process, comparing to 800-1000°C or even higher in gasification and combustion. The pyrolysis process has more advantages over the combustion process due to the economic, the energy utilization and low to none releasing of heavy metal to natural resource. The distribution and characteristics of the pyrolysis products strongly depend on the pyrolysis reactor, the characteristics of raw material and reaction parameters. The liquid, as a major product, contains several different chemicals in varying proportions. It can potentially be either directly used as fuel or extracted for some chemicals. The solid residue is typically composed of mostly stabilized carbon and inorganic compounds, which can be further utilized as a solid fuel or as an adsorbent or even safely goes directly to the disposal.

2.2 Liquid Product Characteristic

Generally, as produced pyrolysis liquid has a higher heating value of about 17 MJ/kg and contains about 25% wt. of water that cannot be separated (Bridgwater *et al.*, 2000). The liquid is often referred to as “oil” or “bio-oil” or “bio-crude” although it will not mix with any hydrocarbon liquids. It is composed of a complex mixture of oxygenated compounds and this mixture provides both the potential and challenge for utilization. There are some important features of this liquid that should be emphasized and the main properties are shown in Table 2.1.

The overview of compound classes and prominent representatives that found in bio-oil is show in Table 2.2. Chemicals from biomass bio-oil by fast pyrolysis are given in Table 2.3. The presence of the several compound classes has

different effects on the bio-oil properties. Bio-oil with a dominating content of oxygenates is highly reactive. These will alter the some properties of the bio-oil such as its bad odour, high viscosity and its instability can be a disadvantage for marketing the oil. Nonetheless, it is possible to improve the characteristics of this oil. Like many other bio-fuel derived oils, it has high oxygen content that induces instability within the oil through polymerization reactions, which then increases the viscosity of the oil.

Esterification of the pyrolysis oil with ethanol and sulfuric acid (as a catalyst) was found to improve the odour characteristics significantly. Moreover, this method not only improves the stability of the oil making it more suitable to be stored for long-term use, but also contributes to an increase in the heating value of the oil by up to 9% (Doshi *et al.*, 2005).

Beside the esterification of bio-oil, the method to upgrade the crude bio-oil for using as a fuel replacing the fossil fuel will discuss in detail in section 2.4.

Table 2.1 Typical properties and characteristics of Wood Derived Crude Pyrolysis Oil (Bridgwater *et al.*, 2000)

| <u>Physical property</u> | <u>Typical value</u> |
|---------------------------------------|-----------------------------|
| Moisture content | 15-30% |
| pH | 2.5 |
| Specific gravity | 1.2 |
| Elemental analysis | |
| C | 56.4% |
| H | 6.2% |
| O | 37.3% |
| N | 0.1% |
| Ash | 0.1% |
| HHV as produced (depends on moisture) | 16-19 MJ/kg |
| Viscosity (at 40°C and 25% water) | 40-100 cp |
| Solids (char) | 1% |
| Vacuum distillation | Max. 50% as liquid degrades |

Characteristics

- Liquid fuel,
- Easy substitution for conventional fuels in many static applications – boilers, engines, turbines,
- Heating value of 17 MJ/kg at 25%wt. water, is about 40% that of fuel oil/diesel,
- Does not mix with hydrocarbon fuels,
- Not as stable as fossil fuels,
- Quality needs definition for each application,
- Standards required,

Table 2.2 An overview compound classes and some representative in pyrolytic liquid (Morf, 2001)

| Compound class | Representatives | Formula |
|------------------|------------------------------|-------------------|
| Acids | Acetic acid | $C_2H_4O_2$ |
| | Propionic acid | $C_2H_6O_2$ |
| | Butanoic acid | $C_4H_8O_2$ |
| Sugars | Levoglucosan | $C_6H_{10}O_5$ |
| | Fructose | $C_6H_{12}O_5$ |
| | Cellobiosan | $C_{12}H_{20}O_6$ |
| Ketones | Acetol | $C_3H_6O_2$ |
| | Cyclopentanone | C_5H_8O |
| | 2-Methyl-2-cyclopenten-1-one | C_6H_8O |
| Phenols, Cresols | Phenol | C_6H_6O |
| | <i>o, m, p</i> -Cresol | C_7H_8O |
| | <i>x, y</i> -Dimethylphenol | $C_8H_{10}O$ |
| | 2-Ethylphenol | $C_8H_{10}O$ |
| Guaiacols | Guaiacol | $C_7H_8O_2$ |
| | 4-Methylguaiacol | $C_8H_{10}O_2$ |
| | 4-Ethylguaiacol | $C_9H_{12}O_2$ |
| Furans | Furan | C_4H_4O |

| Compound class | Representatives | Formula |
|------------------------------------|------------------------|--|
| BTX | Furfural | C ₅ H ₄ O |
| | 5-Methylfurfural | C ₆ H ₆ O ₂ |
| | Benzene | C ₆ H ₆ |
| | Toluene | C ₇ H ₈ |
| | <i>o, m, p</i> -Xylene | C ₈ H ₁₀ |
| Polyaromatic Hydrocarbons (PAH) | Naphthalene | C ₁₀ H ₈ |
| | Anthracene | C ₁₄ H ₁₀ |
| | Benzo [a] pyrene | C ₂₀ H ₁₂ |
| | Coronene | C ₂₄ H ₁₂ |

Table 2.3 Chemicals from biomass bio-oil by fast pyrolysis (Balat M, 2009)

| Chemical | Minimum, wt% | Maximum, wt% |
|------------------------------|--------------|--------------|
| Levoglucosan | 2.9 | 30.5 |
| Hydroxyacetaldehyde | 2.5 | 17.5 |
| Acetic acid | 6.5 | 17.0 |
| Formic acid | 1.0 | 9.0 |
| Acetaldehyde | 0.5 | 8.5 |
| Furfuryl alcohol | 0.7 | 5.5 |
| 1-hydroxy-2-propanone | 1.5 | 5.3 |
| Catechol | 0.5 | 5.0 |
| Methanol | 1.2 | 4.5 |
| Methyl glyoxal | 0.6 | 4.0 |
| Ethanol | 0.5 | 3.5 |
| Cellobiosan | 0.4 | 3.3 |
| 1,6-anhydroglucofuranose | 0.7 | 3.2 |
| Furfural | 1.5 | 3.0 |
| Fructose | 0.7 | 2.9 |
| Glyoxal | 0.6 | 2.8 |
| Formaldehyde | 0.4 | 2.4 |
| 4-methyl-2,6-dimethoxyphenol | 0.5 | 2.3 |

| Chemical | Minimum, wt% | Maximum, wt% |
|---------------------------|--------------|--------------|
| Phenol | 0.2 | 2.1 |
| Propionic acid | 0.3 | 2.0 |
| Acetone | 0.4 | 2.0 |
| Methylcyclopentene-ol-one | 0.3 | 1.9 |
| Methyl formate | 0.2 | 1.9 |
| Hydroquinone | 0.3 | 1.9 |
| Acetol | 0.2 | 1.7 |
| 2-cyclopenten-1-one | 0.3 | 1.5 |
| Syringaldehyde | 0.1 | 1.5 |
| 1-hydroxy-2-butanone | 0.3 | 1.3 |
| 3-ethylphenol | 0.2 | 1.3 |
| Guaiacol | 0.2 | 1.1 |

2.3 Application of Liquid Products

2.3.1 Combustion

Although the heating value of bio-oil is much lower than fossil fuel oil and it contains a significant proportion of water, it has been successfully used as a fuel by many organizations both in test campaigns and commercially. Tests have been successfully carried out at Canmet in Canada (Shaddix, 1997), at MIT, and by Neste in Finland (Gust, 1997), and the bio-oil is routinely used as a boiler fuel by Red Arrow in the USA. Problems reported are the high viscosity which is adjusted by addition of alcohol (Gust, 1997) and by in-line preheating (Shaddix, 1997). In both cases, the boiler or furnace requires preheating with conventional fuels before switching over to bio-oil and a more complex start-up sequence is therefore required as bio-oil is not miscible with fuel oil or diesel. Once burning, emissions are quite acceptable.

2.3.2 Engines

Due to the higher added value of electricity compared to heat and its ease of distribution and marketing, electricity production has attracted considerable attention as an application, which has been encouraged by the various incentives on offer in different countries as described earlier. The results of extended engine tests are reported during which crude bio-oil without any pretreatment has been successfully burnt in a modified 250 kWe dual fuel diesel engine by Ormrod (Leech *et al.*, 1997). Long term operational experience is required to establish optimum conditions and obtain sufficient data for warranties.

2.3.3 Gas Turbines

The successful use of filtered bio-oil in a silo combustor fitted 2.5 MWe gas turbine, and effect of bio-oil combustion in gas turbines in a static test rig (Patnaik *et al.*, 1997). Long term operational experience is required to establish optimum conditions and obtain sufficient data for warranties.

2.3.4 Transport Fuels and Synthetic Fossil Fuels

Two routes to transport fuels are possible - hydrotreating/hydrocracking to a naphtha-like product with upgrading to diesel (Kaiser, 1997); or zeolite cracking to aromatics (Solantausta *et al.*, 1994). None of these routes is proven technically with most concern being over catalyst stability and life. In addition the high pressure and high hydrogen requirement of hydrotreating routes makes this route too expensive. The zeolite route does not have these disadvantages, but still results in unacceptably high product costs.

2.3.5 Chemicals

The production of chemicals is potentially much more attractive due to their high value. A comprehensive review of current work and opportunities was reported (Radlein *et al.*, 1997). The only currently commercial application is for food flavourings such as liquid smoke but other possibilities include speciality chemicals for pharmaceuticals and synthesis, fertilizers, environmental chemicals and resins. The current constraints inhibiting development is lack of defined markets and

inadequately developed production methods. The co-production of chemicals and fuels undoubtedly offers the most interesting opportunities.

The possibilities for the utilization of crude and modified bio-oil are shown in Figure 2.1.

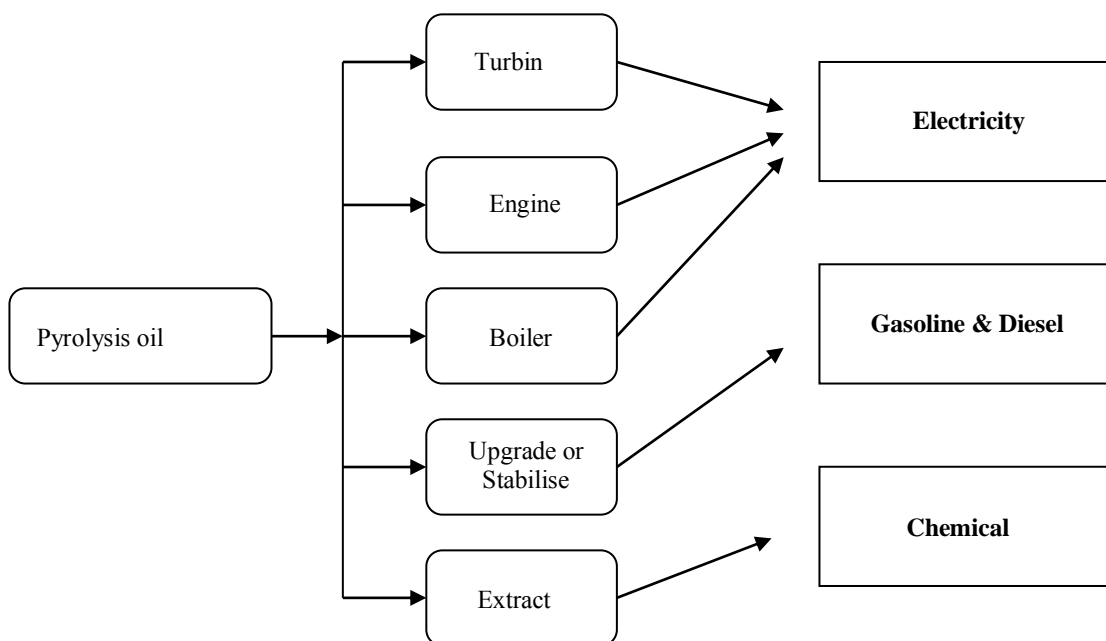


Figure 2.1 Processes and products from pyrolysis of biomass.

2.4 Upgrading of Pyrolytic Liquid

The deleterious properties of high viscosity, thermal instability and corrosiveness present many obstacles to the substitution of fossil derived fuels by bio-oil. Therefore reducing the oxygen content is required for upgrading the bio oil. The recent upgrading techniques are described as follows.

2.4.1 Hydrodeoxygenation

Hydro-process is performed in hydrogen providing solvents activated by the catalysts of Co-Mo, Ni-Mo and their oxides or loaded on Al_2O_3 under pressurized conditions of hydrogen and/or CO. Oxygen is removed as H_2O and CO_2 , and then the energy density is elevated. The volatile from pyrolysis of eucalyptus in a two stage reactor was upgraded by hydrodeoxygenation. Hydro-cracking without catalysts was operated in the first stage, and catalytic hydrotreatment was operative

in the second stage with lower temperature and the same pressure compared with that in the first stage. The analysis indicated that the deactivation of the catalyst did not result from carbon deposition. Instead, the embodiments of volatile components blocked the activated sites in the zeolite catalyst. This hydro-process produced much water and complicated the bio-oil with many impurities. (Pindoria *et al.*, 1997, Pindoria *et al.*, 1998)

Zang *et al.* (2005) separated the bio-oil with a yield of 70% into water and oil phases, and the oil phase was hydrotreated and catalyzed by sulphided Co-Mo-Pt/Al₂O₃. The reaction was operated in an autoclave filled with tetralin (as a hydrogen donor solvent) under the optimum conditions of 360°C and 2 MPa of cold hydrogen pressure. The oxygen content was reduced from 41.8% of the crude oil to 3% of upgraded one, and besides, the crude oil was methanol soluble while the upgraded one was oil soluble.

Elloit and Neuenschwander (1996) examined the hydrocatalytic reactions of bio-oil in a continuous feed fixed bed reactor. Higher conversion was obtained in the down flow configuration compared to the up flow one. The conversion was doubled on NiMo/ γ -Al₂O₃ compared to the CoMo/spinel at elevated temperature.

Weiyang *et al.* (2010) examined the hydrodeoxygenation of phenol, benzaldehyde and acetophenone were used as model compounds of bio-oil. Co-Mo-B amorphous catalysts exhibited high catalytic activity in phenol, benzaldehyde and acetophenone. The catalyst activity was increased with the Co/Mo ratio increase of surface composition. Both the conversion and the total deoxygenation rate could be high to 100%. The high catalytic activity of the Co-Mo-B amorphous catalyst depended on the sufficient supply of free hydrogen and the high content of Mo⁴⁺ Brønsted acid on the catalyst surface.

Zhao *et al.* (2011) studied hydrodeoxygenation of guaiacol as model compound for pyrolysis oil on transition metal phosphide hydroprocessing catalysts. The activity for HDO of guaiacol follows the order: Ni₂P>Co₂P>Fe₂P, WP, MoP. The major products for HDO of guaiacol are phenol, benzene, methoxybenzene, with no catechol formed at higher contact time.

Apparently the hydro-treating process needs complicated equipments, superior techniques and excess cost and usually is halted by catalyst deactivation and reactor clogging.

2.4.2 Emulsification

The simplest way to use bio-oil as a transport fuel seems to be to combine it with Diesel directly. Although the bio-oil are immiscible with hydrocarbons, they can be emulsified by the aid of a surfactant, Chiaramonti *et al.* (2003) prepared emulsified bio-oil by the ratios of 25, 50 and 75 wt% and found the emulsions were more stable than the original ones. The higher the bio-oil content, the higher the viscosity of the emulsion. The optimal range of emulsifier to provide acceptable viscosity was between 0.5% and 2.0%. In particular, the effect of the long term use of emulsions on the stainless steel engine and its subassemblies should be estimated.

Emulsification does not demand redundant chemical transformations, but the high cost and energy consumption input cannot be neglected. The accompanying corrosiveness to the engine and the subassemblies is inevitably serious.

2.4.3 Catalytic Cracking of Pyrolysis Liquid

Oxygen containing bio-oil are catalytically decomposed to hydrocarbons with the removal of oxygen as H₂O, CO₂ or CO. Nokkosmaki *et al.* (2000) proved ZnO to be a mild catalyst on the composition and stability of bio-oils in the conversion of pyrolysis vapors, and the liquid yields were not found to be substantially reduced. Although it had no effect on the water insoluble fraction (lignin derived), it decomposed the diethyl insoluble fraction (water soluble anhydrosugars and polysaccharides). After heating at 80°C for 24 h, the increase in viscosity was significantly lowered for the ZnO-treated oil (55% increase in viscosity) compared to the reference oil without any catalyst (129% increase in viscosity). Despite the indicated deactivation of the catalyst, the improvement in the stability of the ZnO treated oil was clearly observed.

Adijaye and Bakhshi (1995) studied the catalytic performance of the different catalysts for upgrading of bio-oil. Among the five catalysts studied, HZSM-5 was the most effective catalyst for producing the organic distillate fraction, overall hydrocarbons and aromatic hydrocarbons and the least coke formation. Reaction pathways were postulated that bio-oil conversion proceeded as a result of thermal effects followed by thermocatalytic effects. The thermal effects produced separation of the bio-oil in light organics and heavy organics and polymerization of the bio-oil to char. The thermocatalytic effects produced coke, tar, gas, water and the desired organic distillate fraction.

Guo *et al.* (2003) reviewed various catalysts used in bio-oil upgrading in detail and believed that although catalytic cracking is a predominant technique, the catalyst with good performance of high conversion and little coking tendency is demanding much effort.

Hew *et al.* (2010) find the optimum operating condition to upgrade the EFB (Empty Fruit Bunches) derived pyrolysis oil (bio-oil) to liquid fuel, mainly gasoline using Taguchi Method. They found that the zeolite ZSM-5 catalyst is a potential catalyst for conversion of bio-oil to gasoline through the catalytic cracking process. The optimum operating condition for the catalytic cracking process is at 400°C, reaction time of 15 min and utilizing catalyst weight of 30 g that results in the highest yield of gasoline fraction obtained, which is 91.67%.

Although catalytic cracking is regarded as a cheaper route by converting oxygenated feedstocks to lighter fractions, the results seem not promising due to high coking (8-25 wt%) and poor quality of the fuels obtained.

2.4.4 Extraction

Hundreds of the components of bio-oil are determined, and reclaiming one or more kinds of small and valuable chemicals arouses great interests among scholars and businessmen. There are many substances that can be extracted from bio-oil, such as phenols used in the resins industry, volatile organic acids in formation of de-icers, levoglucosan, hydroxyacetaldehyde and some additives applied in the pharmaceutical, fiber synthesizing or fertilizing industry and flavoring agent in food products (Bridgwater and Peacocke, 2000). Commercialization of special chemicals

from bio-oils requires more devotion to developing reliable low cost separation and refining techniques.

2.4.5 Steam-reforming Process

In the steam-reforming reaction, steam reacts with hydrocarbons in the feed to predominantly produce CO and H₂, commonly called synthesis gas. Steam reforming can be applied various solid waste materials including, municipal organic waste, waste oil, sewage sludge, paper mill sludge, black liquor, refuse-derived fuel, and agricultural waste. Steam reforming of natural gas, sometimes referred to as steam CH₄ reforming is the most common method of producing commercial bulk H₂. Steam reforming of natural gas is currently the least expensive method of producing H₂, and used for about half of the world's production of H₂.

Garcia *et al.*, (2000) obtained catalytic steam reforming of bio-oil derived from pyrolysis of biomass is a technically viable process for hydrogen production. Magnesium and lanthanum were used as support modifiers to enhance steam adsorption while cobalt and chromium additives were applied to reduce coke formation reactions. The cobalt-promoted nickel and chromium-promoted nickel supported on MgO-La₂O₃- α -Al₂O₃ catalysts showed the best results in the laboratory tests. At the reaction conditions progressive catalyst deactivation was observed leading to a decrease in the yields of hydrogen and carbon dioxide and an increase in carbon monoxide. The loss of activity also resulted in the formation of higher amounts of methane, benzene and other aromatic compounds.

Yan *et al.* (2010) obtained catalytic steam reforming of bio-oil aqueous fraction. The Ni/CeO₂-ZrO₂ catalyst had superior catalytic activity for hydrogen production by steam reforming of bio-oil as compared to commercial nickel-based catalyst (Z417). The reaction temperature and water-to-bio-oil ratio (W/B) had profound effects on the hydrogen yield and content of the product gas. At T = 800 °C and W/B = 4.9, the hydrogen yield and content reached the maximum value of 69.7% and 61.9% respectively in the range of experimental temperature over the Ni/CeO₂-ZrO₂ (12 wt% Ni, 7.5 wt% Ce) catalyst, which were higher than those of the commercial nickelbased catalysts (Z417).

Seyedeyn-Azad *et al.* 2011 investigated catalytic steam reforming of bio-oil by using Ni/Al₂O₃ catalyst. It was revealed that the Al₂O₃ with 14.1% Ni content gave the highest yield of hydrogen (73%) among the catalysts tested, and the best carbon conversion was 79% under the steam reforming conditions of S/C=5, W_bHSV=13 1/h and temperature=950°C. The H₂ yield increased with increasing temperature and decreasing W_bHSV; whereas the effect of the S/C ratio was less pronounced. In the S/C ratio range of 1 to 2, the hydrogen yield was slightly increased, but when the S/C ratio was increased further, it did not have an effect on the H₂ production yield.

2.5 Catalysts

The number of studies in the literature on steam reforming of oxygenate hydrocarbon catalysts has significantly increased in recent years. Catalysts utilized are mainly Ni, Cu, Co and noble metals, such as Rh, Ru, Re, Pd and Pt (Breen *et al.*, 2002; Liguras *et al.*, 2003; Salge *et al.*, 2005). Although supported noble metal catalysts have been shown to have good performance but the high cost and limited reserves is also cause for concern. As a less expensive alternative, cobalt and nickel-based catalysts have been reported to have superior hydrocarbon steam reforming performance due to their high activity for C-C bond cleavage (Llorca *et al.*, 2002; 2003).

2.5.1 Ni-based Catalysts

Nickel based catalysts are attractive for this reaction due to their high activity and low cost. Hegarty *et al.* (1998) studied steam reforming and partial oxidation of methane over Cu, Co, Fe and Ni supported on ZrO₂ catalysts at the temperatures from 400 to 800°C. The result showed that the activity of the catalysts were found to decrease in the order Ni>Cu>Co>Fe.

Frusteri *et al.* (2004, 2006) studied ethanol reforming over Ni catalyst supported on MgO, and applied it in the molten carbonate fuel cells. It was found that Ni/MgO exhibited high steam reforming activity and H₂ selectivity. However, Ni/MgO also exhibited high selectivity for CO and CH₄. CO was a poison for the

molten carbonate fuel cells. CH₄ seized the hydrogen atom, leading to the decrease of H₂ selectivity, and the decomposition of CH₄ was an important factor for coke formation.

In the work of Galdámez *et al.* (2005) coprecipitated nickel catalysts were investigated, some of them promoted with lanthanum. The results indicate that the highest hydrogen yield was produced with the Ni–Al catalyst. This catalyst had a nickel content (Ni/(Ni + Al)), relative at.% of Ni equal to 33.

The influence of the nickel content has been previously investigated. Thus, coprecipitated Ni–Al catalysts with three different nickel contents (15, 33 and 53 relative at.% of nickel) have been tested in steam reforming of methane by Al-Ubaid and Wolf (1988). Sahli *et al.* (2006) have recently studied Ni–Al catalysts prepared by the sol gel method with different nickel contents. They concluded that it would be of interest to study nickel contents in the catalyst smaller than 33 relative at.% of nickel.

However, Ni is easily deactivated by carbon deposition. It is believed that hydrocarbons dissociate on the nickel surface to produce highly reactive carbon species (C_α) which are probably atomic carbon (McCarty *et al.*, 1979; Bartholomew, 1982). C_α is easily gasified, however, if there is excess of C_α formed or gasification is slow, then polymerisation to C_α is favoured. The carbon may be gasified, may dissolve in the nickel crystallite, or may encapsulate the surface. The dissolved carbon diffuses through the nickel to nucleate and precipitate at the rear of the crystalline. This continuing process leads to the formation of carbon whisker, which lifts the nickel crystallite from the catalyst surface, and eventually results in fragmentation of the catalyst (Trimm, 1977; Rostrup-Nielsen, 1977). Not all of the coke formed on the surface dissolves in nickel. At least some carbon remains on the surface and encapsulates nickel (Trimm, 1977; Rostrup-Nielsen, 1977).

2.5.2 Co-based Catalysts

Co catalysts is alternatives due to their low cost. Co/Al₂O₃ shows considerable activity for the CH₄/CO₂ reaction (Wang and Ruckenstein, 2001; Takanabe *et al.*, 2005), the Fischer-Tropsch synthesis (Schanke *et al.*, 1995; Jacobs *et al.*, 2003; Inache *et al.*, 2004) and the steam reforming of ethanol (Batista *et al.*,

2004). The catalytic activity of cobalt catalysts is influenced by the supporting materials (usually metal oxides), but the cobalt species are believed to be the active center for the cleavage of the C–C bond in ethanol. However, the effect of the supporting materials on catalytic activity has not been investigated thoroughly. The supporting materials could chemically play multiple roles in either modifying the formation of active Co metal species, or in altering the reaction routes where the supporting materials contribute toward active sites with different catalytic functions relative to the Co metal species (Anderson and Fernandez Garcia, 2005).

In steam reforming of ethanol, Al_2O_3 is generally used as a support but its acid sites promote the dehydration of ethanol to ethylene (Fatsikostas, and Verykios, 2004). MgO contains strongly basic sites, which are proposed to be highly active for ethanol dehydrogenation to acetaldehyde (Llorca *et al.*, 2001). Ceria and ceria-containing mixed oxides have also been proposed to be catalytically active components of supported metal catalysts for ethanol conversion reactions due to their high oxygen storage capacities, suggested to improve catalyst stability (Lima *et al.*, 2008; Cai *et al.*, 2008), and because of their ability to promote the dissociation of molecules of the type ROH (e.g., H_2O and ethanol) (Jacobs *et al.*, 2007). In addition, the strong metal-support interaction has been postulated to prevent metal particle sintering, which can contribute to catalyst deactivation (Romero-Sarria *et al.*, 2008).

Hua Song and Umit S. Ozkan (2009) investigated the effect of oxygen mobility on the bio-ethanol steam reforming of ZrO_2 - and CeO_2 -supported cobalt catalysts. The result showed that the significant deactivation of Co/ZrO_2 catalysts through deposition of carbon on the surface, mostly in the form of carbon fibers, the growth of which is catalyzed by the Co particles. The addition of ceria appears to improve the catalyst stability due to its high oxygen mobility, allowing gasification/oxidation of deposited carbon as soon as it forms. The high oxygen mobility of the catalyst not only suppresses carbon deposition and helps maintain the active surface area, but it also allows delivery of oxygen to close proximity of ethoxy species, promoting complete oxidation of carbon to CO_2 , resulting in higher hydrogen yields.

2.5.3 Ceria-Zirconia Mixed Oxides

In general, the deposition of carbon would occur over the metallic sites as well as on the acid sites of the support. Therefore, the studies of highly active and stable catalyst have been focused. Selection of a support material is important to reduce carbon deposit on catalysts. Oxygen storage capacity and redox property of support are promising to gasify carbon deposition. Ceria (CeO_2) has been widely used as a promoter and an oxidation catalyst because of its unique redox properties and high oxygen storage capacity (Trovarelli *et al.*, 1999). However, pure CeO_2 has poor thermal stability. Recently, it has been reported that the addition of Zirconia (ZrO_2) to CeO_2 leads to improvement not only in its oxygen storage capacity, redox properties and catalytic activity, but also resistance to high temperature (Pengpanich *et al.*, 2002).

2.5.4 Promoters

A promoter is a substance that is added in relatively small amounts into the catalyst to improve activity, selectivity or stability. The common additives are alkali metals, and transition metals. In some cases, the precious metals such as Pt, Pd and Rh have been used.

2.5.4.1 Precious Metals

Soyal-Baltacioglu *et al.* (2008) investigated the ethanol reforming on catalysts having 0.2-0.3 wt.% Pt and 10-15 wt.% Ni contents. It was found that the best ethanol steam reforming performance was achieved over 0.3 wt.% Pt-15wt.% Ni/ δ - Al_2O_3 .

Dias and Assaf (2008) studied the effect of introducing small amounts of Pt, Pd and Ir into Ni/ Al_2O_3 catalysts for the autothermal reforming of methane, with the aim of making the reaction ignite without previous reduction of the catalyst with H_2 . It was concluded that the samples promoted with palladium nitrate were very active in the auto-thermal reforming of methane, and this was attributed to expansion of the metal surface.

Luciene P.P. Profeti *et al.* (2009) investigated the ethanol reforming over NiM/LaAl (M=Pt, Pd) catalysts with two different noble metal contents (0.1 and 0.3 wt.%) were prepared by the impregnation method. The result show that the Ni/LaAl promoted catalysts produced a hydrogen-rich gas mixture. In

the experiments performed at 450°C, the Ni/LaAl catalyst showed lower H₂ formation and higher acetaldehyde production than the promoted catalysts. Moreover, the bimetallic catalysts showed a higher ethanol conversion and higher hydrogen yield than the Ni/LaAl catalyst, irrespective of the nature or concentration of the noble metal.

2.5.4.2 Alkali Metals and Transition Metals

Liberatori *et al.* (2007) investigated the catalytic behavior of Ni/Al₂O₃ catalysts modified with La and Ag in the steam reforming of ethanol. They found that the addition of La decreased the coking on Ni catalysts during the steam reforming of ethanol and promoted the selectivity to hydrogen. This resistance to coke deposition on the catalyst was attributed to the formation of lanthanum oxycarbonate, which reacts with surface carbon to form CO and regenerate La₂O₃.

A.C. Basagiannis and X.E. Verykios (2006) investigated the reforming reaction of acetic acid on nickel catalysts. The results shown that the carbon deposition occurs at a high rate in the presence of Al₂O₃, and at a significantly lower rate in the presence of La₂O₃. This is due to the acidity of Al₂O₃ which favours decomposition and polymerization reactions, resulting in the formation of significant carbonaceous species on the carrier, which are of the graphitic type.

Basagiannis *et al.* (2007) studied the steam reforming of aqueous fraction of bio-oil over Ru/MgO/Al₂O₃ catalysts. It was found that the presence of magnesium is improved catalytic activity and decrease coke formation on catalyst. The role of MgO in the catalyst composition seems to be related to enhanced O and/or –OH anion spillover from the carrier onto the metal particles.

Victor A. *et al.* (2008) was studied the effect of iron promoter on cobalt-based catalysts, active in the ethanol steam reforming. Fe_xCo_{3-x}O₄ (0 ≤ x ≤ 0.60) oxides prepared by co-precipitation and an Fe-doped Co₃O₄ prepared by wetness impregnation. Decreasing the production of undesired CO and CH₄ by-products for catalyst derived from Fe_{0.15}Co_{2.85}O₄ is found.

Xun Hu and Gongxuan Lu (2009) were evaluated in acetic acid reforming reaction over Ni/Al₂O₃ catalysts modified with a series of promoters

(Li, Na, K, Mg, Fe, Co, Zn, Zr, La, Ce). The addition of Co, Zr, La, or Ce to Ni/Al₂O₃ promoted the methanation reaction, and consequently promoted methane formation. Conversely, alkali metal modified samples effectively inhibited methane formation, especially the Ni–K/Al₂O₃ catalyst. Besides, the addition of K to a Ni/Al₂O₃ catalyst remarkably enhanced the stability of the Ni catalyst, due to the promotion of K on the gasification of coke deposit.

CHAPTER III

EXPERIMENTAL

In this chapter, the materials used in this research are described. The various experimental techniques utilized in the catalyst preparation, characterization and reaction studies will be explained. Details of the catalytic activity test system are also given.

3.1 Materials

3.1.1 Gases

The gases used in this research were:

1. Helium (He 99.99%) was obtained from Praxair (Thailand) Co.,LTD.
2. Nitrogen (N₂ 99.99%) was obtained from Praxair (Thailand) Co.,LTD.
3. Argon (N₂ 99.99%) was obtained from Praxair (Thailand) Co.,LTD.
4. Air Zero was obtained from Thai Industrial Gas Co.,LTD.
5. Hydrogen (H₂ 99.99%) was obtained from Praxair (Thailand) Co.,LTD.
6. Methane (CH₄ 99.99%) was obtained from Thai Industrial Gas Co.,LTD.

3.1.2 Chemicals

The chemical reagents used in this research were:

1. Cerous (III) nitrate hexahydrate ($\geq 99\%$) was obtained from Fluka Chemie A.G.
2. Zirconium oxychloride ($\geq 99\%$) was obtained from Fluka Chemie A.G.
3. Urea ($\geq 99\%$) was obtained from Fluka Chemie A.G.
4. α -Alumina ($>96\%$) was obtained from Johnson Matthey.

5. Nickel (II) nitrate hexahydrate ($\geq 99\%$) was obtained from Fluka Chemie A.G.
6. Magnesium nitrate ($\geq 99\%$) was obtained from Unilab
7. Potassium chloride ($\geq 99\%$) was obtained from Analar
8. Cobalt (II) nitrate ($\geq 99\%$) was obtained from Univar
9. Acetic acid ($\geq 99.7\%$) was obtained from Lab-Scan, Analytical Sciences.
10. Acetone was obtained from Lab-Scan, Analytical Sciences.
11. Ethanol was obtained from Fluka Chemie A.G.

3.2 Experiment

3.2.1 Catalyst Preparation

3.2.1.1 *Ceria-Zirconia Mixed Oxide*

Mixed oxides of ceria-zirconia samples were prepared via urea hydrolysis. The ceria-zirconia mixed oxide samples were prepared from $\text{Ce}(\text{NO}_3)_3 \cdot 6\text{H}_2\text{O}$ (99.0%, Fluka) and $\text{ZrOCl}_2 \cdot 8\text{H}_2\text{O}$ (99.0%, Fluka). The synthesized procedure has been reported elsewhere (Pengpanich *et al.*, 2002). Briefly, the starting metal salts were dissolved in distilled water to the desired concentration (0.1 M). The ratio between the metal salts was altered depending on the desired concentration: $\text{Ce}_{1-x}\text{Zr}_x\text{O}_2$ in which $x = 0, 0.25, 0.50, 0.75$ and 1.0 . Then, the mixed metal salt solution was added with a 0.4 M of urea (99.0%, Fluka) solution with the salt to urea solution ratio of 2:1 (v/v), and the mixture was kept at $100\text{ }^\circ\text{C}$ for 50 h. The sample was then allowed to cool to room temperature prior to being centrifuged to separate a gel product from the solution. The gel product was washed with ethanol and dried overnight in an oven at $110\text{ }^\circ\text{C}$. The product was then calcined at either $500\text{ }^\circ\text{C}$ for 4 h.

3.2.1.2 *Magnesium Oxide*

Magnesium oxide was prepared via urea hydrolysis. $\text{Ce}(\text{NO}_3)_3 \cdot 6\text{H}_2\text{O}$ (99.0%, Fluka), $\text{Mg}(\text{NO}_3)_2$ was used as sources of Mg. The synthesis procedure of magnesium oxide was similar manner as mention in section 3.2.1.1.

3.2.1.3 *Ni-supported Catalysts*

The catalysts were prepared by the incipient wetness impregnation method. To prepare Ni supported mixed oxide catalysts, Ni (5, 15 and 25 wt.%) was loaded by the incipient wetness impregnation method into the mixed oxide supports using its nitrate salt solution. The catalysts were then calcined at 500°C for 4 h. Ni/ α -Al₂O₃ and Ni/MgO catalyst was also prepared for comparison purposes.

3.2.1.4 Ni-K supported Ce_{0.75}Zr_{0.25}O₂ Catalysts

The catalyst were prepared by a co-impregnation method using aqueous solutions of Ni(NO₃)₂·6H₂O and KNO₃. The nominal loading amount of Ni was kept constant at 15 wt.% and the amount of K loadings was 8 wt.%. The catalysts were then calcined at 500 °C for 4 h in air.

3.2.1.5 Co-supported Catalysts

The catalysts were prepared by the incipient wetness impregnation method. To prepare Co supported mixed oxide catalysts, 15 wt.% Co was loaded by the incipient wetness impregnation method into the mixed oxide supports using its nitrate salt solution. The catalysts were then calcined at 500°C for 4 h.

3.2.2 Catalyst Characterization

3.2.2.1 X-ray Diffraction

An X-ray diffractometer (XRD) system (Rigaku) equipped with a RINT 2000 wide-angle goniometer using Cu K α radiation and a power of 40 kV x 100 mA was used for examination of the crystalline structure. The intensity data were collected at 25 °C over a 2 θ range of 20-90° with a scan speed of 5° (2 θ)/min and a scan step of 0.02° (2 θ).

3.2.2.2 BET Surface Area

The specific surface area, the pore volume and the pore size distribution of the samples were determined from adsorption and desorption isotherms of nitrogen at 77 K using a Quantachrome Corporation Autosorb. Prior to the analysis, the samples were outgassed to eliminate volatile adsorbents on the surface at 250°C for 4 h.

3.2.2.3 *Temperature Programmed Reduction*

Temperature programmed reduction (TPR) measurements were carried out to investigate the redox properties over the resultant materials. About 50 mg of catalyst was placed in a quartz tube and pretreated in a 20 ml/min He atmosphere at 400 °C for 1 h prior to running the TPR experiment, and then cooled down to room temperature in He. The feed of 1% CO in He at a flow rate of 50 ml/min was used as a reducing gas. The temperature of the sample was raised at a constant rate of 10 °C/min. The amount of CO consumption during the increasing temperature period was measured using a mass spectrometer (Balzer Instruments modeled Thermostar GSD 300T).

3.2.2.4 *H₂ Chemisorption*

The dispersion degree of nickel was measured by H₂-pulse chemisorption at 50 °C using an Ar flow of 50 ml/min and each pulse of 0.1 ml (10% H₂ in Ar). For measurements, about 100 mg of sample was placed in a quartz reactor. Prior to the pulse chemisorption, the sample was reduced at 500 °C under H₂ atmosphere for 1 h. Then the sample was purged with Ar at 500 °C for 30 min and cooled to 50 °C in flowing Ar. The H₂ pulses were carried out with an injection interval of 6-8 min until the areas of successive hydrogen peaks were identical. The nickel dispersion was calculated assuming the adsorption stoichiometry of a hydrogen atom per nickel surface atom.

3.2.2.5 *Temperature Programmed Oxidation*

Temperature programmed oxidation (TPO) was carried out in a homemade TPO micro-reactor coupled with an FID detector. TPO was used to determine the amount of carbonaceous deposition on the spent catalysts. Typically, about 30 mg sample was heated in a 2%O₂ in He (40 ml/min) mixture at a heating rate 10°C/min up to 900°C. The output gas was passed to a methanation reactor containing 15 wt% Ni/Al₂O₃ as a catalyst. In this methanation reactor, CO₂ formed from the carbon was completely converted with excess H₂ into methane, to permit precise quantification in a FID detector. After the TPO system reached 900°C, where all carbon had been burned off, the FID signal for methane was calibrated by injecting 100 µl of CO₂ pulses into the methanation reactor, and sending the methane

produced into the FID. By integrating the methane signal during the entire TPO run, it was possible to calculate the amount of carbon removed from catalyst.

3.2.2.6 Thermogravimetric Analysis (TGA)

The amount of carbonaceous deposition on the spent catalysts was carried out using a TG7 Perkin-Elmer thermogravimetric analyzer under N₂ atmosphere. Typically, ca. 5 mg of sample were used for each run. The sample was heated up from ambient temperature to 105°C and held at this temperature for approximately 10 min to ensure that free-water was completely removed. Then, the sample was further heated to 800°C with a heating rate 10°C min⁻¹. By calculating the weight loss during the entire TGA run, it was possible to calculate the amount of carbon removed from catalyst.

3.2.2.7 Transmission Electron Microscope

The morphology of the fresh catalyst and carbon deposition on the spent catalysts was observed by transmission electron microscopy (TEM) with a JEOL (JEM-2010) transmission electron microscope operated at 200 kV. The samples were dispersed in absolute ethanol ultrasonically, and the solutions were then dropped on copper grids coated with a lacey carbon film.

3.2.2.8 Scanning Electron Microscope

The morphology of the fresh catalyst and carbon deposition on the spent catalysts was observed by transmission electron microscopy (TEM) with a JEOL (JEM-2010) Scanning electron Microscope.

3.2.3 Catalytic Activity Tests

3.2.3.1 Catalytic Activity Test for Model Oxygenate Hydrocarbon of Bio-oil aqueous phase Steam Reforming

Catalytic Activity Test for model oxygenate hydrocarbon of the bio-oil aqueous phase (acetic acid, ethanol and acetone) steam reforming were carried out in a differential fixed-bed quartz tube reactor (i.d. 6 mm). Typically, 0.1 g of catalyst was packed between the layers of quartz wool. The reactor was placed in an electric furnace equipped with K-type thermocouples. The temperature of catalyst bed was monitored and controlled using Shinko temperature controllers. A piston metering pump (Eldex) is used as feeding device which fed a liquid mixture

consisting of a known composition of model oxygenate hydrocarbon aqueous solution was introduced into an evaporator at ca. 150 °C to vaporize. Gaseous products were analyzed using a Shimadzu GC 8A equipped with a CTR I (Altech) column and a TCD detector and a Shimadzu GC 17A equipped with a HP-1 (Agilent technologies) column and an FID detector. The schematic diagram of the experimental setup was shown in Figure 3.1. The conversions were determined by dividing the moles of reactant consumed by the moles of initial reactant.

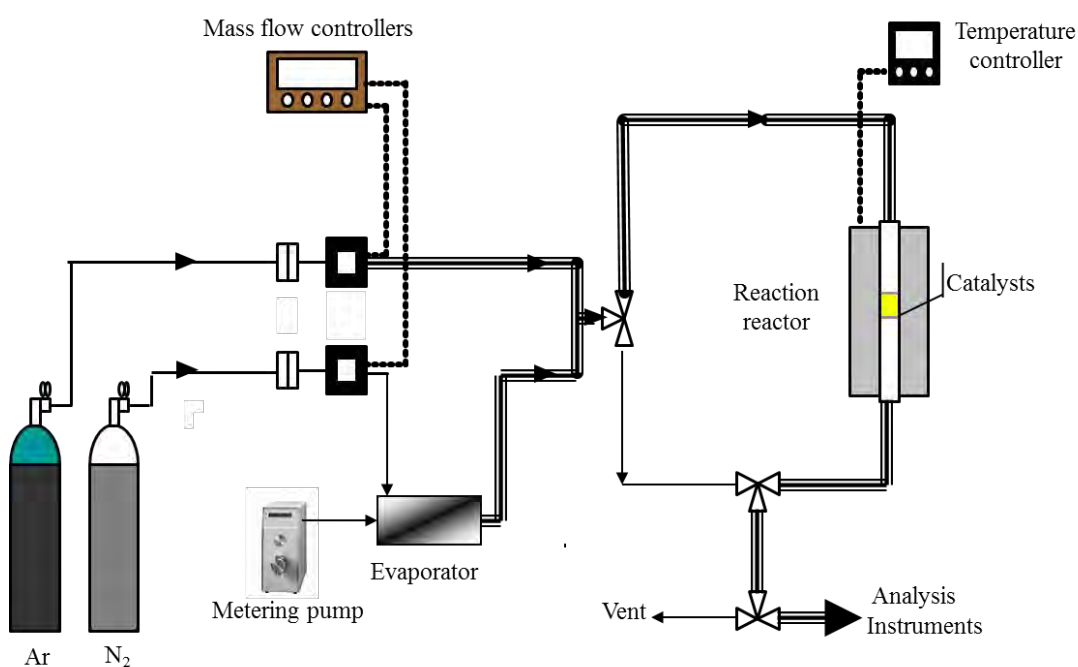


Figure 3.1 Schematic diagram of the experimental setup for model oxygenate hydrocarbon steam reforming.

3.2.3.2 Catalytic Activity Test for Methane Oxidation

Catalytic activity tests for the methane oxidation conducted by using the atmospheric flow experimental system shown in Figure 3.2. A fixed-bed quartz tube microreactor (i.d. \varnothing 6 mm) was used. Typically, 0.1 g of catalyst were packed between the layers of quartz wool. The reactor was placed in an electric furnace equipped with K-type thermocouples. The temperature of catalyst bed was monitored and controlled by Shinko Shinko FCR temperature controllers. 3%CH₄,

10%O₂, and balanced He gases were mixed and fed into the reactor at a gas hourly space velocity (GHSV) of 39 000 h⁻¹ using Brooks 5850 E mass flow controllers. An effluent gas was analyzed using a Varian CP-3380 GC fitted with a TCD.

The kinetic studies were carried out at the temperature range of 400-550°C and atmospheric pressure with variations of methane concentration between 2 and 4%, and of oxygen concentration between 10 and 20%. The kinetic data were attained using the initial rate method at the linear conversion range of less than 20% in all cases as well as conformed to Mears and Weisz criteria to ensure the absence of mass transfer limitations at such reaction conditions.

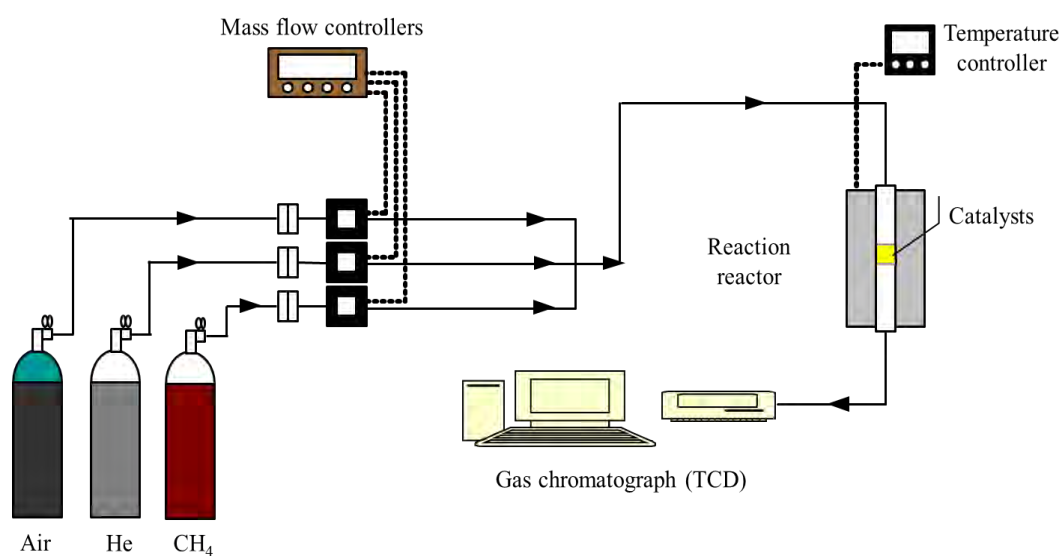


Figure 3.2 Schematic diagram of the experimental setup for methane oxidation.

CHAPTER IV

HYDROGEN PRODUCTION BY STEAM REFORMING OF ACETIC ACID OVER Ni-BASED CATALYSTS

4.1 Abstract

The Ni metallic phase supported metal oxides such as α -Al₂O₃, Ce_{0.75}Zr_{0.25}O₂, and MgO were tested under the steam reforming of acetic acid selected as a representative compound for the aqueous phase of the bio-oil derived from biomass pyrolysis. It was found that the catalytic activity and carbon formation for the catalysts studied were significantly dependent on the Ni content and the nature of support. The 15%Ni/Ce_{0.75}Zr_{0.25}O₂ catalyst exhibited the highest catalytic performance in terms of C-C breakage conversion and hydrogen yield. In addition, the redox property of Ce_{0.75}Zr_{0.25}O₂ provided higher stability than the MgO and α -Al₂O₃ due to its less carbon deposition even at low steam-to-carbon ratios.

4.2 Introduction

Hydrogen is being considered as an environmentally friendly source of energy for power generation with fuel cells. Currently, hydrogen is produced from fossil fuels such as natural gas, naphtha and coal (Peña *et al.*, 1996). However, these resources utilized result in a large quantity of greenhouse gas emission. For this reason, a renewable energy source such as biomass may be used as an alternative feedstock because it appears to have formidably positive environmental properties resulting from no net releases of carbon dioxide (CO₂) and very low sulfur content (Saxena *et al.*, 2009). Biomass can be converted to bio-oils by fast pyrolysis and then the bio-oils can be converted to hydrogen (H₂) by catalytic steam reforming (Czernik *et al.*, 2007; Takanabe *et al.*, 2006; Zhang *et al.*, 2005).

Bio-oils produced from biomass pyrolysis are virtually separated into the oil and water-rich phases. The oil phase contains lignin-derived materials that can be used for the production of more valuable products while the water-rich phase contains mostly carbohydrate-derived compounds that can be catalytically reformed

with steam (Kelley *et al.*, 1997; Shabtai *et al.*, 1997; Jindarom *et al.*, 2007). Since acetic acid is one of the major components of the water-rich phase of bio-oil (Zhang *et al.*, 2005; Bimbela *et al.*, 2007), therefore, steam reforming (SR) of acetic acid has been extensively investigated as a model reaction in order to understand the integrity required for designing the efficient catalysts for use in the SR of the bio-oil water-rich phase.

Ni based catalysts are intensively used for steam reforming of hydrocarbons including oxygenate hydrocarbons (Vizcaíno *et al.*, 2008; Hu and Lu, 2007; Wang *et al.*, 1996). It was reported the major problem of a Ni-based catalyst is its fast deactivation due to carbon deposition and/or metal sintering (Garcia *et al.*, 2000; Baker *et al.*, 1987). Alternative supports such as dolomite, olivine, MgO and MgO-CaO were reported to improve the catalytic stability (Sato and Fujimoto, 2007; Swierczynski *et al.*, 2007; Miyazawa *et al.*, 2006). Recently, it has been reported that $Ce_{1-x}Zr_xO_2$ mixed oxides exhibited a superior resistance to carbon formation on the partial oxidation and steam reforming of hydrocarbons (Bampenrat *et al.*, 2010; Pengpanich *et al.*, 2004), due to the high oxygen vacancy and oxygen mobility. In our early study, we have also found that $Ce_{0.75}Zr_{0.25}O_2$ solid solution exhibited the highest reducibility and activity for oxidation reactions (Bampenrat *et al.*, 2010; Pengpanich *et al.*, 2004; Thammachart *et al.*, 2001). In this study, we investigate the effect of the supports on the steam reforming catalytic activity and stability of acetic acid as a biomass-derived oxygenate compound model over Ni/ $Ce_{0.75}Zr_{0.25}O_2$, Ni/ α - Al_2O_3 and Ni/MgO catalysts

4.3 Experimental

4.3.1 Catalyst Preparation and Characterizations

$Ce_{0.75}Zr_{0.25}O_2$ and MgO were prepared via urea hydrolysis and precipitation method, respectively, whereas α - Al_2O_3 was obtained from a company. $Ni(NO_3)_2$ aqueous solution as Ni precursors was incorporated into the supports by the impregnation method. The desired amounts of Ni loading were 5-25 wt% for $Ce_{0.75}Zr_{0.25}O_2$, and 15wt% for both MgO and α - Al_2O_3 . The catalysts were characterized by BET, XRD, TPR, TPO, and TEM techniques. The detailed

synthesis procedure and characteristics of catalysts were reported elsewhere (Pengpanich *et al.*, 2004).

4.3.2 Catalytic Activity Testing

To compare the catalytic activity and stability of the catalysts on the steam reforming of acetic acid, the reaction was carried out at 650 °C with steam-to-carbon (S/C) ratios ranging from 1 to 6. Typically, 0.1 g of catalyst was packed between the layers of quartz wool in a quartz tube microreactor (i.d. 10 mm) placed in an electric furnace equipped with K-type thermocouples. The temperature of catalyst bed was monitored and controlled using Shinko temperature controllers. A liquid mixture feed consisting of a known composition of acetic acid aqueous solution was introduced into an evaporator at ca. 140 °C to vaporize and mix with a gas stream prior to entering the reactor set at a desired temperature. Gaseous products were analyzed using on-line gas chromatographs in series equipped with TCD and FID detectors. Prior to running the reaction, the catalyst was reduced *in-situ* with a flow of 50% H₂ in N₂ gas at 600 °C for 2 h. The C-C breakage conversion of acetic acid was defined as a molar ratio of the gaseous single carbon compounds (CH₄, CO and CO₂) in the product stream to the acetic acid reactant and the product yield was defined as a molar ratio of the product to the theoretical amount of product produced from steam reforming of acetic acid. The C-C breakage conversion and product yield reported in this work were calculated as follows:

$$\text{C-C breakage conversion (\%)} = \frac{\text{mol}_{\text{CH}_4, \text{out}} + \text{mol}_{\text{CO}, \text{out}} + \text{mol}_{\text{CO}_2, \text{out}}}{2 \times \text{mol}_{\text{AcCH}_3, \text{in}}} \times 100 \quad (1)$$

$$\% \text{Yield}_{\text{H}_2} = \frac{\text{mol}_{\text{H}_2, \text{out}}}{4 \times \text{mol}_{\text{AcCH}_3, \text{in}}} \times 100 \quad (2)$$

$$\% \text{Yield}_{\text{CO}} = \frac{\text{mol}_{\text{CO}, \text{out}}}{2 \times \text{mol}_{\text{AcCH}_3, \text{in}}} \times 100 \quad (3)$$

$$\% \text{Yield}_{\text{CO}_2} = \frac{\text{mol}_{\text{CO}_2, \text{out}}}{2 \times \text{mol}_{\text{AcCH}_3, \text{in}}} \times 100 \quad (4)$$

$$\% \text{Yield}_{\text{CH}_4} = \frac{\text{mol}_{\text{CH}_4, \text{out}}}{2 \times \text{mol}_{\text{AcCH}_3, \text{in}}} \times 100 \quad (5)$$

4.4 Results and Discussion

4.4.1 Catalytic Characterization

The BET surface areas, degree of metal dispersions, and mean size diameters of the catalysts are shown in Table 4.1. As for the Ni/Ce_{0.75}Zr_{0.25}O₂ catalysts, their surface areas are in the range of 58-78 m²/g and decreased with increasing Ni loading. At a given support, the degree of metal dispersion is decreased and the mean size diameter is increased as the Ni loading is increased. This is due to the formation of NiO bulk particles (Pengpanich *et al.*, 2004). However, at a given Ni loading (15wt%), the Ni/Ce_{0.75}Zr_{0.25}O₂ catalyst possesses the highest metal dispersion degree with the smallest mean size diameter. The low metal dispersion degree of 15%Ni/ α -Al₂O₃ is due to the low surface area of the support while that of 15%Ni/MgO is owed to the formation of NiO-MgO solid solution.

The XRD patterns of the Ni/Ce_{0.75}Zr_{0.25}O₂ catalysts indicate a typical cubic fluorite structure of ceria with the presence of NiO phase (37°, 43°, and 62° (2 θ)) as shown in Figure 4.1. However, the Ni or NiO phase was absent in the case of low Ni loading (5 wt%). Since the peak intensity was amplified with increasing Ni loading, it was suggested that NiO species is present in the forms of nano-particles and bulk agglomerated particles at a low- and a high-Ni content, respectively (Pengpanich *et al.*, 2004). This result appears to be in good agreement with the data on degree of metal dispersion. Nevertheless, the XRD pattern of the 15%Ni/ α -Al₂O₃ catalyst reveals the separate phases of NiO and α -Al₂O₃, yet the absence of Ni-Al alloy phase. However, that of the 15%Ni/MgO catalyst indicates a NiO-MgO solid solution as similar to what reported elsewhere (Barbero *et al.*, 2003).

Figure 4.2 depicts the H₂-TPR profiles for Ni/Ce_{0.75}Zr_{0.25}O₂, Ni/ α -Al₂O₃ and Ni/MgO. The results showed that the reducibility of the 15 wt% Ni loading catalysts is in the following order: Ni/Ce_{0.75}Zr_{0.25}O₂ > Ni/ α -Al₂O₃ > Ni/MgO. Noticeably, two H₂ consumption peaks are observed for Ni /Ce_{0.75}Zr_{0.25}O₂ catalyst as compared with that for Ni/ α -Al₂O₃ catalyst. The low temperature peak in the range of 250-300 °C can be associated with the reduction of free NiO particles and the other peak in the range of 300-450 °C can be attributed to the reduction of complex NiO species in intimate contact with the oxide supports (Pengpanich *et al.*, 2004; Roh *et*

al., 2002; Montoya *et al.*, 2000). This suggests that interaction between Ni and the $\text{Ce}_{0.75}\text{Zr}_{0.25}\text{O}_2$ support makes the catalysts more reducible, which probably enhances the oxygen mobility during the reforming reaction. For the Ni/ $\alpha\text{-Al}_2\text{O}_3$ catalyst, only one broad peak attributed to agglomerated Ni is observed at ca. 410 °C. Similar reduction patterns were found in the cases of 5 and 25 wt% Ni loadings on $\text{Ce}_{0.75}\text{Zr}_{0.25}\text{O}_2$ with slightly lower reduction temperatures. It should be noted that the absence of the reduction peak for 15%Ni/MgO catalyst might be due to the incorporation of NiO into the MgO lattice resulting in the formation of NiO-MgO solid solution (Barbero *et al.*, 2003; Wang *et al.*, 2009).

4.4.2 Catalytic Activity for Acetic acid Steam reforming

To investigate the effect of support on the catalytic activity and stability, the $\alpha\text{-Al}_2\text{O}_3$ (inert) and MgO (basic support) were selected to compare with $\text{Ce}_{0.75}\text{Zr}_{0.25}\text{O}_2$ support for steam reforming of acetic acid. The performance of the catalyst was defined as C-C breakage conversion and hydrogen yield. The results showed that 15%Ni/ $\text{Ce}_{0.75}\text{Zr}_{0.25}\text{O}_2$ is the most active catalyst while the 15%Ni/ $\alpha\text{-Al}_2\text{O}_3$ was the least active one for such a steam reforming reaction as shown in Figure 4.3. This could be in part ascribed to the nature of supports steering different degrees of metal dispersion in which these were 3.06, 2.11, and 1.98% for 15%Ni/ $\text{Ce}_{0.75}\text{Zr}_{0.25}\text{O}_2$, 15%Ni/MgO and 15%Ni/ $\alpha\text{-Al}_2\text{O}_3$, respectively. It should be noted that for 15%Ni/ $\alpha\text{-Al}_2\text{O}_3$, the catalytic activity is solely due to Ni metal.

During the course of our experiments H_2 and CO_2 are not only the steam reforming products found, CO and a trace of CH_4 were detected at low steam to carbon ratio (S/C=1). It was reported CO could be generated from ketene decomposition (Basagiannis *et al.*, 2007) as shown in Eq. (6-7). The absence of C_2H_4 in this case would be, then, suggested that CO is probably produced via the decomposition of acetic acid (Eq. 8) as reported elsewhere (Basagiannis *et al.*, 2007) or from the reverse water gas shift reaction (Wang *et al.*, 1996). Since the methanation reaction is not thermodynamically favoured under our conditions, CH_4 might be generated from the decomposition of acetic acid (Eq. (9)) (Wang *et al.*, 1996).



The results also showed that the hydrogen yield increases steadily with the increase in steam to carbon ratio, in parallel with the carbon dioxide concentration, due to the shift in the water gas shift equilibrium toward hydrogen production. The absence of methane in the case of S/C = 3 and 6 for 15%Ni/Ce_{0.75}Zr_{0.25}O₂, and 15%Ni/ α -Al₂O₃ catalysts might be due to the steam reforming reaction of methane. However, a trace amount of CH₄ was still observed on the 15%Ni/MgO catalyst at S/C ratios of 3 and 6, which might be due to the presence of NiO-MgO solid solution.

The effect of Ni loading on the Ce_{0.75}Zr_{0.25}O₂ support was further investigated. It was found that the catalytic activity at a low S/C ratio was dependent on the nickel loading as shown in Table 4.2. The optimal loading is 15 wt%, which is related to the metal surface area and the metal particle size. At a high steam to carbon ratio (S/C = 6), the effect of Ni loading seems to be less pronounced.

4.4.3 Carbon Formation

The results showed that C-C breakage conversion of 15%Ni/ α -Al₂O₃ decreases from 57% to 39% while those of 15%Ni/Ce_{0.75}Zr_{0.25}O₂ and 15%Ni/MgO are rather stable, reported at 76% and 71%, respectively (at S/C =1) as shown in Figure 4.4. This suggests that 15%Ni/Ce_{0.75}Zr_{0.25}O₂ and 15%Ni/MgO are more active and stable than 15%Ni/ α -Al₂O₃. It is noticed that although 15%Ni/ α -Al₂O₃ shows the lowest C-C breakage conversion, the amount of carbon formed is somewhat higher than that of 15%Ni/Ce_{0.75}Zr_{0.25}O₂ and 15%Ni/MgO (Figure 4.5). At higher S/C ratios (S/C = 3 and 6), 15%Ni/Ce_{0.75}Zr_{0.25}O₂ exhibits a better activity with less carbon formation compared to 15%Ni/MgO and 15%Ni/ α -Al₂O₃. This indicates that the synergetic effect of an ease of reducibility and a good oxidation ability of the Ce_{0.75}Zr_{0.25}O₂ mixed oxide could promote the oxidation of carbon precursors on the

nickel surface as similar to reported elsewhere (Pengpanich *et al.*, 2004; Biswas and Kunzru, 2007). The spent catalysts were found to be covered with filamentous carbon as shown in Figure 4.6 and the results conform to the TPO analysis, which indicated mainly high temperature oxidation peak at ca. 650 °C (the results are not shown).

4.5 Conclusions

It can be concluded that the nature of the support affects the catalytic activity and stability by influencing the metal degree of dispersions and water activation. $\text{Ce}_{0.75}\text{Zr}_{0.25}\text{O}_2$ supported catalysts exhibit an excellent activity and stability for an acetic acid steam reforming. This is due to good redox properties and an oxygen mobility of $\text{Ce}_{0.75}\text{Zr}_{0.25}\text{O}_2$; promoting the oxidation of carbon species. At a high steam to carbon ratio ($S/C = 6$), the effect of the support on the activity was found to be less pronounced but was still present on the carbon formation of the catalysts.

4.6 Acknowledgements

This work was supported by the Thailand Research Fund (under Waste-to-Energy project and Royal Golden Jubilee Ph.D. Program: Grant 0170/46), and the Sustainable Petroleum and Petrochemicals Research Unit under the National Center of Excellence for Petroleum, Petrochemicals, and Advanced Materials, Chulalongkorn University.

4.7 References

- Baker, E.G., Brown, L.K.M.D. (1987) Steam gasification of biomass with nickel secondary catalysts. Industrial & Engineering Chemistry Research, 26, 1335–1339.
- Bampenrat, A., Meeyoo, V., Kitiyanan, B., Rangsunvigit, P., Rirksomboon, T. (2010) Naphthalene steam reforming over Mn-doped CeO₂–ZrO₂supported nickel catalysts. Applied Catalysis A: General, 373, 154-159.
- Barbero, J., Peña, M.A., Campos-Martin, J.M., Fierro, J.L.G., Arias, P.L. (2003) Support Effect in Supported Ni Catalysts on Their Performance for Methane Partial Oxidation. Catalysis Letter, 87, 211-218.
- Basagiannis, A.C., Verykios, X.E. (2007) Catalytic steam reforming of acetic acid for hydrogen production. International Journal of Hydrogen Energy, 32, 3343-3355.
- Bimbela, F., Oliva, M., Ruiz, J., García, L., Arauzo, J. (2007) Hydrogen production by catalytic steam reforming of acetic acid, a model compound of biomass pyrolysis liquids. Journal of Analytical and Applied Pyrolysis, 79, 112-120.
- Biswas, P., Kunzru, D. (2007) Steam reforming of ethanol for production of hydrogen over Ni/CeO₂–ZrO₂ catalyst: Effect of support and metal loading. International Journal of Hydrogen Energy, 32, 969-980.
- Czernik, S., Evans, R., French, R. (2007) Hydrogen from biomass-production by steam reforming of biomass pyrolysis oil. Catalysis Today, 129, 265-268.
- Garcia, L., French, R., Czernik, S., Chomet, E. (2000) Catalytic steam reforming of bio-oils for the production of hydrogen: effects of catalyst. Applied Catalysis A: General, 201, 225–239.
- Hu, X., Lu, G. (2007) Investigation of steam reforming of acetic acid to hydrogen over Ni–Co metal catalyst. Journal of Molecular Catalysis A: Chem, 261, 43-48.
- Jindarom, C., Meeyoo, V., Rirksomboon, T., Rangsunvigit, P. (2007) Thermochemical decomposition of sewage sludge in CO₂ and N₂ atmosphere. Chemosphere 67, 1477-1484.

- Kelley, S.S., Wang, X.-M., Myers, M.D., Johnson, D.K., Scahill, J.W. (1997) in: A.V. Bridgwater, D.G.B. Boocock (Eds.), *Developments in Thermochemical Biomass Conversion*, Blackie Academic & Profesional, London, p. 557.
- Miyazawa, T., Kimura, T., Nishikawa, J., Kado, S., Kunimori, K., Tomishige, K. (2006) Catalytic performance of supported Ni catalysts in partial oxidation and steam reforming of tar derived from the pyrolysis of wood biomass. *Catalysis Today*, 115, 254–262.
- Montoya, J.A., Romero-Pascual, E., Gimón, C., Del Angle, P., Monzon, A. (2000) Methane reforming with CO₂ over Ni/ZrO₂–CeO₂ catalysts prepared by sol–gel. *Catalysis Today*, 63, 71-85.
- Peña, M.A., Gómez, J.L.G., Fierro, J.L.G. (1996) New catalytic routes for syngas and hydrogen production. *Applied Catalysis A: General*, 144, 7-57.
- Pengpanich, S., Meeyoo, V., Rirksomboon, T. (2004) Methane partial oxidation over Ni/CeO₂–ZrO₂ mixed oxide solid solution catalysts. *Catalysis Today*, 93-95, 95-105.
- Roh, H., Jun, K., Dong, W., Chang, J., Park, S., Joe, Y. (2002) Highly active and stable Ni/Ce–ZrO₂ catalyst for H₂ production from methane. *Journal of Molecular Catalysis A: Chemical*, 181, 137-142.
- Sato, K., Fujimoto, K. (2007) Development of new nickel based catalyst for tar reforming with superior resistance to sulfur poisoning and coking in biomass gasification. *Catalysis Communications*, 8, 1697–1701.
- Saxena, R.C., Adhikari, D.K., Goyal, H.B. (2009) Biomass-based energy fuel through biochemical routes: A review. *Renewable and Sustainable Energy Reviews*, 13, 167-178.
- Shabtai, J., Zmierzak, W., Chomet, E. (1997) in: R.P.Overend, E. Chornet (Eds.), *Making a Business from Biomass in Energy, Environment, Chemicals, Fibers, and Materials*, vol. 2 Pergamon, Oxford, p. 1037.
- Swierczynski, D., Libs, S., Courson, C., Kiennemann, A. (2007) Steam reforming of tar from a biomass gasification process over Ni/olivine catalyst using toluene as a model compound. *Applied Catalysis B: Environmental*, 74, 211–222.

- Takanabe, K., Aika, K., Inazu, K., Baba, T., Seshan, K., Lefferts, L. (2006) Steam reforming of acetic acid as a biomass derived oxygenate: Bifunctional pathway for hydrogen formation over Pt/ZrO₂ catalysts. Journal of Catalysis, 243, 263-269.
- Thammachart, M., Meeyoo, V., Risksomboon, T., Osuwan, S. (2001) Catalytic activity of CeO₂-ZrO₂ mixed oxide catalysts prepared via sol-gel technique: CO oxidation. Catalysis Today, 68, 53-61.
- Vizcaíno, A.J., Arena, P., Baronetti, G., Carrero, A., Calles, J.A., Laborde, M.A., Amadeo N. (2008) Ethanol steam reforming on Ni/Al₂O₃ catalysts: Effect of Mg addition. International Journal of hydrogen energy, 33, 3489 – 3492.
- Wang, D., Montané, D., Chornet, E. (1996) Catalytic steam reforming of biomass-derived oxygenates: acetic acid and hydroxyacetaldehyde. Applied Catalysis A: General, 143, 245-270.
- Wang, He Y., Mei Liu, H., Qing Xu, B. (2009) Durable Ni/MgO catalysts for CO₂ reforming of methane: Activity and metal-support interaction. Journal of Molecular Catalysis A: Chemical, 299, 44-52.
- Zhang, S., Yan, Y., Li, T., Ren, Z. (2005) Upgrading of liquid fuel from the pyrolysis of biomass. Bioresource Technology, 96, 545-550.

Table 4.1 BET surface area, degree of metal dispersion and mean size diameter of the catalysts

| Catalyst | BET surface area (m ² /g) | Degree of metal dispersion (%) | Mean size diameter* (nm) | Mean size diameter** (nm) |
|--|--------------------------------------|--------------------------------|--------------------------|---------------------------|
| 5%Ni/Ce _{0.75} Zr _{0.25} O ₂ | 78 | 8.29 | - | 12.2 |
| 15%Ni/Ce _{0.75} Zr _{0.25} O ₂ | 68 | 3.06 | 29.5 | 33.0 |
| 25%Ni/Ce _{0.75} Zr _{0.25} O ₂ | 58 | 2.15 | 44.7 | 47.0 |
| 15%Ni/Al ₂ O ₃ | 4 | 1.98 | 47.6 | 51.0 |
| 15%Ni/MgO | 50 | 2.11 | - | 47.8 |

*calculated from XRD

** calculated from H₂-chemisorption

Table 4.2 Acetic acid steam reforming on 0.1 g of 5%Ni/Ce_{0.75}Zr_{0.25}O₂, 15%Ni/Ce_{0.75}Zr_{0.25}O₂ and 25%Ni/Ce_{0.75}Zr_{0.25}O₂ catalysts at T= 650 °C and WHSV (HAc) = 22 h⁻¹

| Catalyst | S/C ratio | Yield* (%) | | | | C-C breakage conversion* (%) |
|--|-----------|----------------|-------|-----------------|-----------------|------------------------------|
| | | H ₂ | CO | CO ₂ | CH ₄ | |
| 5%Ni/Ce _{0.75} Zr _{0.25} O ₂ | 1 | 33.84 | 15.78 | 22.52 | 0.00 | 38.29 |
| | 3 | 64.39 | 10.89 | 57.55 | 0.00 | 68.44 |
| | 6 | 98.52 | 8.46 | 90.53 | 0.00 | 98.98 |
| 15%Ni/Ce _{0.75} Zr _{0.25} O ₂ | 1 | 62.98 | 32.06 | 43.20 | 1.30 | 76.56 |
| | 3 | 93.83 | 19.10 | 80.25 | 0.00 | 99.35 |
| | 6 | 99.34 | 9.59 | 89.15 | 0.00 | 98.84 |
| 25%Ni/Ce _{0.75} Zr _{0.25} O ₂ | 1 | 60.66 | 30.69 | 41.35 | 0.84 | 72.88 |
| | 3 | 73.62 | 11.65 | 65.44 | 0.00 | 77.09 |
| | 6 | 98.74 | 9.31 | 89.43 | 0.00 | 98.74 |

*At time on steam of 40 min.

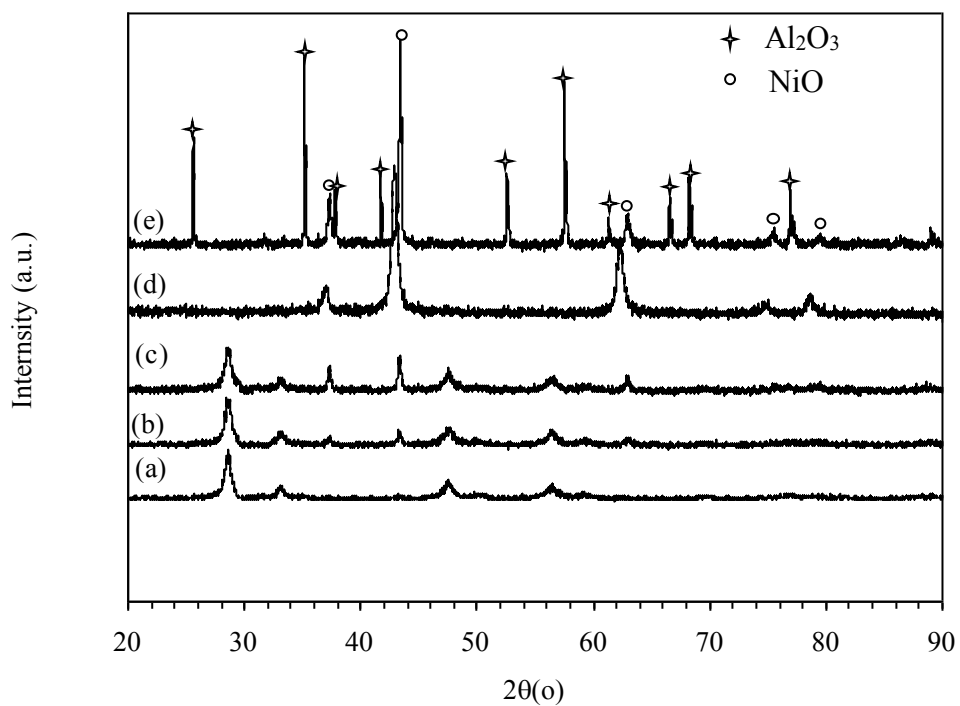


Figure 4.1 XRD patterns for the catalysts investigated (a) 5%Ni/Ce_{0.75}Zr_{0.25}O₂, (b) 15%Ni/Ce_{0.75}Zr_{0.25}O₂, (c) 25%Ni/Ce_{0.75}Zr_{0.25}O₂, (d) 15%Ni/MgO, and (e) 15%Ni/ α -Al₂O₃.

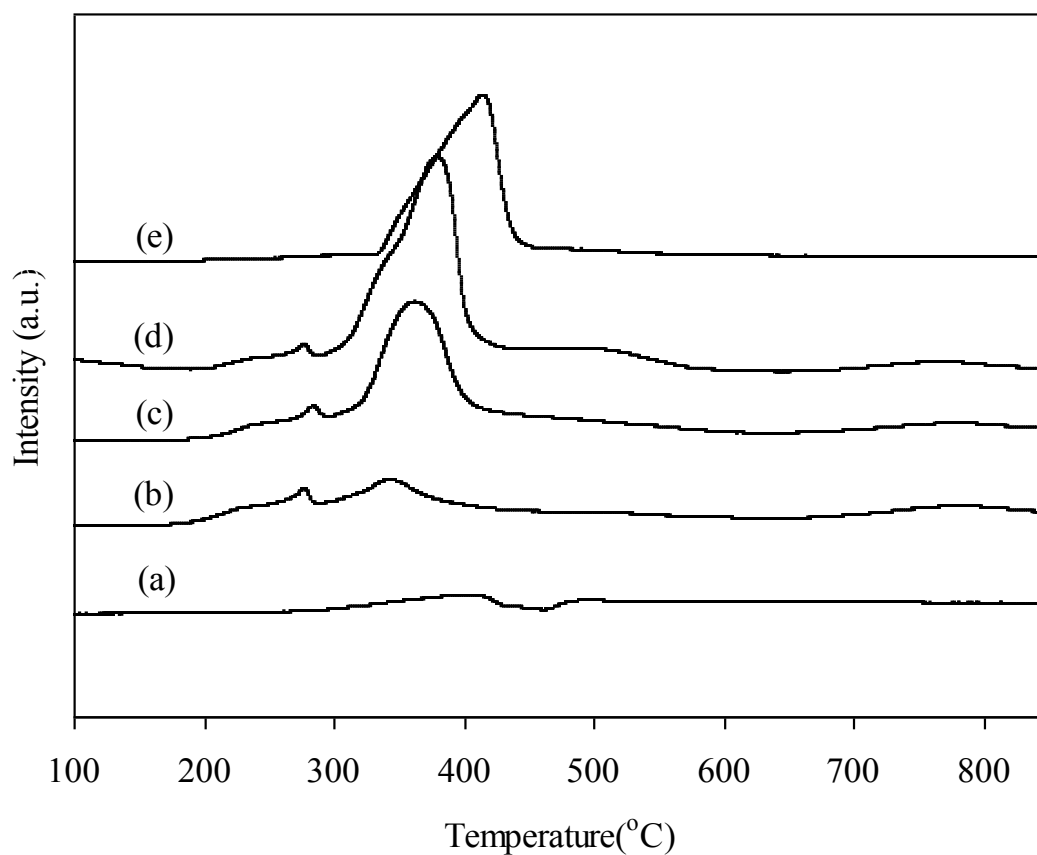


Figure 4.2 H₂-TPR profiles for the catalysts with a heating rate of 10 °C/min, a reducing gas containing 5% H₂ in N₂ with a flow rate of 30 ml/min: (a) 15%Ni/MgO, (b) 5%Ni/Ce_{0.75}Zr_{0.25}O₂, (c) 15%Ni/Ce_{0.75}Zr_{0.25}O₂, (d) 25%Ni/Ce_{0.75}Zr_{0.25}O₂, and (e) 15%Ni/ α -Al₂O₃.

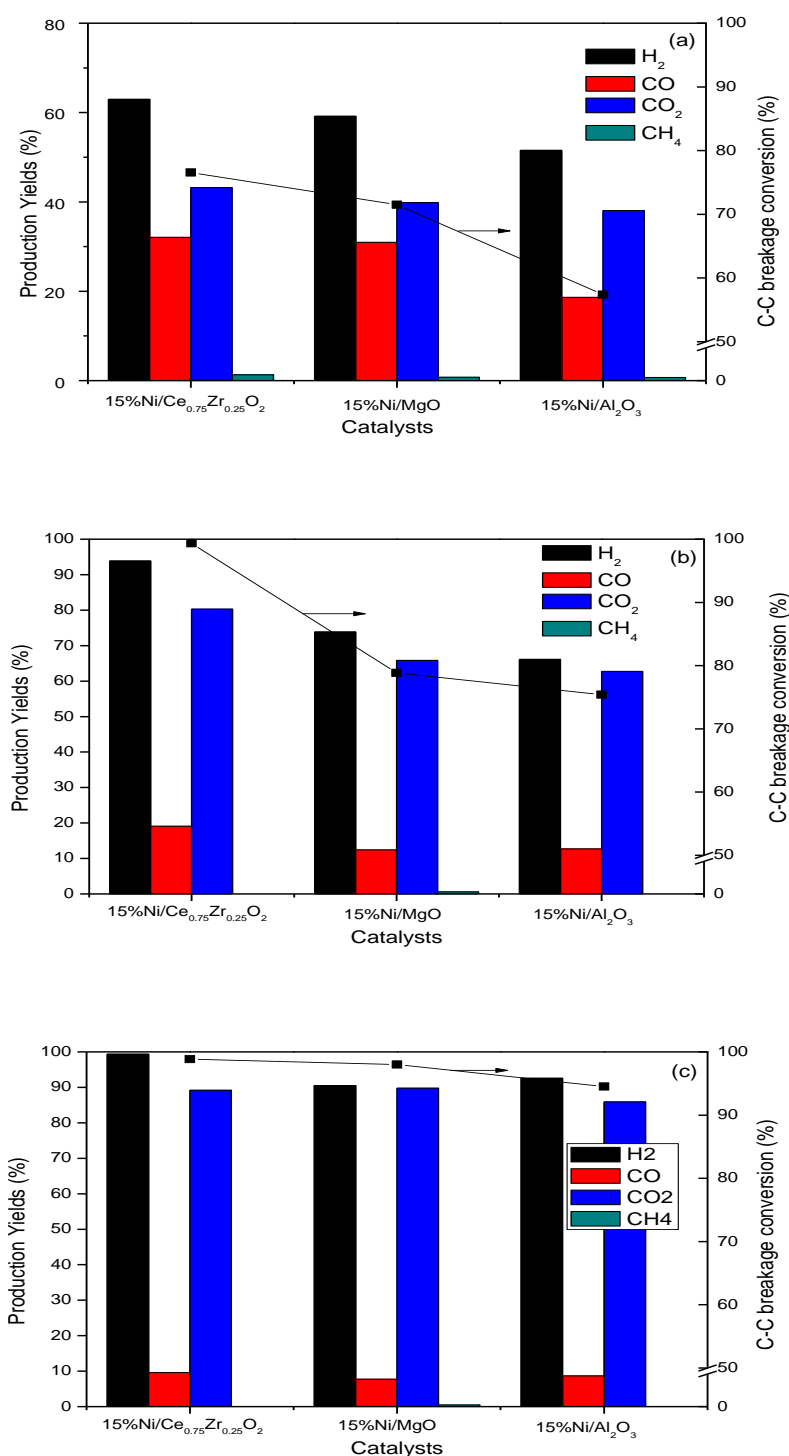


Figure 4.3 Effect of S/C ratio on the C-C breakage conversion, the yields of carbon containing products and hydrogen yield over: 15%Ni/Ce_{0.75}Zr_{0.25}O₂, 15%Ni/MgO and 15%Ni/ α -Al₂O₃ at 650°C and s/c ratio: (a) 1, (b) 3 and (c) 6.

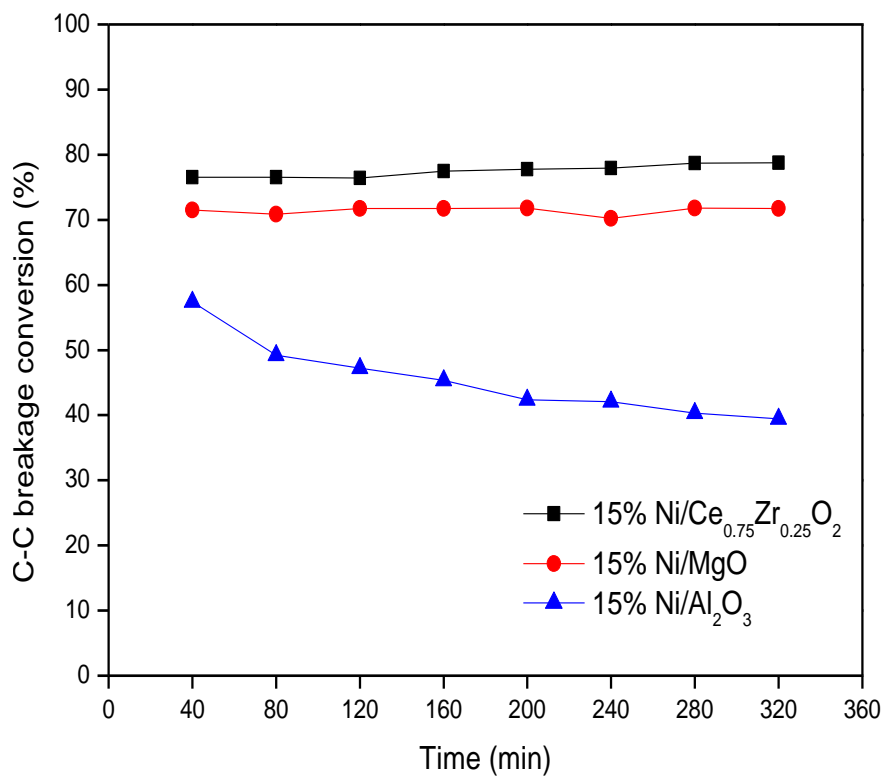


Figure 4.4 Catalytic activity for acetic acid steam reforming over 15%Ni/Ce_{0.75}Zr_{0.25}O₂, 15%Ni/ α -Al₂O₃, and 15%Ni/MgO catalysts: T = 650°C and S/C ratio = 1.

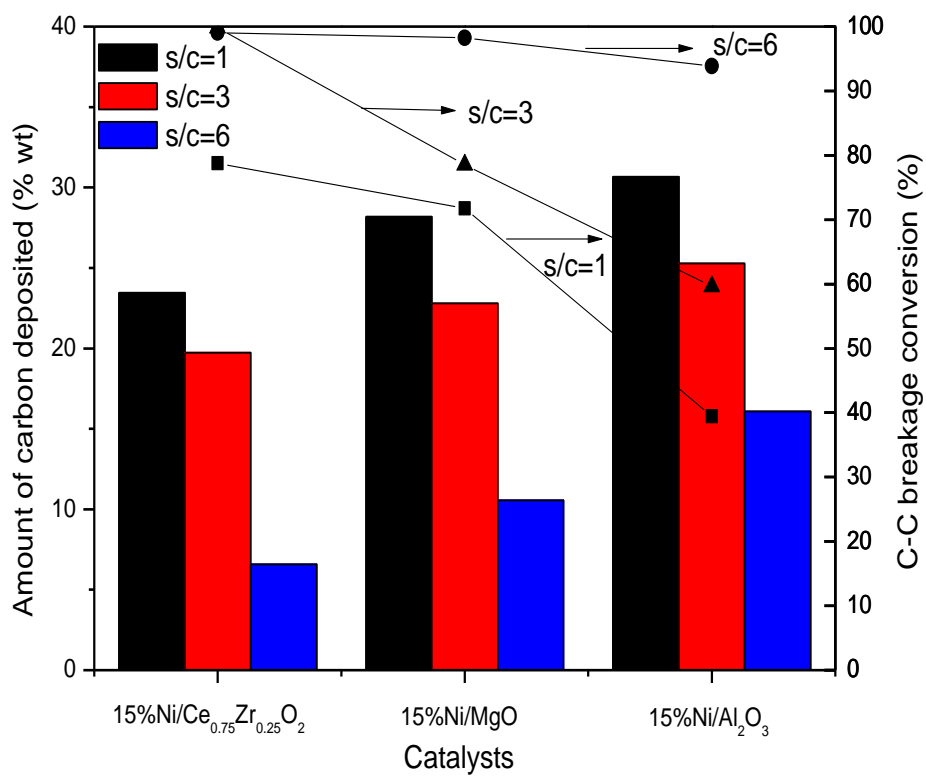


Figure 4.5 Total amount of carbon deposited on catalysts via acetic acid steam reforming over 15%Ni/Ce_{0.75}Zr_{0.25}O₂, 15%Ni/MgO and 15%Ni/ α -Al₂O₃ catalysts; after 320 min on stream, at 650°C, S/C ratios of 1 – 6.

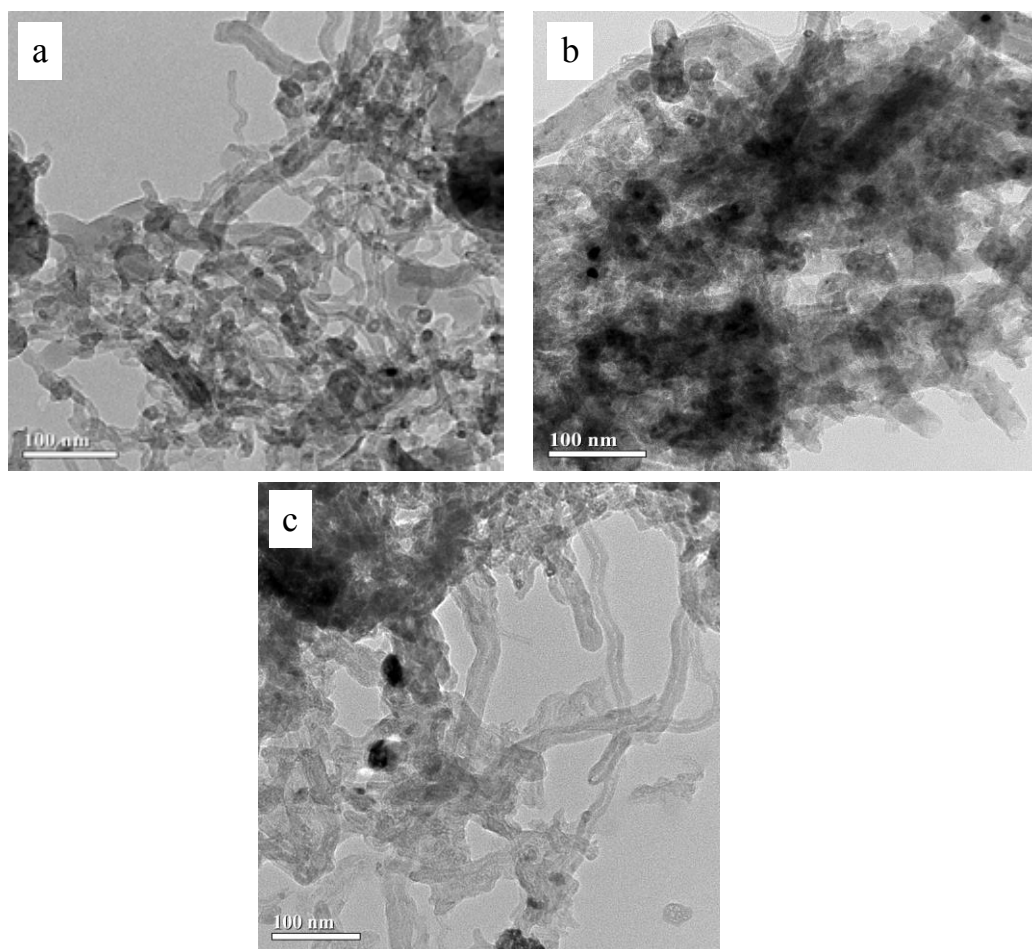


Figure 4.6 TEM images of the spent catalysts: (a) 15%Ni/ α -Al₂O₃, (b) 15%Ni/Ce_{0.75}Zr_{0.25}O₂, (c) 15%Ni/MgO.

CHAPTER V
STEAM REFORMING OF ETHANOL OVER Ni/Ce_{0.75}Zr_{0.25}O₂ AND
Ni-K/Ce_{0.75}Zr_{0.25}O₂ CATALYSTS

5.1 Abstract

In this study, the catalytic activity of Ni/Ce_{0.75}Zr_{0.25}O₂ and Ni-K/Ce_{0.75}Zr_{0.25}O₂ catalysts prepared by urea hydrolysis and incipient wetness impregnation was investigated for steam reforming of ethanol. The results showed that the potassium promoted on Ni/Ce_{0.75}Zr_{0.25}O₂ catalyst exhibit good activity for steam reforming of ethanol. It was found that the presence of K alters the NiO phase rhombohedral phase (R-3m) to cubic phase (Fm-3m), which is more favor for C-C breakage. Moreover it was found that the amount of carbon deposited decrease when potassium introduce to Ni/Ce_{0.75}Zr_{0.25}O₂ catalyst. This might be due to the fact that the presence of K species makes Ni active sites less favor for methane activation resulting in the suppression of carbon deposition.

5.2 Introduction

Currently, hydrogen is produced from fossil fuels such as natural gas, naphtha and coal (Peña *et al.*, 1996). However, these resources utilized result in a large quantity of greenhouse gas emission. For this reason, a renewable energy source such as biomass may be used as an alternative feedstock because it appears to have formidably positive environmental properties resulting from no net releases of carbon dioxide and very low sulfur content (Saxena *et al.*, 2009).

Ethanol has shown good features for hydrogen production (Haryanto *et al.*, 2005) and it owns a series of advantages, mainly handling safety and a renewable origin, since it can be produced in large quantities from several biomass sources (corn, wheat, sugar cane, barley and their waste materials). Thus, ethanol steam reforming is an interesting alternative for hydrogen production. Noble metals such as Rh, Pt, Pd (Breen, *et al.* 2002; Diagne *et al.* 2002; Navarro *et al.* 2005; Liguras *et al.* 2003; Cavallaro *et al.* 2003) bimetallic oxides such as Ni-Rh catalysts (Kugai *et al.*

2005, 2006) and transition metals such as Ni, Co show good catalytic performance for steam reforming of ethanol (SRE) (Chica and Sayas 2009; Fatsikostas and Verykios 2004) The catalysts based on noble metals are reported to be more active and less sensitive to coking than the Ni-based catalysts. However if one considers the aspects of high cost and limited availability of noble metals, it is more practical, from the industrial standpoint to develop Ni- and Co- based catalysts which are resistant to carbon deposition, and exhibit high activity for the reaction. Thus, basic supports (Ruckenstein and Hu, 1995; Chang *et al.*, 1996; Wang *et al.* 2001; Zhang and Verykios 1996), highly dispersed Ni catalysts (Hwang *et al.*, 2001; Tomiya *et al.* 2003) and/or promoters (Tomishige *et al.*, 1998; Lemonidou *et al.* 1998) have been used to lower the rate of coke deposition. The use of metals with catalytic properties for the carbon gasification reaction as promoters for Ni is another promising alternative.

In Ni-based catalysts, CeO₂ has been used as either an effective promoter or support because of its characteristic oxygen storage capacity (OSC), which allows it to store and release oxygen, leading to the presence of highly active oxygen. This makes the catalysts more active in many carbon formation-related reactions of hydrocarbons, such as steam reforming, dry reforming and oxidation. Recently, it has been reported that Ce_{1-x}Zr_xO₂ mixed oxides exhibited a superior resistance to carbon formation on the partial oxidation and steam reforming of hydrocarbons (Pengpanich *et al.* 2004; Thammachart *et al.* 2001; Bampenrat *et al.*, 2010), due to the high oxygen vacancy and oxygen mobility. But, the side reactions such as methanation of carbon oxides may lead to methane formation cause decrease conversion and hydrogen selectivity. This can overcome by the addition of alkali metal over Ni/Al₂O₃ catalyst (Hu *et al.*, 2009). It was reported that the addition K (8 wt%) could remarkably suppress methane production and improve Ni catalyst activity and stability (Hu *et al.*, 2009). Thus, the aim of the present work was to investigate the effect of K on the catalytic steam reforming of ethanol over Ni catalyst on a redox support such Ce/Zr.

5.3 Experimental

5.3.1 Catalyst Preparation and Characterization

$Ce_{0.75}Zr_{0.25}O_2$ was prepared via urea hydrolysis. Cerium nitrate ($Ce(NO_3)_3 \cdot 6H_2O$ (99.0%), Fluka), and zirconium oxychloride ($ZrOCl_2 \cdot 8H_2O$ (99.0%), Fluka) were used as sources of Ce and Zr, respectively. The starting solution was prepared by mixing 0.1 M of metal salt solutions with 0.4 M of urea solution at a 2 to 1 volumetric ratio. The ratio between ceria and zirconia salt was 3 to 1 volumetric ratio. The catalyst were prepared by a co-impregnation method using aqueous solutions of $Ni(NO_3)_2 \cdot 6H_2O$ and KNO_3 . The nominal loading amount of Ni was kept constant at 15 wt.% and the amount of K loadings was 8 wt.%. The catalysts were then calcined at 500 °C for 4 h in air.

Brunauer–Emmett–Teller (BET) surface areas were determined by N_2 adsorption at 77K (seven point BET method using a Quantachrome Corporation Autosorb). Prior to the analysis, the samples were outgassed to eliminate volatile adsorbents on the surface at 250 °C for 6 h.

A Rigagu X-ray diffractometer system equipped with a RINT 2000 wide-angle goniometer using $Cu K\alpha$ radiation and a power of 40 kV x 30 mA was used for examination of the crystalline structure. The intensity data were collected at 25°C over a 2θ range of 20-80° with a scan speed of 5° (2θ)/min and a scan step of 0.02° (2θ).

Temperature programmed reduction (TPR) measurements were carried out to investigate the redox properties over the resultant materials. About 0.1 g of catalyst was placed in a quartz tube and pretreated in a 30 ml/min He atmosphere at 150°C for 30 min prior to running the TPR experiment, and then cooled down to room temperature in He. The feed of 5% H_2 in N_2 at a flow rate of 30 ml/min was used as a reducing gas. The temperature of the sample was raised at a constant rate of 10°C/min. The amount of H_2 consumption during the increasing temperature period was determined by TCD.

The amount of deposited carbon on the spent catalysts was carried out using a TG7 Perkin-Elmer thermogravimetric analyzer. The standard involved the weight change of the sample (10 mg) during its heating in 150 ml.min⁻¹ of N_2 as purge gas and 50 ml.min⁻¹ of O_2 as reactive gas from room temperature to 900°C at a heating rate of 10°C.min⁻¹. The thermogravimetric and differential thermogravimetric

(TG-DTG) data were used to differential the oxidation behavior. The morphology of carbon deposition on the spent catalysts was observed by transmission electron microscopy (TEM) using a JEOL (JEM-2010F) transmission electron microscope operated at 200 kV. The sample was dispersed in absolute ethanol ultrasonically, and the solutions were then dropped on copper grids coated with a lacey carbon film.

5.3.2 Catalyst Activity Tests

To compare the catalytic activity and stability of the catalysts on the SRE, the reaction was carried out at temperature rang 500-650 °C with steam-to-carbon (S/C) ratios ranging from 1 to 6 and GHSV (20000-60000 h⁻¹). Typically, 0.1 g of catalyst was packed between the layers of quartz wool in a quartz tube microreactor (i.d. 10 mm) placed in an electric furnace equipped with K-type thermocouples. The temperature of catalyst bed was monitored and controlled using Shinko temperature controllers. A piston metering pump (Eldex) is used as feeding device which fed a liquid mixture consisting of a known composition of ethanol aqueous solution was introduced into an evaporator at ca. 150 °C to vaporize. The vaporized reaction mixture was then fed into the reactor using Ar as the carrier gas. Gaseous products were analyzed using on-line gas chromatographs with TCD detectors. Prior to running the reaction, the catalyst was reduced *in-situ* with a flow of 50% H₂ in N₂ gas at 600 °C for 2 h. The C-C breakage conversion of ethanol was defined as a molar ratio of the gaseous single carbon compounds (CH₄, CO and CO₂) in the product steam to the ethanol reactant and the product yield was defined as a molar ratio of the product to the theoretical amount of product produced from steam reforming of ethanol. The C-C breakage conversion, hydrogen yield and product selectivity reported in this work were calculated as follows:

$$\text{C-C breakage conversion (\%)} = \frac{[CO]_{out} + [CO_2]_{out} + [CH_4]_{out}}{2 \times [C_2H_6O]} \times 100 \quad (1)$$

$$\%Yield_{H_2} = \frac{[H_2]_{out}}{6 \times [C_2H_6O]} \times 100 \quad (2)$$

$$\%S_{CO} = \frac{[CO]_{out}}{[CO]_{out} + [CO_2]_{out} + [CH_4]_{out}} \times 100 \quad (3)$$

$$\%S_{CO_2} = \frac{[CO_2]_{out}}{[CO]_{out} + [CO_2]_{out} + [CH_4]_{out}} \times 100 \quad (4)$$

$$\%S_{CH_4} = \frac{[CH_4]_{out}}{[CO]_{out} + [CO_2]_{out} + [CH_4]_{out}} \times 100 \quad (5)$$

Where $[C_2H_6O]$ is the concentration of ethanol entering the reactor, and $[CO]_{out}$, $[CO_2]_{out}$, $[CH_4]_{out}$ and $[H_2]_{out}$ are the concentrations of carbon monoxide, carbon dioxide, methane, and hydrogen leaving the reactor, respectively. N₂ was particularly used as an internal standard for chromatographic analysis.

5.4 Results and Discussion

5.4.1 Catalyst Characterization

5.4.1.1 BET surface area, XRD and SEM analysis

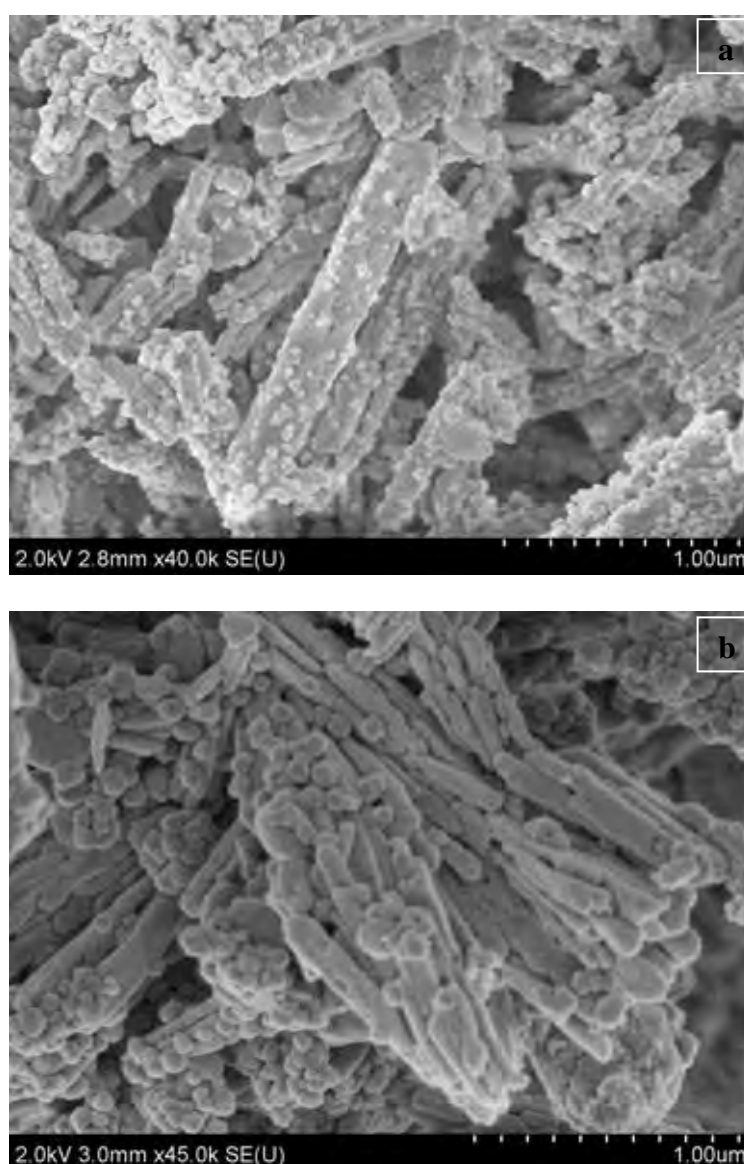
The results showed that the BET surface area of Ni/Ce_{0.75}Zr_{0.25}O₂ decreased drastically with the presence of K as reported in Table 5.1. This might be due to the blockage of mesopores by the presence K is confirmed by the SEM images as shown in Figure 5.1.

The X-ray diffraction patterns of Ni/Ce_{0.75}Zr_{0.25}O₂ and Ni-K/Ce_{0.75}Zr_{0.25}O₂ catalysts are presented in Figure 5.2 indicating typical peaks of CeO₂ cubic fluorite structure at about 29°, 33°, 47°, and 58° (2θ) with several small peaks characteristic of NiO rhombohedral phase observed at about 37.31°, 43.35°, 62.99 ° and 75.88° (2θ). The results are similar to those reported elsewhere (Pengpanich *et al.*, 2004; Bampenrat *et al.*, 2010). The addition of K over Ni/Ce_{0.75}Zr_{0.25}O₂ reveals typical peaks of K cubic structure at 23.59° and 41.48° (2θ) with the absence of K₂O peaks. However, the TPR results showed a reduction of K₂O at ca. 550 and 570 °C for Ni-K/Ce_{0.75}Zr_{0.25}O₂ and K/Ce_{0.75}Zr_{0.25}O₂, respectively. This suggests that K₂O might be well dispersed on Ce_{0.75}Zr_{0.25}O₂ and cannot be detected by XRD. It was also noticed that the presence of K alters the NiO phase from a rhombohedral to a cubic phase indicating by a shift in a diffraction pattern to a value of 37.09°, 43.08°, 62.59° and 75.25° (2θ).

Table 5.1 Textural properties of Ni/Ce_{0.75}Zr_{0.25}O₂ and Ni-K/Ce_{0.75}Zr_{0.25}O₂ catalysts

| Catalysts | Ni ^a particle size (nm) | K ^a particle size (nm) | BET surface area (m ² /g) |
|---|------------------------------------|-----------------------------------|--------------------------------------|
| Ni/Ce _{0.75} Zr _{0.25} O ₂ | 47.00 | - | 56.68 |
| Ni-K/Ce _{0.75} Zr _{0.25} O ₂ | 56.00 | 74.00 | 6.44 |

^a Determined by XRD

**Figure 5.1** SEM images of Ni/Ce_{0.75}Zr_{0.25}O₂ (a) and Ni-K/Ce_{0.75}Zr_{0.25}O₂ (b) catalysts.

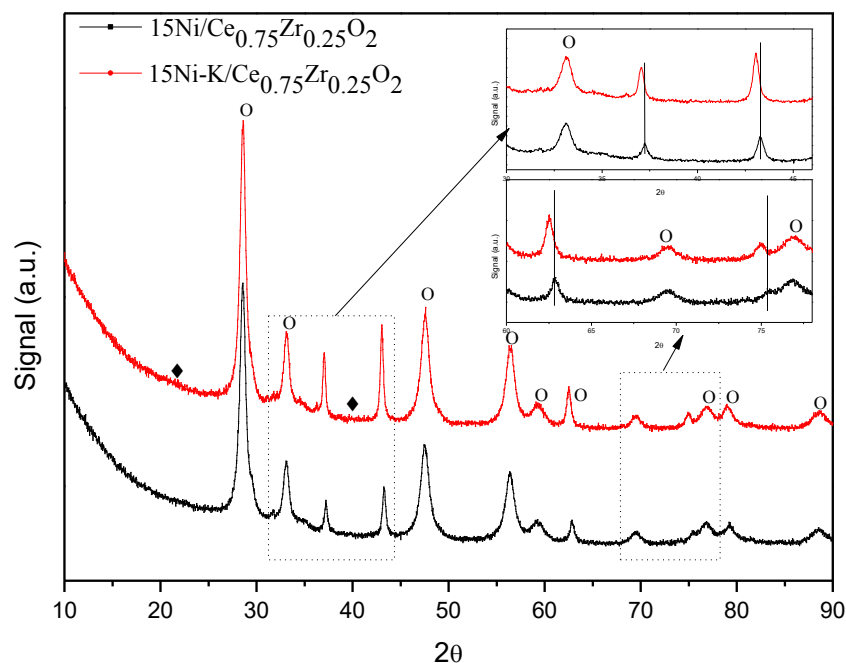


Figure 5.2 XRD patterns of Ni/Ce_{0.75}Zr_{0.25}O₂ and Ni-K/Ce_{0.75}Zr_{0.25}O₂ catalysts.

5.4.1.2 H₂-Temperature Programmed Reduction

Figure 5.3 shows the H₂-TPR profiles of the Ni/Ce_{0.75}Zr_{0.25}O₂ and Ni-K/Ce_{0.75}Zr_{0.25}O₂ catalysts. The results showed that Ni/Ce_{0.75}Zr_{0.25}O₂ exhibits three distinct H₂ consumption peaks that show maxima at 262 °C, 354 °C and 810 °C. The first two peaks at 262 and 354 °C indicate the reduction of NiO to Ni⁰ whereas the others are assigned to the reduction of support (Roh *et al.*, 2002). Typically, for supported Ni catalysts, the lower temperature peak (262 °C) is attributed to the reduction of the relatively free NiO particles while the higher temperature one (354 °C) is attributed to the reduction of complex NiO species in intimate contact with the oxide support (Montoya *et al.* 2000; Pengpanich *et al.*, 2004; Roh *et al.*, 2002). The addition of K over Ni/Ce_{0.75}Zr_{0.25}O₂ catalyst was found to increase the reducibility of NiO. The reduction peak at 354 °C was shifted to 426 °C with the disappearance of the peak at 262 °C indicating that the strong interaction between nickel and potassium.

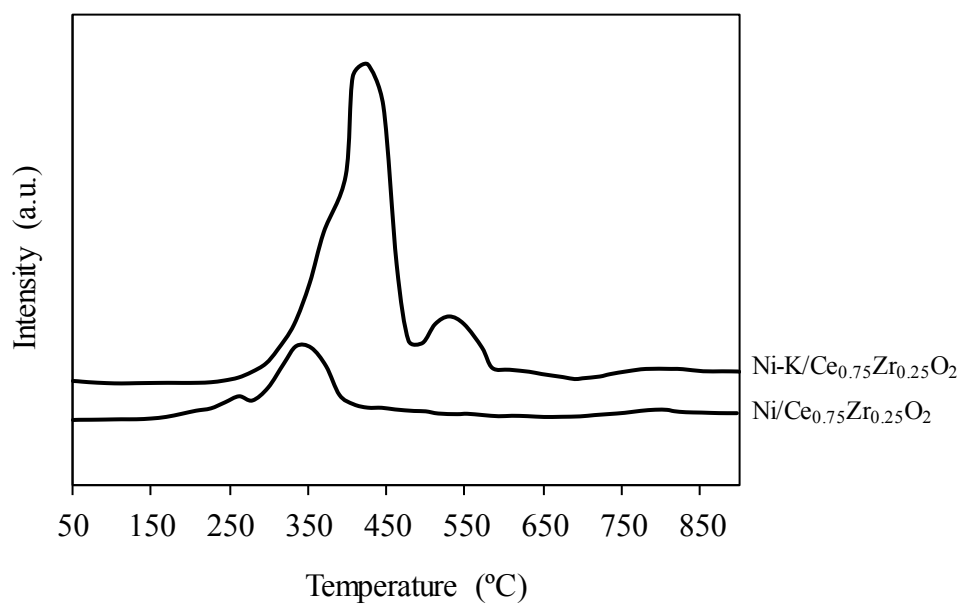


Figure 5.3 TPR profiles of the Ni/Ce_{0.75}Zr_{0.25}O₂ and Ni-K/Ce_{0.75}Zr_{0.25}O₂ catalysts. The reducing gas contains 5% H₂ in N₂ with a flow rate of 30 ml/min and a heating rate of 10°C/min.

5.4.2 Catalytic Activities and Stability for Steam reforming of Ethanol

The typical products for ethanol steam reforming detected in this study are H₂, CO₂, CO and CH₄ with the absence of other hydrocarbons as shown in Table 5.2. It was suggested that the steam reforming of ethanol occurs through the dehydrogenation of ethanol to acetaldehyde route following with the decomposition of acetaldehyde to methane and carbon monoxide or ethanol dehydration route (Chica and Sayas 2009; Fatsikostal and Verykios 2004). Hydrogen and carbon dioxide are the products for methane steam reforming and a water-gas-shift reaction. The results showed that at low temperature (500°C), the catalytic activity and stability of Ni-K/Ce_{0.75}Zr_{0.25}O₂ is obviously higher than that of Ni/Ce_{0.75}Zr_{0.25}O₂. This suggested that the presence of K species interact with nickel by forming a partial coverage and/or modify the structure of Ni particle as indicated by XRD, to form highly active Ni sites (plane 1,1,1) which are more favor for C-C breakage (Hu *et al.*, 2009; Nandinik *et al.*, 2005). The presence of the alkaline metal was also found to suppress the reaction pathway for methane formation (Hu *et al.*, 2009), indicating by low methane selectivity at low temperature for Ni-K/Ce_{0.75}Zr_{0.25}O₂. At higher temperatures, the catalyst activity and stability of both catalysts are rather similar. It was reported (Horiuchi *et al.*, 1996; Nandinik *et al.*, 2005) that the surface of the Ni catalyst with basic metal oxides was favor for CO₂ adsorption while the surface without them was rich in adsorbed CH₄. This creates an unfavorable condition for methane activation and, as a result, carbon deposition was suppressed during the reforming reaction on Ni-K/Ce_{0.75}Zr_{0.25}O₂, which is also indicated by lower H₂ yield and selectivity.

It is also found that by increasing GHSV from 20 000 to 60 000 h⁻¹, the catalytic activity of Ni/Ce_{0.75}Zr_{0.25}O₂ is drastically decreased while Ni-K/Ce_{0.75}Zr_{0.25}O₂ is slightly decreased with increasing GHSV as show in Figure 5.4. This suggests that Ni with present of potassium catalyst is more active than the other.

Table 5.2 C-C breakage conversion (%), products distribution (%), temperature and time on stream for the steam reforming of ethanol over the Ni/Ce_{0.75}Zr_{0.25}O₂ and Ni-K/Ce_{0.75}Zr_{0.25}O₂, steam-to-carbon ratio = 6, GHSV = 20 000 h⁻¹

| Catalysts | T _R (°C) | t (min) | C-C breakage conversion(%) | (% Yield) _{H₂} | Selectivity (%) | | | |
|---|------------------------|------------|-------------------------------|------------------------------------|-----------------|------|-----------------|-----------------|
| | | | | | H ₂ | CO | CO ₂ | CH ₄ |
| Ni/Ce _{0.75} Zr _{0.25} O ₂ | 500 | 40 | 51.9 | 29.1 | 71.1 | 2.8 | 62.9 | 34.2 |
| | | 200 | 22.5 | 9.3 | 65.5 | 7.9 | 59.5 | 32.6 |
| | | 360 | 10.4 | 2.6 | 49.4 | 8.3 | 53.8 | 37.8 |
| | 550 | 40 | 96.4 | 71.4 | 89.0 | 11.7 | 74.5 | 13.8 |
| | | 200 | 97.1 | 72.3 | 89.1 | 12.0 | 74.3 | 13.7 |
| | | 360 | 97.0 | 71.7 | 88.7 | 12.2 | 73.7 | 14.1 |
| | 600 | 40 | 96.9 | 79.1 | 96.9 | 14.4 | 81.6 | 4.0 |
| | | 200 | 97.0 | 79.3 | 96.9 | 14.4 | 81.7 | 3.9 |
| | | 360 | 95.7 | 79.6 | 96.9 | 14.3 | 81.7 | 4.0 |
| | 650 | 40 | 97.0 | 83.6 | 99.2 | 13.7 | 85.2 | 1.1 |
| | | 200 | 96.4 | 84.0 | 99.1 | 13.7 | 85.1 | 1.2 |
| | | 360 | 97.1 | 84.6 | 99.1 | 13.8 | 85.1 | 1.2 |
| Ni-K/Ce _{0.75} Zr _{0.25} O ₂ | 500 | 40 | 62.7 | 37.7 | 76.8 | 12.7 | 59.9 | 27.3 |
| | | 200 | 38.0 | 18.9 | 70.4 | 9.6 | 58.9 | 31.4 |
| | | 360 | 23.9 | 10.3 | 66.1 | 9.7 | 57.1 | 33.2 |
| | 550 | 40 | 96.4 | 75.3 | 91.5 | 8.4 | 80.6 | 10.9 |
| | | 200 | 97.0 | 75.3 | 91.4 | 8.3 | 80.7 | 11.0 |
| | | 360 | 96.8 | 74.5 | 91.4 | 8.3 | 80.8 | 10.8 |
| | 600 | 40 | 96.8 | 75.8 | 93.3 | 9.3 | 82.2 | 8.5 |
| | | 200 | 96.9 | 75.2 | 93.0 | 9.1 | 82.2 | 8.7 |
| | | 360 | 96.2 | 75.7 | 93.3 | 9.5 | 82.0 | 8.5 |
| | 650 | 40 | 96.3 | 77.2 | 94.8 | 8.7 | 84.7 | 6.6 |
| | | 200 | 96.5 | 77.9 | 94.9 | 8.5 | 85.0 | 6.5 |
| | | 360 | 96.6 | 77.5 | 94.6 | 8.6 | 84.6 | 6.8 |

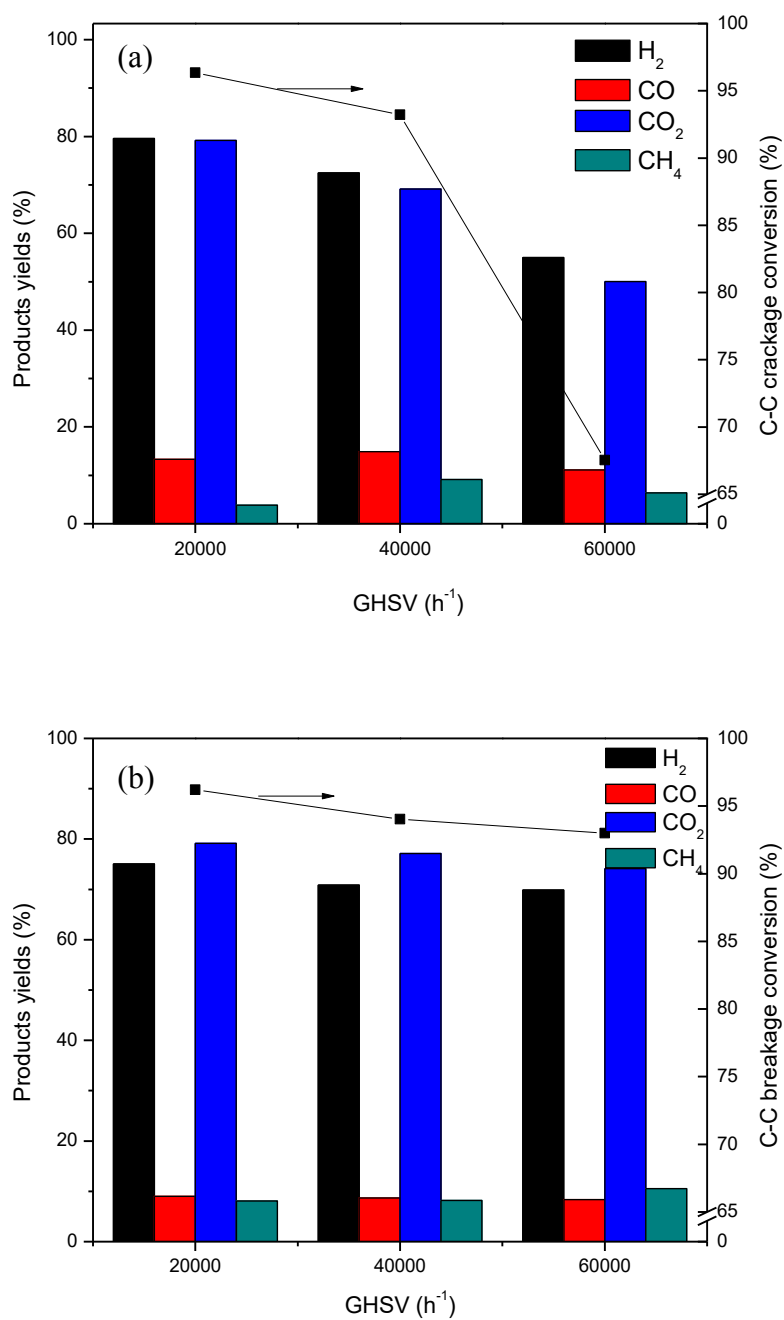


Figure 5.4 C-C breakage conversion (%) and products distribution (%) vs. GHSV for the steam reforming of ethanol over (a) Ni/Ce_{0.75}Zr_{0.25}O₂ and (b) Ni-K/Ce_{0.75}Zr_{0.25}O₂ catalysts; steam-to-carbon ratio = 6, temperature = 600°C.

5.4.3 Effect of Steam-to-Carbon Ratio

The effect of the steam to carbon ratio (s/c) on the catalytic activity of Ni/Ce_{0.75}Zr_{0.25}O₂ and Ni-K/Ce_{0.75}Zr_{0.25}O₂ catalysts was investigated by varying the s/c ratios from 1 to 6 at 600 °C. As show in Figure 5.5, it was found that the C-C breakage conversion increases with increasing s/c ratio, in parallel with hydrogen and carbon dioxide yields indicating that the steam reforming of ethanol reaction is shifted to the right due to the H₂O surplus. Carbon monoxide and methane are not favored by the high steam content in the feed (Sahoo *et al.*, 2007). Especially for methane, the s/c ratio necessary to achieve negligible concentration to the product mixture is about 6. The effect of potassium is more pronounce at lower s/c ratios (1 to 3). It was found that C-C breakage conversion of the potassium-containing catalyst is higher due to highly active Ni sites as above mentioned. The results showed that the ethanol steam reforming over Ni/Ce_{0.75}Zr_{0.25}O₂ and Ni-K/Ce_{0.75}Zr_{0.25}O₂ catalysts might favor ethanol dehydrogenation route at low s/c ratio (1) as indicated by no C₂H₄, which produced from ethanol dehydration route, detected in the product streams. It was also found that CH₄ yield of Ni-K/Ce_{0.75}Zr_{0.25}O₂ is higher than Ni/Ce_{0.75}Zr_{0.25}O₂ due to less adsorb CH₄ over Ni-K which mention above.

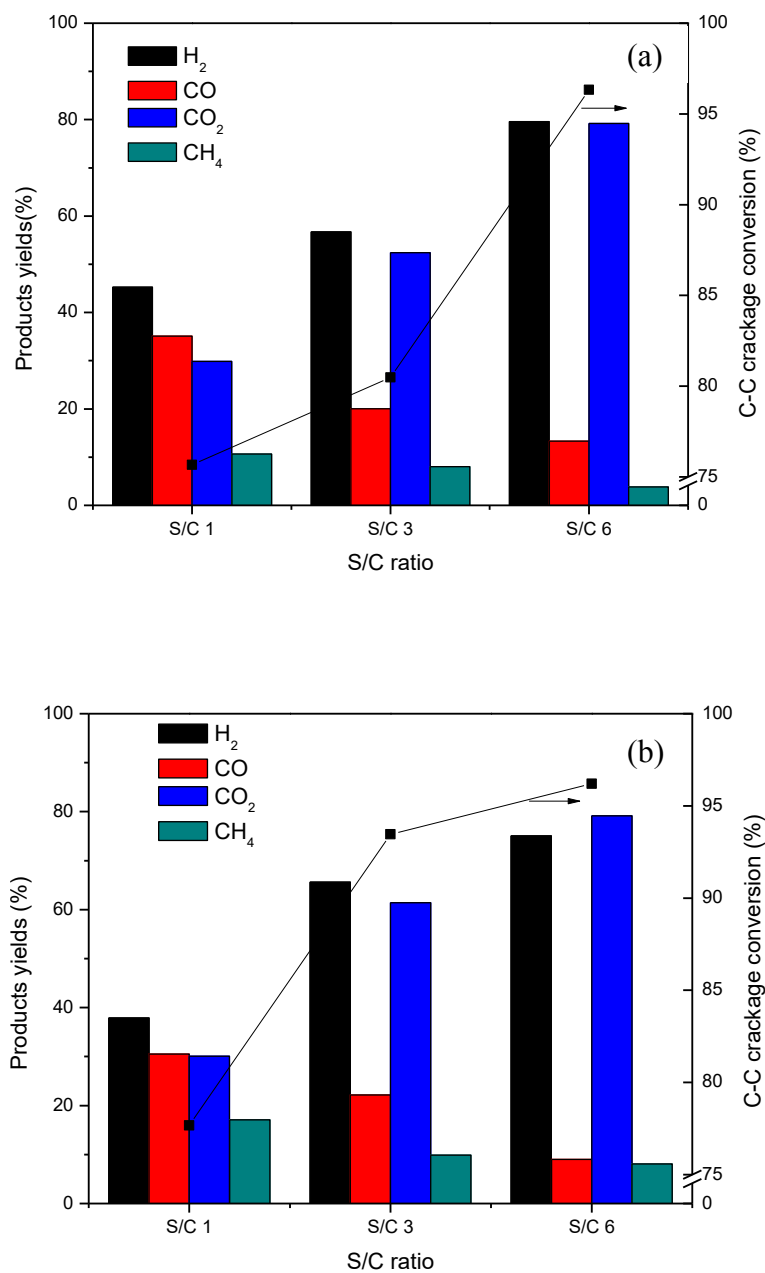


Figure 5.5 C-C breakage conversion (%) and products distribution (%) vs. steam-to-carbon ratio (S/C) for the steam reforming of ethanol over (a) Ni/Ce_{0.75}Zr_{0.25}O₂ and (b) Ni-K/Ce_{0.75}Zr_{0.25}O₂; GHSV = 20 000, temperature = 600°C.

5.4.4 Carbon Deposition

Figure 5.6 shows the amount of carbon deposited (%) for the spent Ni/Ce_{0.75}Zr_{0.25}O₂ and Ni-K/Ce_{0.75}Zr_{0.25}O₂ catalysts after 6 h of reaction at 550°C are 43%.% and 34wt.%, respectively. This indicated that the carbon deposition is strongly inhibited in the presence of K. TEM images (Figure 5.7) reveal that carbon deposited on the potassium containing catalyst is mainly amorphous while that of Ni/Ce_{0.75}Zr_{0.25}O₂ contains both amorphous and filament. This might be due to the fact that the presence of K species makes Ni active sites less favor for methane activation resulting in the suppression of carbon deposition or potassium can work as a catalyst for the coke gasification (Hu *et al.*, 2009; Nandinik *et al.*, 2005).

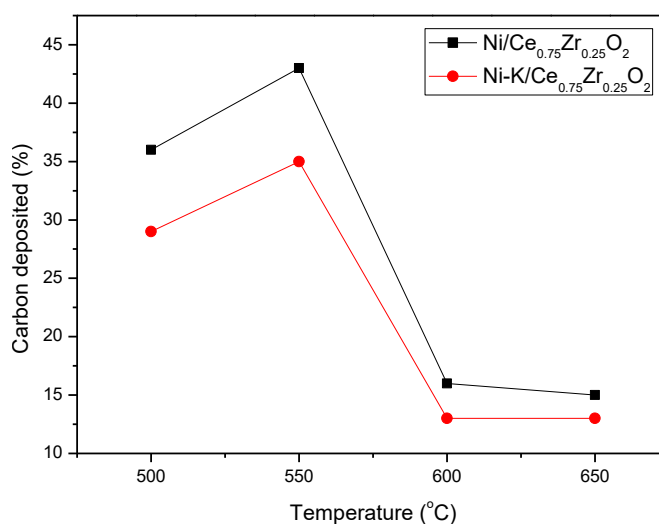


Figure 5.6 Carbon deposited (%) vs. temperature for the steam reforming of ethanol over the Ni/Ce_{0.75}Zr_{0.25}O₂ and Ni-K/Ce_{0.75}Zr_{0.25}O₂ steam-to-carbon ratio = 3, GHSV = 20000 h⁻¹.

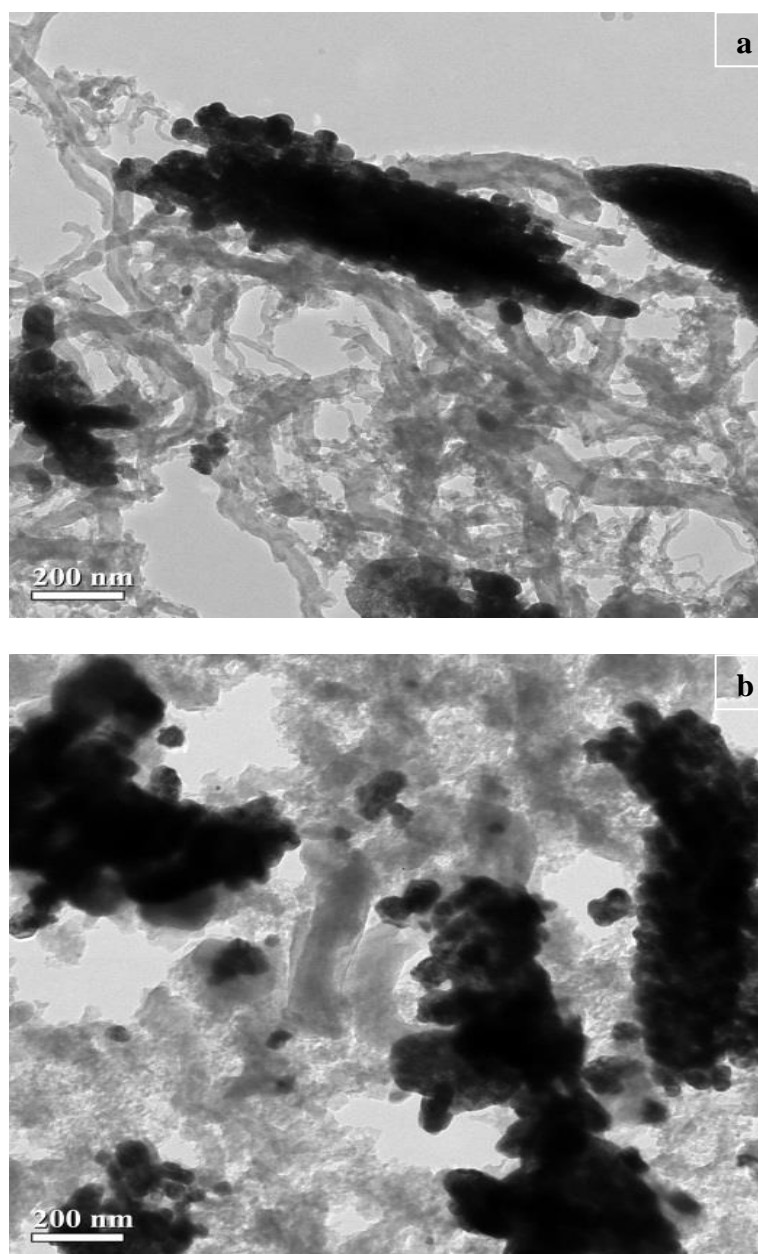


Figure 5.7 TEM images of (a) Ni/Ce_{0.75}Zr_{0.25}O₂ and (b) Ni-K/Ce_{0.75}Zr_{0.25}O₂ catalysts after steam reforming of ethanol steam-to-carbon ratio = 3, GHSV = 20000 h⁻¹ for 6 h.

5.5 Conclusions

The Ni-K/Ce_{0.75}Zr_{0.25}O₂ catalyst exhibit high activities and stabilities for steam reforming of ethanol. The potassium promoted over Ni/Ce_{0.75}Zr_{0.25}O₂ catalyst is able to modify NiO phase from a rhombohedral to a cubic phase which is more favor for C-C breakage or interact with nickel, resulting in the improvement of catalytic properties of the Ni/ Ce_{0.75}Zr_{0.25}O₂ catalyst. Furthermore, the presence of K species makes Ni active sites less favor for methane activation resulting in the suppression of carbon deposition or potassium can work as a catalyst for the coke gasification.

5.6 Acknowledgements

This work was supported by the Thailand Research Fund (under Waste-to-Energy project and Royal Golden Jubilee Ph.D. Program: Grant 0170/46), National Metal and Materials Technology Center (Project No. MT-B-50-END-74-038-G), and the Sustainable Petroleum and Petrochemicals Research Unit under the National Center of Excellence for Petroleum, Petrochemicals, and Advanced Materials, Chulalongkorn University.

5.7 References

- Bampenrat, A., Meeyoo, V., Kitiyanan, B., Rangsunvigit, P., Rirksomboon, T. (2010) Naphthalene steam reforming over Mn-doped CeO₂-ZrO₂supported nickel catalysts. Applied Catalysis A: General, 373, 154-159.
- Breen, J.P., Burch, R., Coleman, H.M. (2002) Metal-catalysed steam reforming of ethanol in the production of hydrogen for fuel cell applications. Applied Catalysis B: Environmental, 39, 65-74.

- Cavallaro, S., Chiodo, V., Freni, S., Mondello, N., Frusteri, F. (2003) Performance of Rh/Al₂O₃ catalyst in the steam reforming of ethanol: H₂ production for MCFC. Applied Catalysis A: General, 249, 119–128.
- Chang, J.S., Park, S.E., Chon, H. (1996) Catalytic activity and coke resistance in the carbon dioxide reforming of methane to synthesis gas over zeolite-supported Ni catalysts. Applied Catalysis A: General, 145, 111-124.
- Chica, A., Sayas, S. (2009) Effective and stable bioethanol steam reforming catalyst based on Ni and Co supported on all-silica delaminated ITQ-2 zeolite. Catalysis Today, 146, 37-43.
- Diagne, D., Idriss, H., Kiennemann, A. (2002) Hydrogen production by ethanol reforming over Rh/CeO₂–ZrO₂ catalysts. Catalysis Communications, 3, 565–571.
- Fatsikostas, N.A., Verykios, X.E. (2004) Reaction network of steam reforming of ethanol over Ni-based catalysts. Journal of Catalysis, 225, 439–452.
- Haryanto, A., Fernando, S., Murali, N., Adhikari, S. (2005) Current Status of Hydrogen Production Techniques by Steam Reforming of Ethanol: A Review. Energy Fuels, 19, 2098–2106.
- Horiuchi, T., SaKuma, K., Fukui, K., Kubo, Y., Osaki, T., Mori, T. (1996) Suppression of carbon deposition in the CO₂-reforming of CH₄ by adding basic metal oxides to a Ni/Al₂O₃ catalyst. Applied Catalysis A: General, 144, 111-120.
- Hu, X., Lu, G. (2009) Inhibition of methane formation in steam reforming reactions through modification of Ni catalyst and the reactants. Green Chemistry, 11, 724-732.
- Hwang, K.S., Zhu, H.Y., Lu, G.Q. (2001) New nickel catalysts supported on highly porous alumina intercalated laponite for methane reforming with CO₂. Catalysis Today, 68, 183-190.
- Kugai, J., Velu, S., Song, C.S. (2005) Low-temperature reforming of ethanol over CeO₂-supported Ni-Rh bimetallic catalysts for hydrogen production. Catalysis Letter, 101, 255–264.
- Kugai, J., Velu, S., Song, C.S., Engelhard, M.H., Chin, Y.H. (2006) Effects of nanocrystalline CeO₂ supports on the properties and performance of Ni–Rh

- bimetallic catalyst for oxidative steam reforming of ethanol. Journal of Catalysis, 238, 430–440.
- Lemonidou, A.A., Goula, M.A., Vasalos, I.A. (1998) Carbon dioxide reforming of methane over 5 wt.% nickel calcium aluminate catalysts – effect of preparation method. Catalysis Today, 46, 175-183.
- Liguras, D.K., Kondarides, D.I., Verykios, X.E. (2003) Production of hydrogen for fuel cells by steam reforming of ethanol over supported noble metal catalysts. Applied Catalysis B: Environmental, 43, 345–354.
- Montoya, J.A., Romero-Pascual, E., Gimón, C., Del Angle, P., Monzon, A. (2000) Methane reforming with CO₂ over Ni/ZrO₂–CeO₂ catalysts prepared by sol–gel. Catalysis Today, 63, 71-85.
- Nandini, A., Pant, K.K., Dhingra, S.C. (2005) K-, CeO₂-, and Mn-promoted Ni/Al₂O₃ catalysts for stable CO₂ reforming of methane. Applied Catalysis A: General, 290, 166-174.
- Navarro, R.M., Alvarez-Galvan, M.C.A., Sanchez-Sanchez, M.C., Rosa, F., Fierro, J.L.G. (2005) Production of hydrogen by oxidative reforming of ethanol over Pt catalysts supported on Al₂O₃ modified with Ce and La. Applied Catalysis B: Environmental, 55, 229–241.
- Peña, M.A., Gómez, J.L.G., Fierro, J.L.G. (1996) New catalytic routes for syngas and hydrogen production. Applied Catalysis A: General, 144, 7-57.
- Pengpanich, S., Meeyoo, V., Rirksomboon, T. (2004) Methane partial oxidation over Ni/CeO₂–ZrO₂ mixed oxide solid solution catalysts. Catalysis Today, 93-95, 95-105.
- Roh, H., Jun, K., Dong, W., Chang, J., Park, S., Joe, Y. (2002) Highly active and stable Ni/Ce–ZrO₂ catalyst for H₂ production from methane. Journal of Molecular Catalysis A: Chemical, 181, 137-142.
- Ruckenstein, E., Hu, Y.H. (1995) Carbon dioxide reforming of methane over nickel/alkaline earth metal oxide catalysts. Applied Catalysis A: General, 133, 149-161.
- Sahoo, D.R., Vajpai, S., Patel, S., Pant, K.K. (2007) Kinetic modeling of steam reforming of ethanol for the production of hydrogen over Co/Al₂O₃ catalyst. Chemical Engineering Journal, 125, 139-147.

- Saxena, R.C., Adhikari, D.K., Goyal, H.B. (2009) Biomass-based energy fuel through biochemical routes: A review. Renewable and Sustainable Energy Reviews, 13, 167-178.
- Thammachart, M., Meeyoo, V., Risksomboon, T., Osuwan, S. (2001) Catalytic activity of CeO₂-ZrO₂ mixed oxide catalysts prepared via sol-gel technique: CO oxidation. Catalysis Today, 68, 53-61.
- Tomishige, K., Yamazaki, O., Chen, Y.G., Yokoyama, K., Li, X., Fujimoto, K. (1998) Development of ultra-stable Ni catalysts for CO₂ reforming of methane. Catalysis Today, 45, 35-39.
- Tomiyama, S., Takahashi, R., Sato, S., Sodesawa, T., Yoshida, S. (2003) Preparation of Ni/SiO₂ catalyst with high thermal stability for CO₂-reforming of CH₄. Applied Catalysis A: General, 241, 349-361.
- Wang, J.B., Tai, Y.L., Dow, W.P., Huang, T.J. (2001) Study of ceria-supported nickel catalyst and effect of yttria doping on carbon dioxide reforming of methane. Applied Catalysis A: General, 218, 69-79.
- Zhang, Z., Verykios, X.E. (1996) Carbon dioxide reforming of methane to synthesis gas over Ni/La₂O₃ catalysts. Applied Catalysis A: General, 138, 109-133.

CHAPTER VI

CATALYTIC STEAM REFORMING OF ACETONE OVER $\text{Co/Ce}_{1-x}\text{Zr}_x\text{O}_2$ CATALYSTS

6.1 Abstract

In this study, the catalytic steam reforming of acetone was carried out over $\text{Co/Ce}_{1-x}\text{Zr}_x\text{O}_2$ ($x = 0, 0.25, 0.5, 0.75$ and 1) catalysts. It was found that the catalytic activity was significantly dependent on the reducibility and the metal dispersion. The $\text{Co/Ce}_{0.75}\text{Zr}_{0.25}\text{O}_2$ catalyst exhibited the highest catalytic performance in terms of hydrogen yield. The results showed that with $\text{Co/Ce}_{1-x}\text{Zr}_x\text{O}_2$ ($x \leq 0.5$), the catalytic steam reforming of acetone occur simultaneously on both supports and metal phases. Roles of the supports are to promote the water gas shift reaction and prohibit the metal sintering with subjected to the amount of Zr in the Ce-Zr mixed oxides. The amount of carbon deposited on the catalysts is not related to the reducibility of the support, and hence, the deactivation is found to be from the aggregation of metals.

6.2 Introduction

In recent years, there are many researches in new sources of energy, especially clean energy. Biomass has been proposed as an alternative feedstock for hydrogen production not only because it is renewable but also because it is a CO_2 neutral energy supply. Biomass converts to bio-oil by fast pyrolysis and then the bio-oil converts to hydrogen (H_2) by catalytic steam reforming (Czernik *et al.* 2007; Takanabe *et al.* 2006; Zhang *et al.* 2005). Bio-oil is a mixture of oxygenated compounds including acids, alcohols, ketones, esters, ethers, aldehydes, phenols, and derivatives, as well as carbohydrates, and a large proportion (20–30 wt.%) of lignin-derived oligomers (Oasmaa *et al.* 2002). By the addition of water, bio-oil can be separated into a hydrophobic-lignin derived fraction and an aqueous fraction (50 wt.% of the bio-oil) containing mostly carbohydrate-derived monomeric compounds (Piskorz *et al.* 1988). Steam reforming of the single compound such as acetic acid in the aqueous fraction of bio-oil has been the subject of many research efforts (Birot *et*

al. 2008; Sun *et al.* 2008). Acetone (C_3H_6O) is the model compound selected as a representative of the ketones present in bio-oil at appreciable amounts up to 2.8% (Diebold 1999). Therefore, steam reforming of acetone has been investigated as a model reaction in order to understand the requirements for the design efficient catalysts for the steam reforming of bio-oil. Up to now, very limited reports (Rioche *et al.* 2005; Hu and Lu 2009; Vagia and Lemonidou 2008) in producing hydrogen from acetone have been published, and only few catalysts have been investigated, for example, Rh/Al₂O₃, Pd/CeZrO₂ and cordierite catalysts.

The number of studies in the literature on steam reforming of oxygenated hydrocarbon catalysts has significantly increased in recent years. Catalysts utilized are mainly Ni, Cu, Co and noble metals, such as Rh, Ru, Re, Pd and Pt (Breen *et al.* 2002; Liguras *et al.* 2003). Although, supported noble metal catalysts have shown to have a good performance but the high cost and limited reserves are also causes for concerns. As a less expensive alternative, cobalt-based catalysts have been reported to have superior hydrocarbon steam reforming performance due to their high activity for C-C bond cleavage (Mielenz 2001; Llorca *et al.* 2002, 2003). Various metal oxides such as TiO₂, V₂O₅, ZnO, La₂O₃ and CeO₂ have been used to support Co in order to provide large surface area as well as good thermal stability, leading to high cobalt dispersion even at high temperatures (Llorca *et al.* 2002). CeO_x-ZrO_x mixed oxides exhibited a superior resistance to carbon formation due to high oxygen vacancy and oxygen mobility (Bampenrat *et al.* 2010; Pengpanich *et al.* 2004). Yet, the redox supports such as Ce_{1-x}Zr_xO₂ mixed oxides, which reported a good carbon resistant, were rarely used with cobalt for steam reforming reaction. It was reported that Ce_{1-x}Zr_xO₂ supporting Ni showed a superior resistant to coke formation during steam reforming of acetic acid, naphthalene and methane partial oxidation (Bampenrat *et al.* 2010; Pengpanich *et al.* 2004; Thaicharoensutcharittham *et al.* 2011). Here, this leads us to investigate of the effect of Ce_{1-x}Zr_xO₂ supports and the catalytic activity of Co for steam reforming of acetone.

6.3 Experimental

6.3.1 Catalyst Preparation

$Ce_{1-x}Zr_xO_2$ mixed oxides were prepared via urea hydrolysis. Cerium nitrate ($Ce(NO_3)_3 \cdot 6H_2O$ (99.0%), Fluka), and zirconium oxychloride ($ZrOCl_2 \cdot 8H_2O$ (99.0%), Fluka) were used as sources of Ce and Zr, respectively. The starting solution was prepared by mixing 0.1 M of metal salt solutions with 0.4 M of urea solution at a 2 to 1 volumetric ratio. The ratio between each metal salt was altered depending on desired solid solution concentration: $Ce_{1-x}Zr_xO_2$, where $x = 0, 0.25, 0.5, 0.75$ and 1.0 . The synthesis procedure has been reported elsewhere (Pengpanich *et al.* 2004).

Co was loaded onto the support via wetness impregnation method using cobalt nitrate solution. The nominal loading amount of Co was kept constant at 15 wt.%. The catalysts were then calcined at 400°C for 4 h in air.

6.3.2 Catalyst Characterization

Brunauer–Emmett–Teller (BET) surface areas were determined by N_2 adsorption at 77K (seven point BET method using a Quantachrome Corporation Autosorb). Prior to the analysis, the samples were outgassed to eliminate volatile adsorbents on the surface at 250°C for 6 h.

A Rigagu X-ray diffractometer system equipped with a RINT 2000 wide-angle goniometer using $Cu K\alpha$ radiation and a power of 40 kV x 30 mA was used for examination of the crystalline structure. The intensity data were collected at 25°C over a 2θ range of 20-80° with a scan speed of 5° (2θ)/min and a scan step of 0.02° (2θ).

Temperature programmed reduction (TPR) measurements were carried out to investigate the redox properties over the resultant materials. About 0.1 g of catalyst was placed in a quartz tube and pretreated in a 30 ml/min He atmosphere at 150°C for 30 min prior to running the TPR experiment, and then cooled down to room temperature in He. The feed of 5% H_2 in N_2 at a flow rate of 30 ml/min was used as a reducing gas. The temperature of the sample was raised at a constant rate of 10°C/min. The amount of H_2 consumption during the increasing temperature period was determined by TCD

The dispersion degree of cobalt was measured by H_2 -pulse chemisorption at 50°C using an Ar flow of 50 ml min^{-1} and individual pulses of 0.1

ml (10% H₂ in Ar). For measurements, about 100 mg of sample was placed in a quartz reactor. Prior to the pulse chemisorption, the sample was reduced at 500°C under H₂ atmosphere for 1 h. Then the sample was purged with Ar at 500°C for 30 min and cooled to 50°C in flowing Ar. The H₂ pulses were continued with an injection interval of 6–8 min until the areas of successive hydrogen peaks were identical. The cobalt dispersion was calculated assuming the adsorption stoichiometry of one hydrogen atom per cobalt surface atom.

The amount of deposited carbon on the spent catalysts was quantitatively determined by temperature-programmed oxidation (TPO) technique, which was carried out in a TPO reactor analyzer coupled with an FID, was used to quantify the amount of coke formation in the spent catalysts. Typically, about 40 mg of sample was heated at a constant rate of 10°C/min from room temperature to 800°C using 2% O₂ in He as an oxidizing gas at a flow rate of 40 ml/min. The output gas was passed to a methanizer packed with 15% Ni/Al₂O₃ as a catalyst prior to the FID detector. After the temperature reached 800°C, 100 µl of CO₂ pulses was injected in order to evaluate the quantity of coke formed.

6.3.3 Catalytic Activity Tests

To compare the catalytic activity and stability of the catalysts on the steam reforming of acetone, the reaction was carried out at temperature rang 550-700°C with steam-to-carbon (S/C) ratios 6 and LHSV of 15.3 h⁻¹. Typically, ca. 0.1 g of catalyst was packed between the layers of quartz wool in a quartz tube microreactor (i.d. 6 mm) placed in an electric furnace equipped with K-type thermocouples. The temperature of catalyst bed was monitored and controlled using Shinko temperature controllers. A liquid mixture feed consisting of a known composition of acetone aqueous solution was introduced into an evaporator at ca. 150°C to vaporize. The vaporized reaction mixture was then fed into the reactor using Ar as the carrier gas. Gaseous products were analyzed using on-line gas chromatographs in series equipped with FID and TCD detectors. Prior to running the reaction, the catalyst was reduced *in-situ* with a flow of 50% H₂ in N₂ gas at 600°C for 2 h. The conversion and product yield reported in this work were calculated as follows:

$$\text{Conversion (\%)} = \frac{\text{mol}_{\text{Acet one},in} - \text{mol}_{\text{Acet one},out}}{\text{mol}_{\text{Acet one},in}} \times 100 \quad (1)$$

$$\%Yield_{\text{H}_2} = \frac{\text{mol}_{\text{H}_2,out}}{8 \times \text{mol}_{\text{Acet one},in}} \times 100 \quad (2)$$

$$\%Yield_{\text{CO}} = \frac{\text{mol}_{\text{CO},out}}{3 \times \text{mol}_{\text{Acet one},in}} \times 100 \quad (3)$$

$$\%Yield_{\text{CO}_2} = \frac{\text{mol}_{\text{CO}_2,out}}{3 \times \text{mol}_{\text{Acet one},in}} \times 100 \quad (4)$$

$$\%Yield_{\text{CH}_4} = \frac{\text{mol}_{\text{CH}_4,out}}{3 \times \text{mol}_{\text{Acet one},in}} \times 100 \quad (5)$$

6.4 Results and Discussion

6.4.1 Catalyst Characterization

6.4.1.1 *BET surface area, metal dispersion, SEM and XRD analysis*

The BET surface areas and metal dispersion of the catalysts are shown in Table 6.1. The surface areas of Co/Ce_{1-x}Zr_xO₂ ($x = 0, 0.25, 0.5, 0.75$ and 1) catalysts are in the range of 49-65 m²/g, where the Co/ZrO₂ exhibits the lowest. This might be due to a low metal-interaction between cobalt and zirconia resulting the sintering of cobalt, and zirconia itself, possesses a low surface area (Fornasiero *et al.* 1996). The degree of metal dispersion was found in the following decreasing order: Co/Ce_{0.75}Zr_{0.25}O₂ > Co/CeO₂ > Co/Ce_{0.50}Zr_{0.50}O₂ > Co/Ce_{0.25}Zr_{0.75}O₂ > Co/ZrO₂ as depicted in Table 6.1, indicating that Co particles are better dispersed on CeO₂ than ZrO₂. As shown in Fig. 6.1 small particles of Co₃O₄ well disperse on CeO₂, resulting from a strong metal-integration of Co₃O₄ with CeO₂ bulk phase, While Co₃O₄ sintered to form large particles on ZrO₂ surface.

Table 6.1 BET surface areas and metal dispersion of the catalysts

| Catalysts | BET surface area (m ² /g) | Metal dispersion (%) |
|---|--------------------------------------|----------------------|
| Co/CeO ₂ | 58.52 | 1.98 |
| Co/Ce _{0.75} Zr _{0.25} O ₂ | 62.65 | 2.13 |
| Co/Ce _{0.50} Zr _{0.50} O ₂ | 63.14 | 0.69 |
| Co/Ce _{0.25} Zr _{0.75} O ₂ | 64.70 | 0.60 |
| Co/ZrO ₂ | 49.65 | 0.58 |

The X-ray diffraction (XRD) patterns of Ce_{1-x}Zr_xO₂ mixed oxides impregnated with 15% Co (Co/Ce_{1-x}Zr_xO₂) are presented in Fig. 6.2, showing typical peaks of CeO₂ cubic fluorite structure at about 29°, 33°, 47°, and 58° (2θ), similar to what reported elsewhere (Thammachart *et al.* 2001). The presence of only the cubic phase in the samples (Ce_{1-x}Zr_xO₂, where $x < 0.5$) indicates that Ce and Zr are highly homogeneously distributed. Conversely, the evidence of a tetragonal phase was found when x is higher than 0.5 and the presence of a monoclinic phase is also observed at a higher ZrO₂ content. Several small peaks characteristic of Co₃O₄ are observed at about 36°, 44° and 65° (2θ), corresponding to the (3 1 1), (4 0 0), and (4 4 0) planes, respectively. There are no peaks of CoO and other CoO_x as also observed by Lin *et al.* (2009) indicating that Co₃O₄ are preferably formed on the surface of CeO₂-ZrO₂ mixed oxide.

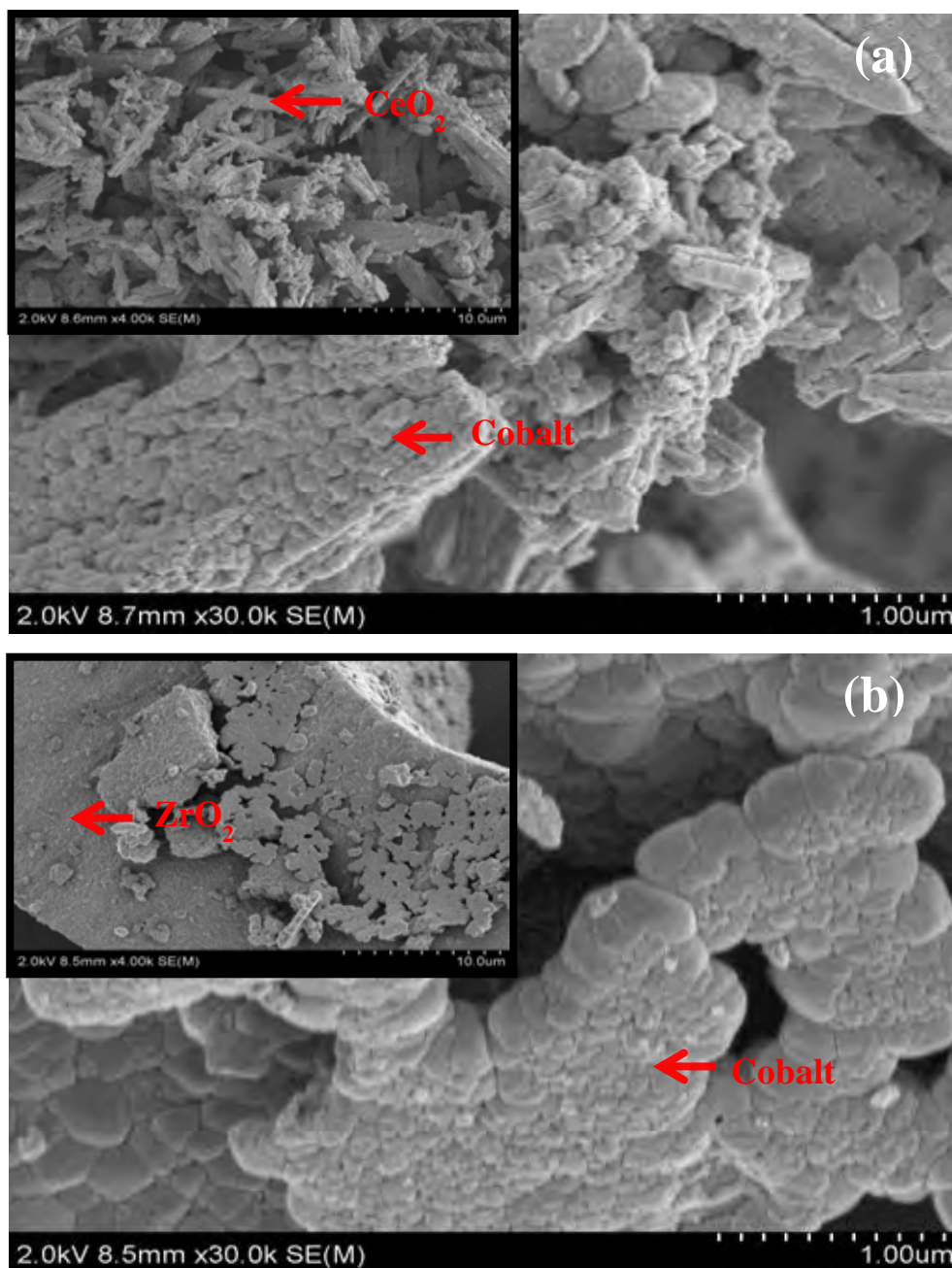


Figure 6.1 SEM images of (a) Co/CeO₂ and (b) Co/ZrO₂ catalysts.

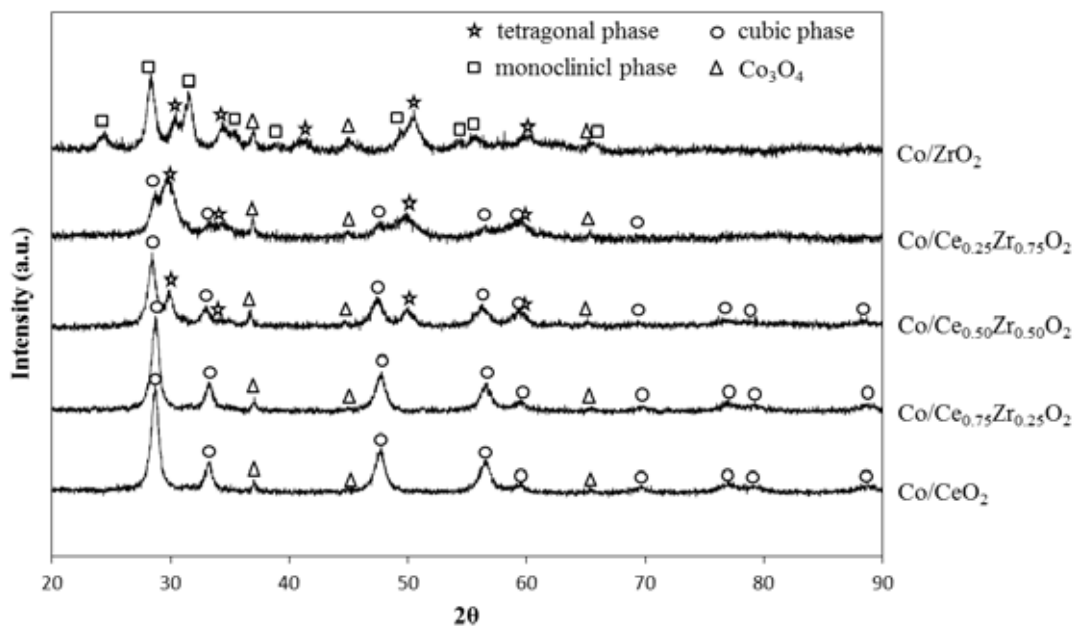


Figure 6.2 XRD patterns of $\text{Co/Ce}_{1-x}\text{Zr}_x\text{O}_2$ catalysts ($x = 0, 0.25, 0.5, 0.75$ and 1)

6.4.1.2 H_2 -Temperature Programmed Reduction

H_2 -TPR profiles of catalysts are shown in Fig. 6.3. For the unsupported Co_3O_4 , two main reduction peaks were observed for which the first peak (at 320°C) and the other one (at 390°C) are attributed to the reductions of $\text{Co}_3\text{O}_4 \rightarrow \text{CoO}$ and $\text{CoO} \rightarrow \text{Co}$, respectively (Paryjczak *et al.* 1980). However, in the presence of the support, the TPR profile are different due to the metal support interaction. The H_2 -TPR profile of Co/ZrO_2 still shows a two-step reduction: $\text{Co}_3\text{O}_4 \rightarrow \text{CoO} \rightarrow \text{Co}$, but shift to higher temperatures. We speculate that this shift in the high temperature region is a result of the irreducible structure of the material caused by ZrO_2 . The results showed that the reduction temperature was shifted to the lower temperature when Ce was present. It is apparent that the reducibility of the catalysts was found the in the similar order as the supports in the following order: $\text{Co/Ce}_{0.75}\text{Zr}_{0.25}\text{O}_2 > \text{Co/CeO}_2 > \text{Co/Ce}_{0.50}\text{Zr}_{0.50}\text{O}_2 > \text{Co/Ce}_{0.25}\text{Zr}_{0.75}\text{O}_2 > \text{Co/ZrO}_2$. This, then, suggests that the reducibility of cobalt oxide is modified by the interaction between Co and supports. It was found that the metal interaction is improved with

the presence of Ce in the mixed oxide supports. This is similar to what reported elsewhere with Ni/Ce_{1-x}Zr_xO₂ (Pengpanich *et al.* 2004).

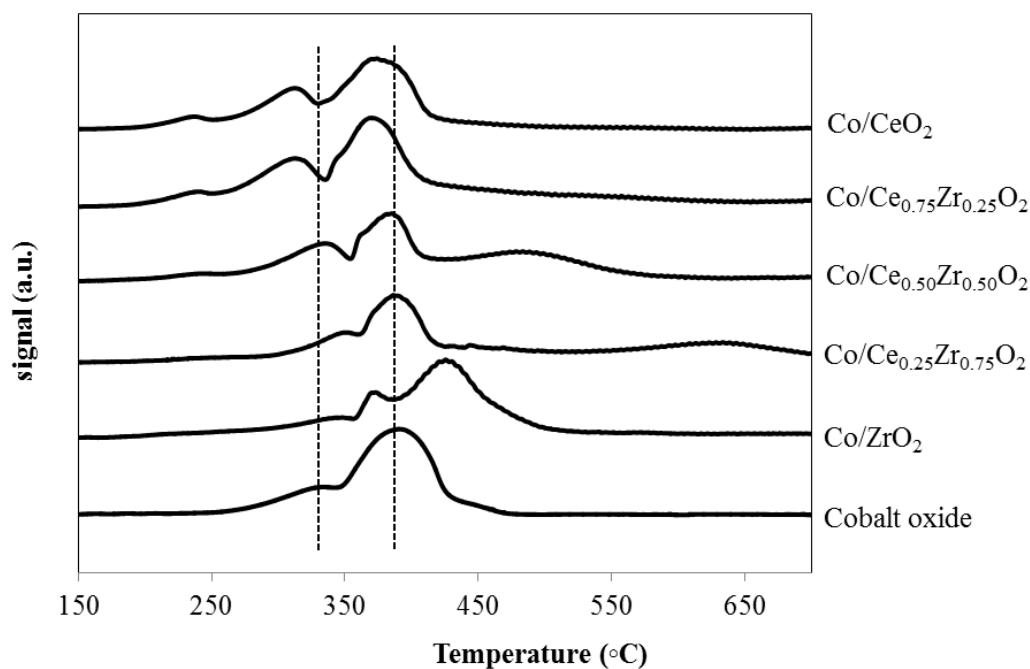


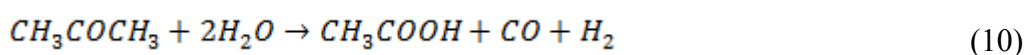
Figure 6.3 TPR profiles of the Co/Ce_{1-x}Zr_xO₂ catalysts ($x = 0, 0.25, 0.5, 0.75$ and 1) and cobalt oxide. The reducing gas contains 5% H₂ in N₂ with a flow rate of 30 ml/min and a heating rate of 10 °C/min.

6.4.2 Catalytic activity and stability for steam reforming of acetone

6.4.2.1 *Steam reforming of Acetone over Ce_{1-x}Zr_xO₂ ($x = 0, 0.25, 0.5, 0.75$ and 1)*

Firstly, steam reforming of acetone was carried out on the bare Ce_{1-x}Zr_xO₂ mixed oxides support. The reaction was carried out in a temperature range of 550-700°C with a s/c ratio of 6 and LHSV of 15.3 h⁻¹. The results showed that the catalytic activity of the Ce_{1-x}Zr_xO₂ ($x = 0, 0.25, 0.5$ and 0.75) mixed oxide is higher than that of ZrO₂ and found to relate to their reducibilities as show in Table 6.2 and Fig. 6.4. The catalytic activity for acetone steam reforming is decreased in the following order: Ce_{0.75}Zr_{0.25}O₂ > CeO₂ > Ce_{0.50}Zr_{0.50}O₂ > Ce_{0.25}Zr_{0.75}O₂ > ZrO₂. Ce_{0.75}Zr_{0.25}O₂ was found to exhibit the highest acetone conversion as related to the

highest reducibility amongst the mixed oxides, which was similar to what reported in our previous work on naphthalene steam reforming (Bampenrat *et al.* 2010). The gaseous products found during the reaction are mainly CH₄, CO₂, CO, H₂ and a trace of C₂H₄. However, ZrO₂ does not yield the reforming products at temperature below 650 °C, which suggests that Zr rich mixed oxides are less active for the steam reforming of acetone. The high yield of methane indicates that the reaction mainly occurs via the decomposition of acetone to ketene (6) and its further hydration to the formation of CH₄ and CO₂ (7) (Duan and Page 1995). These contribute to the CH₄ yield prevails over CO₂ about to 2 times. The small amounts of ethylene were found in the products stream. This might be produced from ketene convert to ethylene and CO via reaction (8) (Rice and Vollrath 1929). The amounts of acetic acid may also arise from the ketene hydration to acetic acid (9) and/or the alternative reforming of acetone via reaction (10) (Smith *et al.* 1943). The purposed reaction scheme of acetone steam reforming over Ce_xZr_{1-x}O₂ is illustrated in Figure 6.5.



It should be noted that carbon balance loss ca. 10-20% was observed throughout the catalytic tests, which suggests that the acetone undergoes cracking and leave carbon deposited on the surface of the mixed oxides. This is similar to the case of acetone reforming over Pt/ZrO₂ where there was a carbon balance loss up to 30% (Takanabe *et al.* 2006).

Table 6.2 Conversion (%) and products yields (%) for the steam reforming of acetone over $Ce_{1-x}Zr_xO_2$ ($x = 0, 0.25, 0.5, 0.75$ and 1), steam-to-carbon ratio = 6,

| Catalysts | Temperature (°C) | Conversion (%) | Product yields (%) | | | | | |
|--|------------------|----------------|--------------------|-------|-----------------|-----------------|-------------|-------------------------------|
| | | | H ₂ | CO | CO ₂ | CH ₄ | Acetic acid | C ₂ H ₄ |
| CeO ₂ | 550 | 51.16 | 0.00 | 2.69 | 9.39 | 21.02 | 0.00 | 2.82 |
| | 600 | 73.61 | 6.33 | 10.81 | 14.73 | 27.93 | 0.28 | 2.81 |
| | 650 | 84.34 | 10.02 | 16.39 | 20.15 | 32.69 | 0.26 | 2.39 |
| | 700 | 90.63 | 13.46 | 21.83 | 21.55 | 34.28 | 0.35 | 2.30 |
| Ce _{0.75} Zr _{0.25} O ₂ | 550 | 58.71 | 2.14 | 5.45 | 14.47 | 26.43 | 0.00 | 1.22 |
| | 600 | 76.41 | 5.54 | 7.62 | 17.63 | 39.41 | 0.00 | 1.22 |
| | 650 | 86.33 | 10.18 | 18.23 | 19.16 | 34.01 | 0.18 | 2.34 |
| | 700 | 95.30 | 15.25 | 21.86 | 24.54 | 42.12 | 0.19 | 1.55 |
| Ce _{0.5} Zr _{0.5} O ₂ | 550 | 50.76 | 0.00 | 3.17 | 9.62 | 20.90 | 0.52 | 2.60 |
| | 600 | 67.47 | 3.77 | 6.49 | 9.48 | 29.79 | 0.60 | 3.51 |
| | 650 | 79.64 | 9.41 | 13.56 | 20.36 | 30.34 | 0.59 | 3.51 |
| | 700 | 88.54 | 12.61 | 22.45 | 21.95 | 31.74 | 0.00 | 2.13 |
| Ce _{0.25} Zr _{0.75} O ₂ | 550 | 12.63 | 0.00 | 1.60 | 0.77 | 1.52 | 0.00 | 0.00 |
| | 600 | 21.84 | 1.97 | 2.88 | 1.95 | 3.85 | 0.00 | 0.20 |
| | 650 | 29.26 | 2.91 | 7.01 | 2.82 | 5.41 | 0.00 | 0.20 |
| | 700 | 35.44 | 7.28 | 7.99 | 3.96 | 7.09 | 0.00 | 0.20 |
| ZrO ₂ | 550 | 12.18 | 0.00 | 0.00 | 0.00 | 0.00 | 0.00 | 0.00 |
| | 600 | 12.62 | 0.00 | 0.00 | 0.00 | 0.00 | 0.00 | 0.00 |
| | 650 | 27.96 | 1.28 | 3.35 | 0.96 | 3.80 | 0.00 | 0.00 |
| | 700 | 35.26 | 4.80 | 8.91 | 1.69 | 5.80 | 0.00 | 0.16 |

LHSV of 15.3 h⁻¹, time on stream = 2 h, temperature range of 550-700 °C

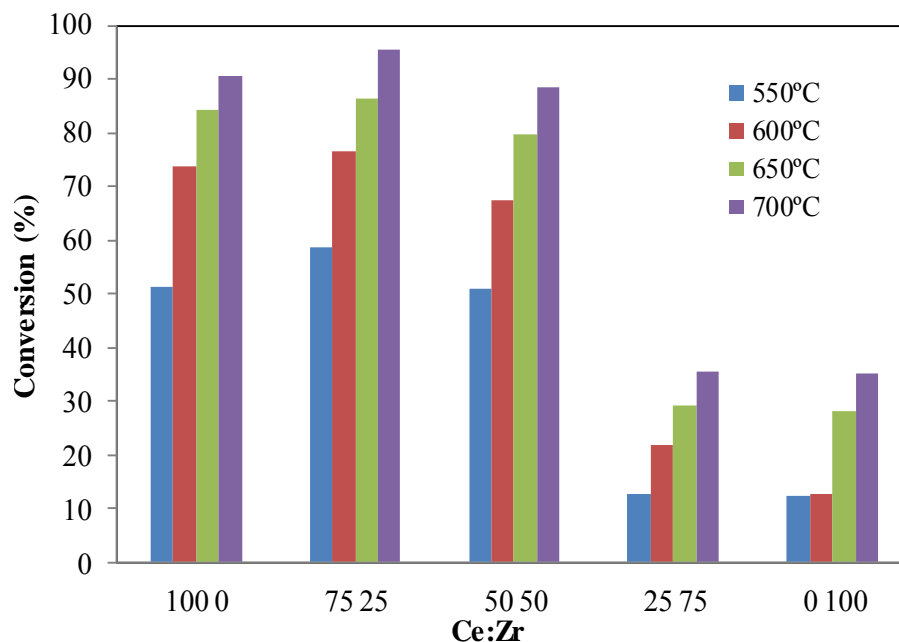


Figure 6.4 Conversion (%) for the steam reforming of acetone over $\text{Ce}_{1-x}\text{Zr}_x\text{O}_2$ ($x = 0, 0.25, 0.5, 0.75$ and 1), steam-to-carbon ratio = 6, LHSV of 15.3 h^{-1} , time on stream = 2 h, temperature range of 550-700 °C.

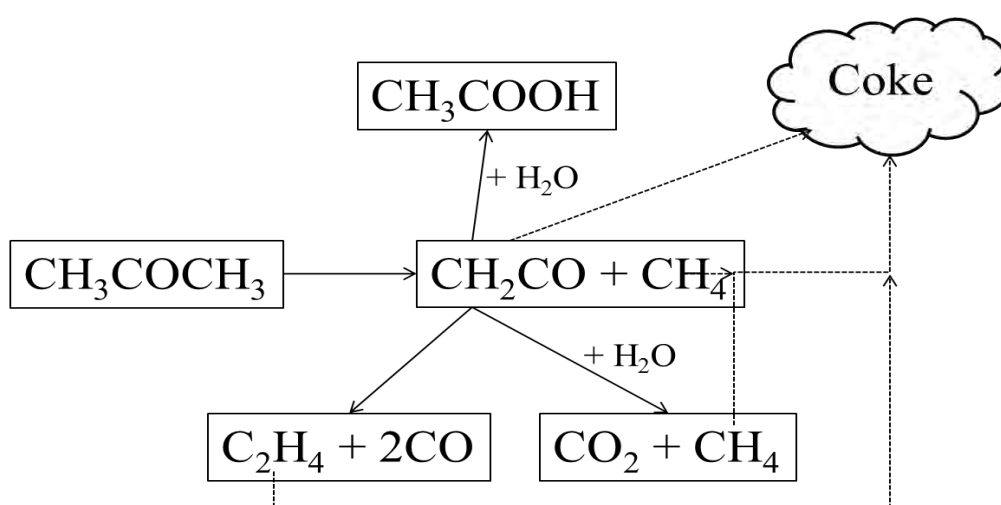


Figure 6.5 Diagram for the possible reaction of acetone over $\text{Ce}_{1-x}\text{Zr}_x\text{O}_2$ mixed oxide.

6.4.2.2 Steam Reforming of Acetone over Ni/Ce_{0.75}Zr_{0.25}O₂ and Co/Ce_{1-x}Zr_xO₂ Catalysts

Figure 6.6 summarizes the catalytic activity of Co/Ce_{1-x}Zr_xO₂ catalysts for steam reforming of acetone. It was found that the acetone conversion increases with increasing reaction temperature. Hydrogen, carbon monoxide and carbon dioxide yields are also increased. Unlike the catalytic reforming over the mixed oxides support, the typical products detected in the case of Co/Ce_{1-x}Zr_xO₂ are mainly H₂, CO₂, CO and a trace of CH₄ with the absence of other hydrocarbons. The absence of C₂H₄ and other hydrocarbons may be due to the further reforming of these compounds by cobalt phases or the reaction pathway might not follow the aforementioned reaction scheme. In all cases, no significant carbon loss was observed (>98% carbon-balance). It was reported that metallic phases of the cobalt-base catalyst are effective for hydrogen production by steam reforming of acetic acid and ethanol with high selectivity at low temperature (Hu and Lu 2007; Lin *et al.* 2009). As depicted in Table 6.2, ZrO₂ is not active for reforming reaction at temperature below 600°C. By introducing cobalt phases, the reforming reaction was found to improve immensely. The acetone conversion and hydrogen yield were comparable to those of Co/Ce_{1-x}Zr_xO₂ ($x \leq 0.5$). This, in turn, suggests that cobalt phases are essential for the steam reforming of acetone.

Interestingly, with Ce_{1-x}Zr_xO₂ ($x \leq 0.5$) supports, the acetone conversion was not improved with the presence of cobalt phases but increases the hydrogen yield. This suggests that cobalt phases might play role in reforming of the products originating from the supports, particularly CH₄. It is believed that the increase in hydrogen yield is through the steam reforming of methane as indicated by the diminishing methane yield. The difference in hydrogen yield of the catalysts was found to owe to the different water gas shift activity of the supports, which is related to the redox properties (Pengpanich *et al.* 2004; Bampenrat *et al.* 2010) and metal dispersions of the catalysts. It is apparent that the catalytic activities of Co/Ce_{1-x}Zr_xO₂ ($x = 0, 0.25, 0.5, 0.75$ and 1) are in the following order: Co/Ce_{0.75}Zr_{0.25}O₂ > CoCeO₂ > Co/Ce_{0.50}Zr_{0.50}O₂ > Co/Ce_{0.25}Zr_{0.75}O₂ > Co/ZrO₂ which is similar to the activity of the support. This seems that a superior activity of Co/Ce_{0.75}Zr_{0.25}O₂ for catalytic

6.4.2.3 Catalyst Stability and Carbon Formation

The stability of Co/Ce_{1-x}Zr_xO₂ catalysts for steam reforming of acetone was compared with that of Ni/Ce_{0.75}Zr_{0.25}O₂ catalyst. It was found that the catalytic activity of Co/Ce_{1-x}Zr_xO₂ ($x = 0.25, 0.5, 0.75, 1$) and Ni/Ce_{0.75}Zr_{0.25}O₂ remained unchanged for at least 6 h on stream whereas a slightly deactivation was observed for Co/CeO₂ catalyst after 3 h on stream as shown in Fig.6.7. The catalytic activity of Co/CeO₂ decreases about 5% and 12% at the reaction temperature 600 °C and 700 °C, respectively. The carbon deposition on the catalysts after 6 h of reaction at 600°C and 700°C and s/c ratio of 6 was quantified by using TPO technique. As shown in Fig. 6.8, the amount of carbon deposition was found to slightly decrease with decreasing Ce/Zr ratio for Co/Ce_{1-x}Zr_xO₂ ($x = 0, 0.25, 0.5, 0.75, 1$) at 600°C, following the catalytic activity. It is noticed the carbon deposition on Ni/Ce_{0.75}Zr_{0.25}O₂ is considerably higher than that on Co/Ce_{0.75}Zr_{0.25}O₂ even the acetone conversion is rather similar. This indicates that carbon formation is less favour when Co is an active metal.

It was reported that Ce_{0.75}Zr_{0.25}O₂ support help minimizing carbon deposition by enhancing gasification of carbon formed on the surface in the case of Ni/Ce_{0.75}Zr_{0.25}O₂ (Thaicharoensutcharittham *et al.* 2011). However, the effect of Ce_{1-x}Zr_xO₂ ($x = 0, 0.25, 0.5, 0.75$ and 1) supports on the carbon formation is not pronounced in the case of Co/Ce_{1-x}Zr_xO₂ attribute to the carbon formation on these catalysts is not much different, mainly related to the acetone conversion. Ever, the carbon deposition is not much different, Co/CeO₂ showed an obvious deactivation during the course of reaction. As shown in Fig. 6.9, the Co particles of spent catalyst are larger especially in the case of CeO₂ and less in the case of ZrO₂, This, in turn, indicated that the deactivation of the catalyst is mainly caused by the aggregation of Co particles.

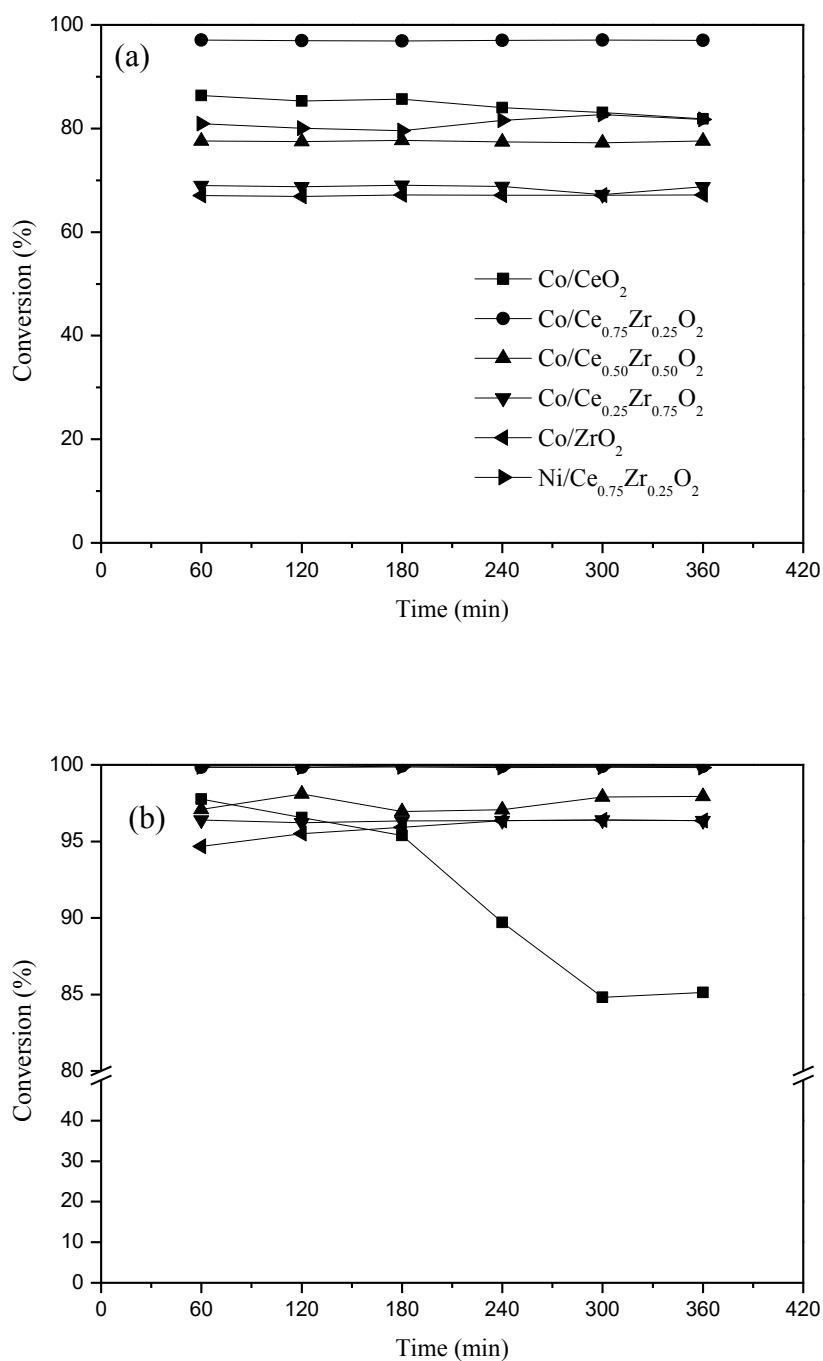


Figure 6.7 Conversion (%) vs. time on stream for the steam reforming of acetone over Co/Ce_{1-x}Zr_xO₂ (x = 0, 0.25, 0.5, 0.75 and 1) and Ni/Ce_{0.75}Zr_{0.25}O₂ catalysts, steam-to-carbon ratio = 6, LHSV of 15.3 h⁻¹ at temperature 600°C (a), 700°C (b).

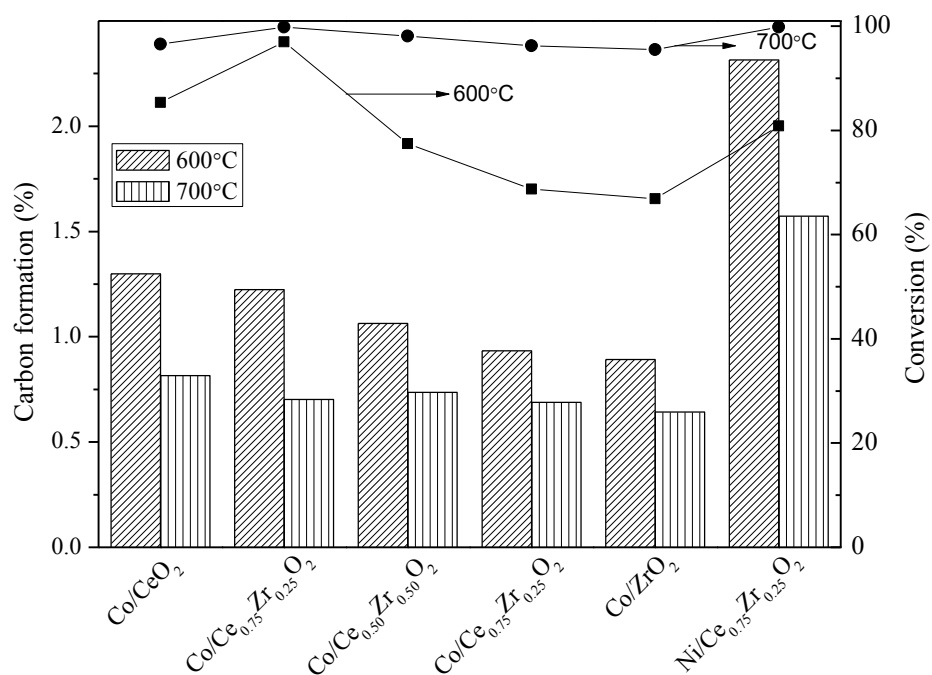


Figure 6.8 Carbon deposition for the steam reforming of acetone over Co/Ce_{1-x}Zr_xO₂ (x = 0, 0.25, 0.5, 0.75 and 1) and Ni/Ce_{0.75}Zr_{0.25}O₂ catalysts, steam-to-carbon ratio = 6, LHSV of 15.3 h⁻¹ at temperature 600 °C and 700°C time on stream 6 h.

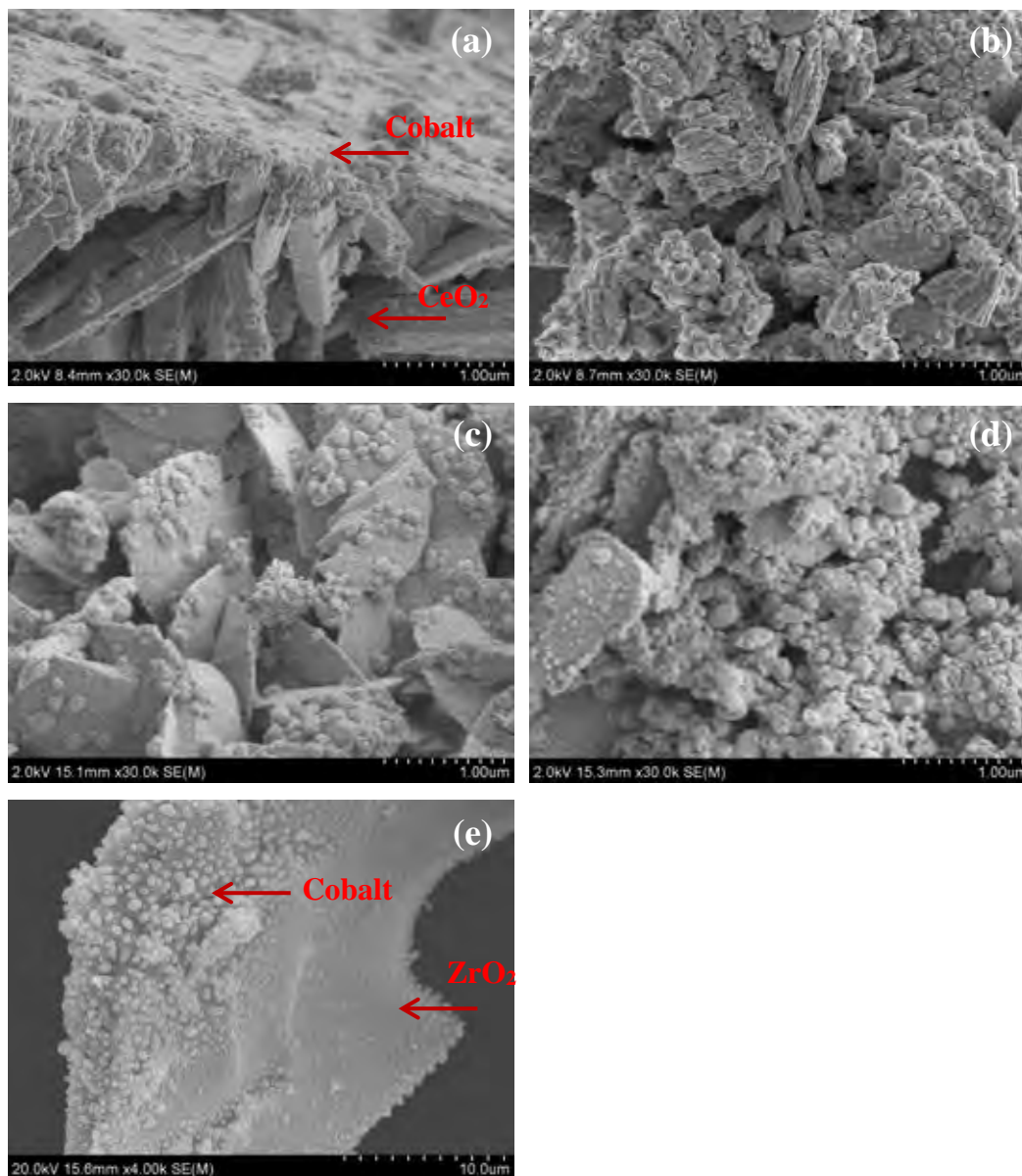


Figure 6.9 SEM images of (a) Co/CeO₂, (b) Co/Ce_{0.75}Zr_{0.25}O₂, (c) Co/Ce_{0.50}Zr_{0.50}O₂, (d) Co/Ce_{0.25}Zr_{0.75}O₂, (e) Co/ZrO₂ after 3 h of steam reforming of acetone reaction at 700°C.

6.5 Conclusions

In conclusion, it was found that the $\text{Co/Ce}_{1-x}\text{Zr}_x\text{O}_2$ catalysts exhibit excellent activity for steam reforming of acetone. The catalytic steam reforming of acetone occurred on both mixed oxides supports and metal phases with $\text{Co/Ce}_{1-x}\text{Zr}_x\text{O}_2$ ($x \leq 0.5$) and mainly on the metal phases when x is greater than 0.5. The nature of the support also influenced the catalytic activity and stability. It was found that the activity decreases with a decrease in Ce/Zr ratio. Due to high reducibility, the $\text{Co/Ce}_{0.75}\text{Zr}_{0.25}\text{O}_2$ catalyst was reported to have the highest activity and stability among mixed oxide catalysts. The roles of the support are to enhancing the decomposition of acetone and water gas shift reaction with the ceria rich mixed oxides and to prohibit the metal sintering when Zr is present.

6.6 Acknowledgements

This work was supported by the Thailand Research Fund (under Waste-to-Energy project and Royal Golden Jubilee Ph.D. Program: Grant 0170/46), and the Research Unit for Petrochemical and Environmental Catalysts, Ratchadapisek Somphot Endowment Fund, and the National Center of Excellence for Petroleum, Petrochemicals and Advanced Materials, Chulalongkorn University.

6.7 References

- Bampenrat, A., Meeyoo, V., Kitiyanan, B., Rangsunvigit, P., Rirksomboon, T. (2010) Naphthalene steam reforming over Mn-doped $\text{CeO}_2\text{-ZrO}_2$ supported nickel catalysts. *Applied Catalysis A: General*, 373, 154-159.
- Birot, A., Epron, F., Descorme, C., Duprez, D. (2008) Ethanol steam reforming over $\text{Rh/Ce}_x\text{Zr}_{1-x}\text{O}_2$ catalysts: Impact of the $\text{CO-CO}_2\text{-CH}_4$ interconversion reactions on the H_2 production. *Applied Catalysis B: Environmental*, 79, 17-25.

- Breen, J.P., Burch, R., Coleman, H.M. (2002) Metal-catalysed steam reforming of ethanol in the production of hydrogen for fuel cell applications. Applied Catalysis B: Environmental, 39, 65–74.
- Czernik, S., Evans, R., French, R. (2007) Hydrogen from biomass-production by steam reforming of biomass pyrolysis oil. Catalysis Today, 129, 265-268.
- Diebold, JP. A review of the chemical and physical mechanisms of the storage stability of fast pyrolysis bio-oils. National renewable energy laboratory (NREL) internal report, vol. 26. August 1999. p. 1–51.
- Duan, X., Page, M., (1995) Theoretical investigation of competing mechanisms in the thermal unimolecular decomposition of acetic acid and the hydration reaction of ketene. Journal American Chemical Society, 117, 5114–5119.
- Fornasiero, P., Balducci, G., Di Monte, R., Kašpar, J., Sergo, V., Gubitosa, G., Ferrero, A., Graziani, M. (1996) Modification of the Redox Behaviour of CeO₂ Induced by Structural Doping with ZrO₂. Journal of Catalysis, 164, 173-183.
- Hu, X., Lu, G. (2007) Investigation of steam reforming of acetic acid to hydrogen over Ni–Co metal catalyst. Journal of Molecular Catalysis A: Chem, 261, 43-48.
- Hu, X., Lu, G. (2009) Investigation of the steam reforming of a series of model compounds derived from bio-oil for hydrogen productio. Applied Catalysis B: Environmental, 88, 376-385.
- Liguras, D.K., Kondarides, D.I., Verykios, X.E. (2003) Production of hydrogen for fuel cells by steam reforming of ethanol over supported noble metal catalysts. Applied Catalysis B: Environmental, 43, 345–354.
- Lin, S.S.Y., Daimon, H., Ha, S.Y. (2009) Co/CeO₂-ZrO₂ catalysts prepared by impregnation and coprecipitation for ethanol steam reforming. Applied Catalysis A: General, 366, 252-261.
- Lin, S.S.Y., Kim, D.H., Ha, S.Y. (2009) Metallic phases of cobalt-based catalysts in ethanol steam reforming: The effect of cerium oxide. Applied Catalysis A: General, 355, 69-77

- Llorca, J., Homs, N., Sales, J., Piscina, P.R. (2002) Efficient Production of Hydrogen over Supported Cobalt Catalysts from Ethanol Steam Reforming. Journal of Catalysis, 209, 306–317.
- Llorca, J., Piscina, P.R., Dalmon, J.A., Sales, J., Homs, N. (2003) CO-free hydrogen from steam-reforming of bioethanol over ZnO-supported cobalt catalysts: Effect of the metallic precursor. Applied Catalysis B: Environmental, 43, 355–369.
- Mielenz, J.R. (2001) Ethanol production from biomass: technology and commercialization status. Current Opinion in Microbiology, 4, 324–329.
- Oasmaa, A., Meier, D. in: A.V. Bridgwater (Ed.), *Fast Pyrolysis of Biomass: A Handbook*, vol. 2, CPL Press, Newbury, UK, 2002, pp. 41–58.
- Paryjczak, T., Rynkowski, J., Karski, S. (1980) Thermoprogrammed reduction of cobalt oxide catalysts. Journal of Chromatography A, 188, 254–256.
- Pengpanich, S., Meeyoo, V., Rirksomboon, T. (2004) Methane partial oxidation over Ni/CeO₂–ZrO₂ mixed oxide solid solution catalysts. Catalysis Today, 93-95, 95-105.
- Piskorz, J., Scott, S.D., Radlein, D., in: E.J. Soltes, T.A. Milne (Eds.), *Pyrolysis Oils from Biomass: Producing, Analyzing and Upgrading*. ACS Symposium Series 376, American Chemical Society, Washington, DC, 1988, pp. 167–178
- Rice, F.O., Vollrath, R.E. (1929) The thermal decomposition of acetone in the gaseous state. Chemistry, 15, 702–705.
- Rioche, C., Kulkarni, S., Meunier, F. C., Breen, J.P., Burch, R. (2005) Steam reforming of model compounds and fast pyrolysis bio-oil on supported noble metal catalysts. Applied Catalysis B: Environmental, 61, 130-139.
- Smith, J.R.E., Phil, D., Hinshelwood, C.N. (1944) The Thermal Decomposition of Acetone. Proceedings of the Royal Society of London. Series A, Mathematical and Physical Sciences, 183, 33–37.
- Sun, G.B., Hidajat, K., Wu, X.S., Kawi, S. (2008) A crucial role of surface oxygen mobility on nanocrystalline Y₂O₃ support for oxidative steam reforming of ethanol to hydrogen over Ni/Y₂O₃ catalysts. Applied Catalysis B: Environmental, 81, 303-312.

- Takanabe, K., Aika, K., Inazu, K., Baba, T., Seshan, K., Lefferts, L. (2006) Steam reforming of acetic acid as a biomass derived oxygenate: Bifunctional pathway for hydrogen formation over Pt/ZrO₂ catalysts. Journal of Catalysis, 243, 263-269.
- Thaicharoensutcharittham, S., Meeyoo, V., Kitiyannan, B., Rangsunvigit, P., Rirksomboon, T. (2011) Hydrogen production by steam reforming of acetic acid over Ni-based catalysts. Catalysis Today, 164, 257-261.
- Thammachart, M., Meeyoo, V., Risksomboon, T., Osuwan, S. (2001) Catalytic activity of CeO₂-ZrO₂ mixed oxide catalysts prepared via sol-gel technique: CO oxidation. Catalysis Today, 68, 53-61.
- Vagia, E.Ch., Lemonidou, A.A. (2008) Hydrogen production via steam reforming of bio-oil components over calcium aluminate supported nickel and noble metal catalysts. Applied Catalysis A: General, 351, 111-121.
- Zhang, S., Yan, Y., Li, T., Ren, Z. (2005) Upgrading of liquid fuel from the pyrolysis of biomass. Bioresource Technology, 96, 545-550.

CHAPTER VII

CATALYTIC COMBUSTION OF METHANE OVER NiO/Ce_{0.75}Zr_{0.25}O₂ CATALYST

7.1 Abstract

In this work, methane combustion over Ce_{0.75}Zr_{0.25}O₂ and NiO/Ce_{0.75}Zr_{0.25}O₂ catalysts was investigated in the temperature range of 300-800°C. Kinetic studies of the methane combustion over the catalysts were performed using the initial rate method. It was found that the NiO/Ce_{0.75}Zr_{0.25}O₂ catalyst yields higher activity for methane combustion than Ce_{0.75}Zr_{0.25}O₂ catalyst. The reaction order determined is in good agreement with a pseudo first order with respect to methane. The two-term model associated with the most adopted surface kinetic mechanism suggests differences of the NiO and Ce_{0.75}Zr_{0.25}O₂ active sites whose activation energies for methane combustion are observed as 63.10 ± 2.51 and 74.26 ± 2.40 kJ/mol, respectively.

7.2 Introduction

In recent years, catalytic combustion of methane has been extensively studied as an alternative to conventional thermal combustion (Trimm, 1983; Pfefferle *et al.*, 1987; Zwinkels *et al.*, 1993). This catalytic combustion has shown to be high efficient in gas turbine combustors and effective in reduction of emitting pollutants such as carbon monoxide and nitrogen oxides (Pfefferle *et al.*, 1987; Saint-Just and Kinderen, 1996). Another main application of catalytic total oxidation of hydrocarbons is the abatement of methane emissions from natural gas or methane combustion devices. Because methane is a potent greenhouse gas, it is important to reduce its amounts emitted into the atmosphere. This would, in turn, cover a wide range of applications such as abatement of methane emissions from lean-burn natural gas vehicles (NGVs) and power generation processes.

Catalysts in catalytic combustion typically are noble metals or transition metal oxides that are supported on a substrate. Precious metal such as Pt and Pd, and

mixed metal oxide catalysts are typically employed for the oxidation of hydrocarbons (Lee and Trimm, 1995; Gélin and Primet, 2002). However, due to its rapid deactivation other various supports are being scrutinized. Ceria (CeO_2) has been extensively employed as a textural and structural promoter for the supported noble metal catalysts because of its unique redox properties and high oxygen storage capacity (Trovarelli *et al.*, 1999). However, pure CeO_2 possesses poor thermal stability. Recently, it has been reported that the addition of Zirconia (ZrO_2) to CeO_2 leads to the improvement of not only its oxygen storage capacity, redox properties, and catalytic activity but also resistance to high temperatures (Fornasiero *et al.*, 1996; Hori *et al.*, 1998). CeO_2 or ZrO_2 oxides make themselves of interest for use as a support in oxidation reactions. In fact, CeO_2 - ZrO_2 mixed oxides have shown the catalytic activity for methane oxidation (Pengpanich *et al.*, 2002).

Reducing the high cost of noble metal catalysts by making use inexpensive metals for the complete oxidation of hydrocarbons remains the major research target. Recently, it has been demonstrated that NiO/CeO_2 and NiO/ZrO_2 catalysts are active for methane oxidation (Pakulska and Grgicak, 2007). As our previous studies showed that $\text{Ni}/\text{Ce}_{0.75}\text{Zr}_{0.25}\text{O}_2$ catalyst is superior to methane partial oxidation with an insignificant coke formation (Pengpanich *et al.*, 2004), thus, we explored the catalytic activity and kinetics of $\text{NiO}/\text{Ce}_{0.75}\text{Zr}_{0.25}\text{O}_2$ catalyst for methane total oxidation.

7.3 Experimental

7.3.1 Catalyst Preparation and Characterization

$\text{Ce}_{0.75}\text{Zr}_{0.25}\text{O}_2$ mixed oxide was prepared via urea hydrolysis of Cerium nitrate and zirconium oxychloride. The $\text{NiO}/\text{Ce}_{0.75}\text{Zr}_{0.25}\text{O}_2$ catalyst at which its Ni loading was 5% was prepared by the incipient wetness impregnation method. The catalysts were characterized by BET surface areas, X-ray diffraction (XRD), and H_2 temperature programmed reduction (H_2 -TPR). The detailed synthesis procedure and characteristics of catalysts were reported elsewhere (Pengpanich *et al.*, 2002).

7.3.2 Catalytic Activity tests and Kinetic Studies

Catalytic activity tests for methane oxidation were carried out in a differential quartz tube micro reactor (i.d. 10 mm). Typically, 0.1 g of catalyst were packed between the layers of quartz wool. The reactor was placed in an electric furnace equipped with K-type thermocouples. The temperature of catalyst bed was monitored and controlled by Shinko FCR temperature controllers. 3%CH₄, 10%O₂, and balanced He gases were mixed and fed into the reactor at a gas hourly space velocity (GHSV) of 39 000 h⁻¹ using Brooks 5850 E mass flow controllers. An effluent gas was analyzed using a Varian CP-3380 GC fitted with a TCD.

The kinetic studies were carried out at the temperature range of 400-550°C and atmospheric pressure with variations of methane concentration between 2 and 4%, and of oxygen concentration between 10 and 20%. The kinetic data were attained using the initial rate method at the linear conversion range of less than 20% in all cases as well as conformed to Mears (1971) and Weisz (1954) criteria to ensure the absence of mass transfer limitations at such reaction conditions.

7.4 Results and discussion

7.4.1 Catalyst Characterization

BET surface areas of Ce_{0.75}Zr_{0.25}O₂ and NiO/Ce_{0.75}Zr_{0.25}O₂ catalysts determined by N₂ adsorption at 77K (five point BET method using a Quantachrome Corporation Autosorb) are 89.3 and 77.9 m²/g, respectively. The presence of NiO appears to some extent lead to a diminution of the surface area of its Ce_{0.75}Zr_{0.25}O₂ support. XRD patterns of the catalysts yield a typical cubic fluorite structure of ceria, without separate phases of Ni and NiO, similar to those reported elsewhere (Pengpanich *et al.*, 2004).

H₂-TPR profiles of catalysts are shown in Figure 7.1. For the Ce_{0.75}Zr_{0.25}O₂ catalyst, two peaks were observed for which the first peak (517 °C) and the other one (810°C) are attributed to the reductions of surface oxygen and bulk oxygen, respectively (Pengpanich *et al.*, 2002). On the other hand, four peaks were observed for the NiO/Ce_{0.75}Zr_{0.25}O₂ catalyst. The first two peaks at 244 and 340°C indicate the reduction of NiO to Ni⁰ whereas the others are assigned to the reduction of support (Roh *et al.*, 2002). Typically, for supported Ni catalysts, the lower

temperature peak (244 °C) is attributed to the reduction of the relatively free NiO particles while the higher temperature one (340 °C) is attributed to the reduction of complex NiO species in intimate contact with the oxide support (Pengpanich *et al.*, 2004; Roh *et al.*, 2002; Montoya *et al.*, 2000).

7.4.2 Catalytic Activities for Methane Oxidation and Kinetic Studies

Figure 7.2 reveals that the NiO/Ce_{0.75}Zr_{0.25}O₂ catalyst at which its temperature for 50% conversion (T_{50%}) of methane was reduced to 480°C yields higher activity than Ce_{0.75}Zr_{0.25}O₂ catalyst having its T_{50%} of 590°C. This might be related to the degree of reducibility of the catalysts, where NiO/Ce_{0.75}Zr_{0.25}O₂ shows the highest reducibility, as indicated by H₂-TPR results (Figure 7.1). Interestingly, T_{50%} of the NiO/Ce_{0.75}Zr_{0.25}O₂ catalyst is significantly lower than those reported for the methane combustion over perovskite type oxides (525-780°C) (Arai *et al.*, 1986), NiO/CeO₂ and NiO/ZrO₂ (550-805°C)(Pakulska and Crgicak, 2007).

For kinetic studies of methane combustion, the effects of the variations of the methane and oxygen partial pressures on the rate of reaction at 450°C are presented in Figure 7.3. It is apparent that the reaction rate is strongly influenced by the methane partial pressure whereas it is insignificantly dependent on the oxygen partial pressure. Based on a power law model, the reaction order with respect to methane is found to be 0.95 ± 0.1 (ca. 1.0) while that with respect to oxygen is 0.15 ± 0.02 (ca. 0). This conforms to the dependency of the partial pressure of each reactant on the reaction rate. Such values are quite similar to those reported for the methane combustion over cobalt oxides (Bahlawane, 2006), NiO/CeO₂ and NiO/ZrO₂ (Pakulska and Crgicak, 2007) in which they were about zeroth order for oxygen and a first order for methane. The apparent activation energy obtained from the Arrhenius plot for a pseudo-first-order model is 55.68 ± 1.43 kJ/mol. This value falls in the range of the activation energies reported for methane combustion over Pd, Pt, and metal oxide catalysts (30-120 kJ/mol) (Pengpanich *et al.*, 2002; Pakulska and Crgicak, 2007; Bahlawane, 2006; Hurtado *et al.*, 2004; Klvana *et al.*, 1994).

The kinetic models purposed for methane combustion in the literature are mainly categorized into four types; Langmuir-Hinshelwood models (LH), Eley-Rideal models (ER), Mars-van Krevelen models (MVK), and a two-term model (TT)

(Pengpanich *et al.*, 2002; Arai *et al.*, 1986; Klvana *et al.*, 1994; Vangiezen *et al.*, 1999). The details of each model are summarized in Table 7.1.

By performing a multi-linear regression analysis as presented in Table 7.2, it was found that LH1 and LH2 models assumed surface reaction as a rate determining-step fit the experimental reaction rate well in the temperature range of 400-500 °C but descend to predict beyond 550 °C. Although the ER and MVK models frequently used to describe the oxidation of organic compounds over noble metals and metal oxides (Hurtado *et al.*, 2004; Klvana *et al.*, 1994; Vangiezen *et al.*, 1999; Ciuparu *et al.*, 2002; Mccarty and Wise, 1990) yield positive parameters for the reaction studied with R^2 's of 0.998 and 0.997, respectively, they cannot be used to clarify the catalytic reactions that take place at the coexisting two active sites as the methane oxidation over NiO/Ce_{0.75}Zr_{0.25} might occur on two different active sites simultaneously.

A two-term model modified from the ER model for two active sites was then purposed in conjunction with few assumptions made. The rate expression of CH₄ oxidation over NiO can be expressed as $k_1 P_{CH_4}$ by assuming a fast supply of oxygen while that of over Ce_{0.75}Zr_{0.25}O₂ can be expressed as $k_2 P_{CH_4} \sqrt{P_{O_2}}$ by assuming a small coverage of oxygen. Therefore, the overall rate expression can be written as follows:

$$-r_{CH_4} = k_1 P_{CH_4} + k_2 P_{CH_4} \sqrt{P_{O_2}} \quad (1)$$

where P_{CH_4} and P_{O_2} denote the partial pressures of methane and oxygen, respectively, k_1 and k_2 denote the reaction rate constants over NiO and Ce_{0.75}Zr_{0.25}O₂, respectively.

Figure 7.4 illustrates that the two-term model gives an excellent agreement ($R^2 = 0.998$) with the experimental rate. Based on such a model, it should be pointed out that the rate of methane oxidation over NiO sites is much higher as three times than that over Ce_{0.75}Zr_{0.25}O₂ sites at a given temperature. Notably, the methane oxidation rate of Ce_{0.75}Zr_{0.25}O₂ sites is relatively close to what reported in

our previous study (Pengpanich *et al.*, 2002). The kinetic parameters for the two-term model are graphically shown in Figure 7.5. The activation energies for NiO and Ce_{0.75}Zr_{0.25}O₂ sites are determined to be 63.10 ± 2.51 and 74.26 ± 2.40 kJ/mol, respectively, which are in the range of values reported for other transition oxides (Bahlawane, 2006; Hurtado *et al.*, 2004; Klvana *et al.*, 1994; Vangiezen *et al.*, 1999; Ciuparu *et al.*, 2002; Mccarty and Wise, 1990).

7.5 Conclusions

NiO/Ce_{0.75}Zr_{0.25}O₂ catalyst possesses high activity for methane combustion. Based on the kinetic studies, the reaction rate of catalytic methane combustion strongly depends on methane concentration in which the reaction occurs simultaneously on NiO and Ce_{0.75}Zr_{0.25}O₂ sites with a vigorously pronounced activity of NiO. The reaction mechanism can be expressed as the two-term model for which the dissociative oxygen reacting with methane is a rate-determining step.

7.6 Acknowledgements

This work was supported by the Thailand Research Fund (under Waste-to-Energy project and Royal Golden Jubilee Ph.D. Program: Grant 0170/46), and the Research Unit for Petrochemical and Environmental Catalysis, Ratchadapisek Somphot Endowment Fund, Chulalongkorn University, and the Center of Excellence for Petroleum, Petrochemicals and Advanced Materials (PPAM), Chulalongkorn University.

7.7 References

- Arai, H., Yamada, T., Eguchi, K., Seiyama, T. (1986) Catalytic combustion of methane over various perovskite-type oxides. *Applied Catalysis*, 26, 265-276.
- Bahlawane, N. (2006) Kinetics of methane combustion over CVD-made cobalt oxide catalysts. *Applied Catalysis B: Environmental*, 67, 168-176.

- Ciuparu, D., Lyubowsky, M., Altman, E., Pfefferle, L. D., Datye, A. (2002) Catalytic combustion of methane over palladium-based catalysts. Catalysis Reviews: Science and Engineering, 44, 593-649.
- Fornasiero, P., Balducci, G., Di Monte, R., Kašpar, J., Sergio, V., Gubitosa, G., Ferrero, A., Graziani, M. (1996) Modification of the Redox Behaviour of CeO₂ Induced by Structural Doping with ZrO₂. Journal of Catalysis, 164, 173-183.
- Gélin, P., Primet, M. (2002) Complete oxidation of methane at low temperature over noble metal based catalysts: a review. Applied Catalysis B: Environmental, 39, 1-37.
- Hori, C.E., Permana, H., Simon Ng, K.Y.S., Brenner, A., More, K., Rahmoeller, K.M., Belton, D.N. (1998) Thermal stability of oxygen storage properties in a mixed CeO₂-ZrO₂ system. Applied Catalysis B: Environmental, 16, 105-117.
- Hurtado, P., Ordóñez, S., Sastre, H., Díez, F. V. (2004) Development of a kinetic model for the oxidation of methane over Pd/Al₂O₃ at dry and wet conditions. Applied Catalysis B: Environmental, 51, 229-238.
- Klvana, D., Vaillancourt, J., Kirchnerova, J., Chaouki, J. (1994) Combustion of methane over La_{0.66}Sr_{0.34}Ni_{0.3}Co_{0.7}O₃ and La_{0.4}Sr_{0.6}Fe_{0.4}Co_{0.6}O₃ prepared by freeze-drying. Applied Catalysis A: General, 109, 181-193.
- Lee, J. H., Trimm, D. L. (1995) Catalytic combustion of methane, Fuel Processing Technology, 42, 339-359.
- Mccarty, J. G., Wise, H. (1990) Perovskite catalysts for methane combustion. Catalysis Today, 8, 231-248.
- Mears, D.E. (1971) Tests for transport limitations in experimental catalytic reactors. Industrial and Engineering Chemistry Product Research and Development, 10, 541-547.
- Montoya, J.A., Romero-Pascual, E., Gimón, C., Del Angle, P., Monzon, A. (2000) Methane reforming with CO₂ over Ni/ZrO₂-CeO₂ catalysts prepared by sol-gel. Catalysis Today, 63, 71-85.

- Pakulska, M. M., Grgicak, C. M. (2007) The effect of metal and support particle size on NiO/CeO₂ and NiO/ZrO₂ catalyst activity in complete methane oxidation. Applied Catalysis A: General, 332, 124-129.
- Pengpanich, S., Meeyoo, V., Rirksomboon, T. (2004) Methane partial oxidation over Ni/CeO₂-ZrO₂ mixed oxide solid solution catalysts. Catalysis Today, 93-95, 95-105.
- Pengpanich, S., Meeyoo, V., Risksomboon, T., Bunyakiat, K. (2002) Catalytic oxidation of methane over CeO₂-ZrO₂ mixed oxide solid solution catalysts prepared via urea hydrolysis. Applied Catalysis A: General, 234, 221-233.
- Pfefferle, L. D., Pfefferle, W. C. (1987) Catalysis in Combustion. Catalysis Reviews: Science and Engineering, 29, 219-267.
- Roh, H., Jun, K., Dong, W., Chang, J., Park, S., Joe, Y. (2002) Highly active and stable Ni/Ce-ZrO₂ catalyst for H₂ production from methane. Journal of Molecular Catalysis A: Chemical, 181, 137-142.
- Saint-Just, J., Der Kinderen, J. (1996) Catalytic combustion: from reaction mechanism to commercial applications, Catalysis Today, 29, 387-395.
- Trimm, D. L. (1983) Catalytic combustion. Applied Catalysis, 7, 249-282.
- Trovarelli, A., Leitenburg, C., Boaro, M., Dolcetti, G. (1999) The utilization of ceria in industrial catalysis, Catalysis Today, 50, 353-367.
- Vangiezen, J. C., VandenBerg, F. N., Kleinen, J. L., Vandilen, A. J., Geus, J. W. (1999) The effect of water on the activity of supported palladium catalysts in the catalytic combustion of methane, Catalysis Today, 47, 287-293.
- Weisz, P.B., Prater, C.D. (1954) Interpretation of measurements in experimental catalysis. Advances in Catalysis, 6, 143-196.
- Zwinkels, M. F. M., Järås, S. G., Menon, P. G., Griffin, T. A. (1993) Catalytic Materials for High-Temperature Combustion. Catalysis Reviews: Science and Engineering, 35, 319-358.

Table 7.1 Kinetic models tested in fitting the methane combustion for NiO/Ce_{0.75}Zr_{0.25}O₂ catalyst

| Model | Assumption | Reaction mechanism | Rate determining step | Rate expression |
|-------|--|---|--|---|
| LH1 | Surface reaction between dissociative adsorption of oxygen and adsorption of methane | $\frac{1}{2} O_2 + X \xrightleftharpoons{k_1} O - X;$ $CH_4 + X \xrightleftharpoons{k_2} CH_4 - X;$ $CH_4 - X + O - X \xrightarrow{k_3} product - X + X;$ $product - X \xrightarrow{k_4} product + X;$ | $\frac{1}{2} O_2 + X \rightleftharpoons O - X;$ $CH_4 + X \rightleftharpoons CH_4 - X;$ $CH_4 - X + O - X \rightleftharpoons product + X + X;$ | $-r_{CH_4} = k_1 \frac{\sqrt{P_{O_2}}}{(1 + k_2 P_{CH_4})}$ $-r_{CH_4} = k_2 \frac{P_{CH_4}}{(1 + k_1 \sqrt{P_{O_2}})}$ $-r_{CH_4} = k_3 \frac{k_1 k_2 P_{CH_4} \sqrt{P_{O_2}}}{(1 + k_1 \sqrt{P_{O_2}} + k_2 P_{CH_4})^2}$ |
| LH2 | Surface reaction between molecular adsorption of oxygen and adsorption of methane | $O_2 + X \xrightleftharpoons{k_1} O_2 - X;$ $CH_4 + X \xrightleftharpoons{k_2} CH_4 - X;$ $CH_4 - X + O_2 - X \xrightarrow{k_3} product - X + X;$ $product - X \xrightarrow{k_4} product + X;$ | $O_2 + X \rightleftharpoons O_2 - X;$ $CH_4 + X \rightleftharpoons CH_4 - X;$ $CH_4 - X + O_2 - X \rightleftharpoons product - X + X;$ | $-r_{CH_4} = k_1 \frac{P_{O_2}}{(1 + k_2 P_{CH_4})}$ $-r_{CH_4} = k_2 \frac{P_{CH_4}}{(1 + k_1 P_{O_2})}$ $-r_{CH_4} = k_3 \frac{k_1 k_2 P_{CH_4} P_{O_2}}{(1 + k_1 P_{O_2} + k_2 P_{CH_4})^2}$ |
| ER | Surface reaction between dissociative adsorption of oxygen and gaseous methane | $\frac{1}{2} O_2 + X \xrightleftharpoons{k_1} O - X;$ $CH_4 + O - X \xrightarrow{k_2} product - X + X;$ $product - X \xrightarrow{k_3} product + X;$ | $CH_4 + O - X \xrightarrow{k_2} product - X + X;$ | $-r_{CH_4} = k_2 \frac{k_1 P_{CH_4} \sqrt{P_{O_2}}}{1 + k_1 \sqrt{P_{O_2}}}$ |
| MVK | The reaction takes place through alternative oxidation and reduction of the catalyst surface | $[O]_{lattice} + CH_4 \xrightarrow{k_{red}} [intermediate]$ $\frac{(2\gamma-1)[O]_{lattice}}{2[O]_{lattice}} \rightarrow product + 2\gamma[VS]_{lattice}$ $[VS]_{lattice} + O_2 \xrightarrow{k_{ox}} [O_2] \xrightarrow{[VS]_{lattice}} 2[O]_{lattice}$ | - | $-r_{CH_4} = \frac{k_{red} P_{CH_4} k_{ox} P_{O_2}}{\gamma k_{red} P_{CH_4} + k_{ox} P_{O_2}}$ |
| TT | The oxidation on catalyst surface by two roots: via the lattice oxygen and via the adsorbed oxygen | $1. [O]_{lattice} + CH_4 \xrightarrow{k_1} product + [VS]_{lattice}$ $2. [O - X] + CH_4 \xrightarrow{k_2} product + X$ | - | $-r_{CH_4} = k_1 P_{CH_4} + k_2 \sqrt{P_{O_2}} P_{CH_4}$ |

Table 7.2 Summary of kinetic parameters over NiO/Ce_{0.75}Zr_{0.25}O₂ catalyst

| Model | Rate expression | Rate parameter | Temperature (°C) | | | | R ² |
|-------|---|--|---|---|---|---|----------------|
| | | | 400 | 450 | 500 | 550 | |
| LH1 | $-r_{CH_4} = k_1 \frac{\sqrt{P_{O_2}}}{(1 + k_2 P_{CH_4})}$ | k ₁ (x10 ⁷) k ₂ (x10) | 2.863 ± 0.492 -1.548 ± 0.274 | 6.530 ± 1.071 -1.643 ± 0.241 | 12.310 ± 2.051 -1.709 ± 0.231 | 22.620 ± 3.235 -1.758 ± 0.189 | 0.784 |
| | $-r_{CH_4} = k_2 \frac{P_{CH_4}}{(1 + k_1 \sqrt{P_{O_2}})}$ | k ₁ (x10) k ₂ (x10 ⁷) | -0.536 ± 0.315 5.605 ± 0.863 | -0.557 ± 0.138 13.430 ± 0.920 | -0.555 ± 0.239 26.470 ± 3.122 | -0.740 ± 0.181 45.720 ± 4.542 | 0.975 |
| | $-r_{CH_4} = k_3 \frac{k_1 k_2 P_{CH_4} \sqrt{P_{O_2}}}{(1 + k_1 \sqrt{P_{O_2}} + k_2 P_{CH_4})^2}$ | k ₁ (x10) k ₂ (x10) k ₃ (x10 ³) | 1.877 ± 0.412 0.600 ± 0.229 0.059 ± 0.020 | 1.646 ± 0.177 0.217 ± 0.093 0.361 ± 0.146 | 1.536 ± 0.511 0.004 ± 0.261 40.863 ± 29.949 | 1.105 ± 0.317 -0.155 ± 0.175 -1.853 ± 2.218 | 0.988 |
| LH2 | $-r_{CH_4} = k_1 \frac{P_{O_2}}{(1 + k_2 P_{CH_4})}$ | k ₁ (x10 ⁷) k ₂ (x10) | 0.717 ± 0.270 -1.548 ± 0.600 | 1.634 ± 0.592 -1.644 ± 0.533 | 3.089 ± 1.111 -1.705 ± 0.500 | 5.639 ± 1.843 -1.766 ± 0.428 | 0.199 |
| | $-r_{CH_4} = k_2 \frac{P_{CH_4}}{(1 + k_1 P_{O_2})}$ | k ₁ (x10) k ₂ (x10 ⁷) | -0.078 ± 0.051 6.231 ± 0.557 | -0.081 ± 0.023 15.010 ± 0.616 | -0.080 ± 0.042 29.620 ± 2.179 | -0.112 ± 0.033 53.180 ± 3.290 | 0.974 |
| | $-r_{CH_4} = k_3 \frac{k_1 k_2 P_{CH_4} P_{O_2}}{(1 + k_1 P_{O_2} + k_2 P_{CH_4})^2}$ | k ₁ (x10) k ₂ (x10) k ₃ (x10 ³) | 0.665 ± 0.104 0.670 ± 0.331 0.052 ± 0.022 | 0.585 ± ± 0.048 0.238 ± 0.147 0.316 ± 0.182 | 0.547 ± 0.093 0.017 ± 0.018 8.425 ± 4.432 | 0.447 ± 0.067 -0.205 ± 0.212 -1.225 ± 1.356 | 0.985 |
| ER | $-r_{CH_4} = k_2 \frac{k_1 P_{CH_4} \sqrt{P_{O_2}}}{1 + k_1 \sqrt{P_{O_2}}}$ | k ₁ (x10) k ₂ (x10 ⁶) | 7.201 ± 0.441 9.776 ± 0.599 | 6.718 ± 0.400 23.936 ± 1.424 | 5.672 ± 0.465 49.302 ± 0.311 | 5.050 ± 0.319 96.661 ± 6.099 | 0.998 |
| MVK | $-r_{CH_4} = \frac{k_{red} P_{CH_4} k_o x P_{O_2}}{k_{red} P_{CH_4} + k_o x P_{O_2}}$ | k _R (x10) k _O (x10) | 8.638 ± 0.838 1.659 ± 0.161 | 19.667 ± 1.180 5.389 ± 0.323 | 37.898 ± 3.415 11.759 ± 1.059 | 66.638 ± 6.431 52.724 ± 5.088 | 0.997 |
| TT | $-r_{CH_4} = k_1 P_{CH_4} + k_2 P_{CH_4} \sqrt{P_{O_2}}$ | k ₁ (x10 ⁷) k ₂ (x10 ⁷) | 5.160 ± 0.665 0.524 ± 0.174 | 12.182 ± 0.730 1.309 ± 0.191 | 22.726 ± 2.235 2.862 ± 0.583 | 40.874 ± 4.317 5.927 ± 1.127 | 0.998 |

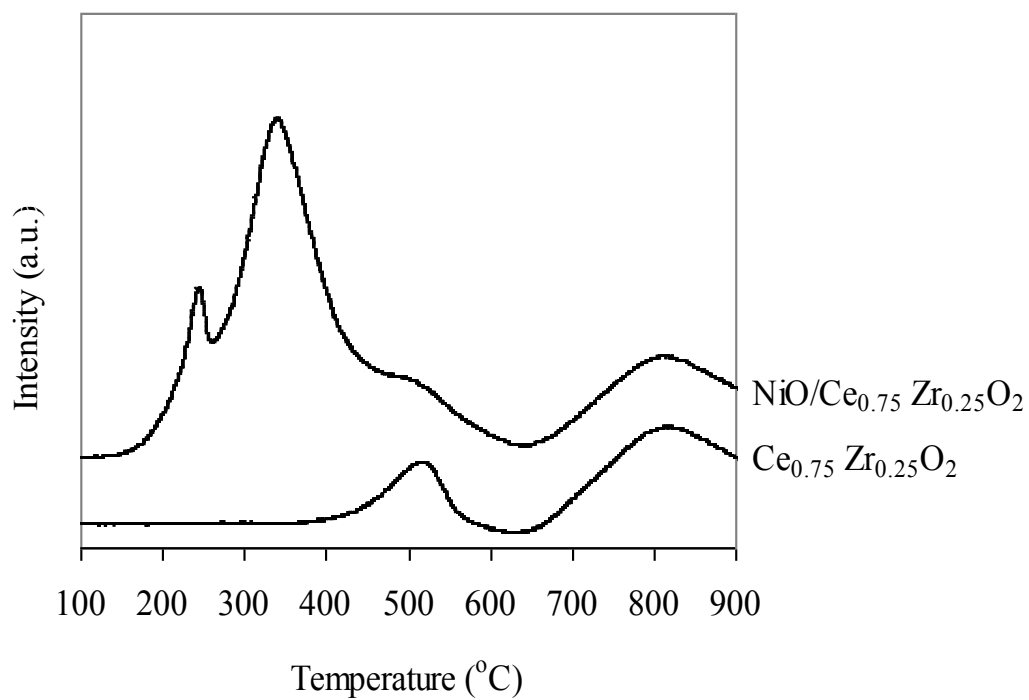


Figure 7.1 TPR profiles of Ce_{0.75}Zr_{0.25}O₂ and NiO/Ce_{0.75}Zr_{0.25}O₂ catalysts. The reducing gas contains 5.32% H₂ in N₂ with a flow rate of 30 ml/min and a heating rate of 10 °C/min.

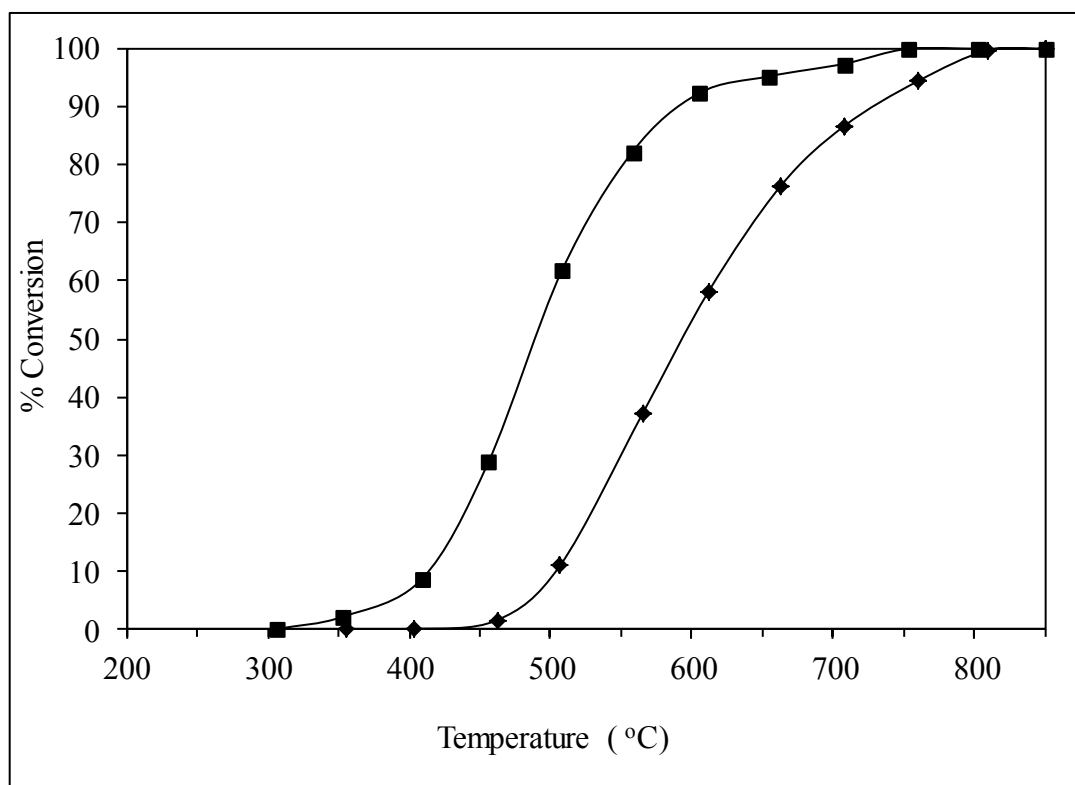


Figure 7.2 Light-off curves for $\text{Ce}_{0.75}\text{Zr}_{0.25}\text{O}_2$ and $\text{NiO}/\text{Ce}_{0.75}\text{Zr}_{0.25}\text{O}_2$ catalysts. The gas mixture contains 3.0% CH_4 , 10.0% O_2 in balanced He with a total flow rate of 100 ml/min.

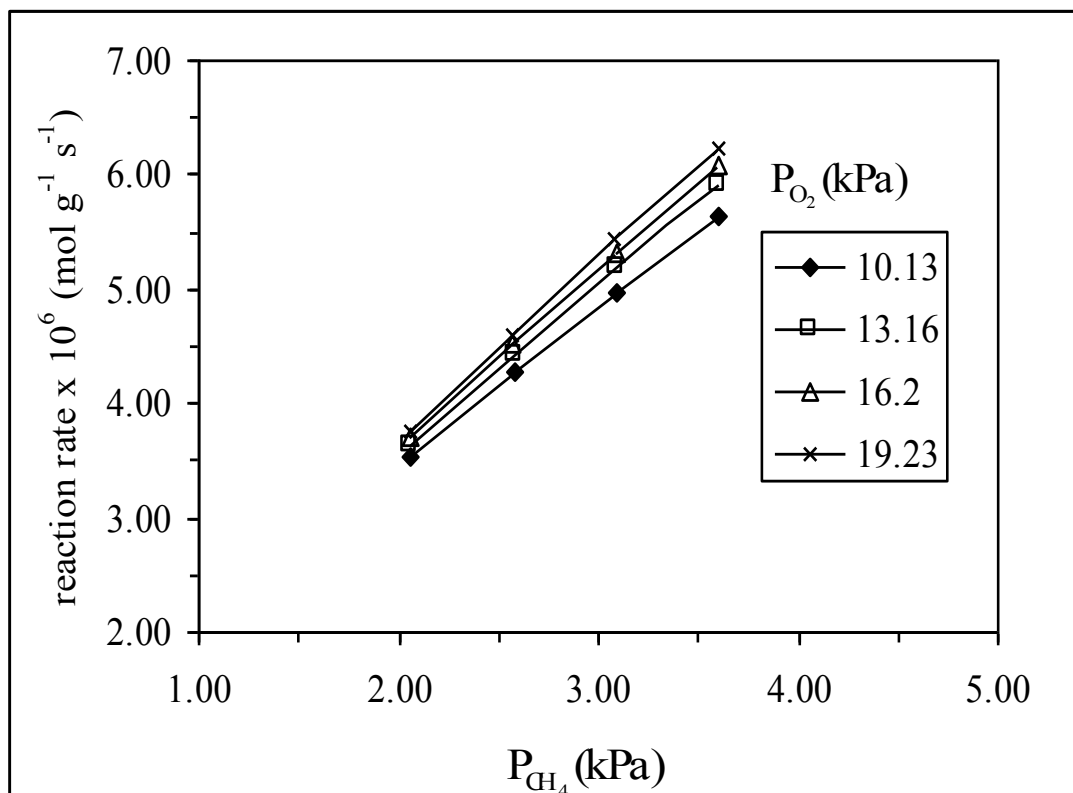


Figure 7.3 Experimental reaction rate (r_{CH_4}) vs. methane partial pressure (P_{CH_4}) with different oxygen partial pressures (P_{O_2}) for NiO/Ce_{0.75}Zr_{0.25}O₂ catalyst at 450°C.

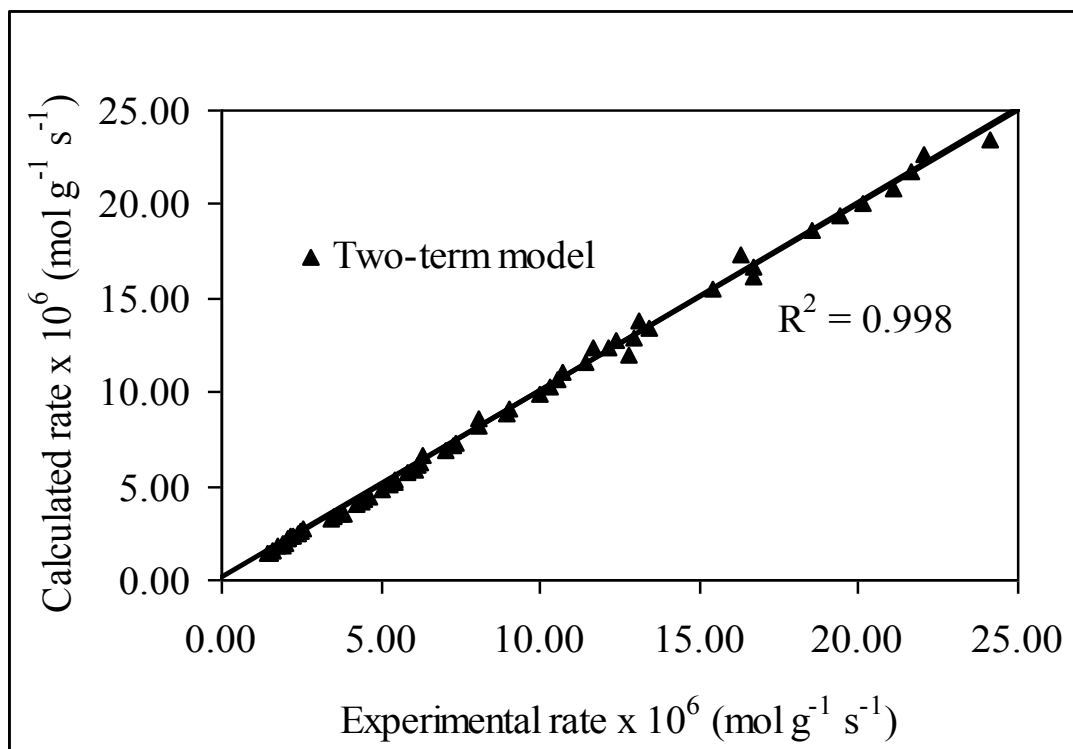


Figure 7.4 The comparison between experimental reaction rates and calculated reaction rates based on the two-term model for methane combustion over $\text{NiO/Ce}_{0.75}\text{Zr}_{0.25}\text{O}_2$ catalyst.

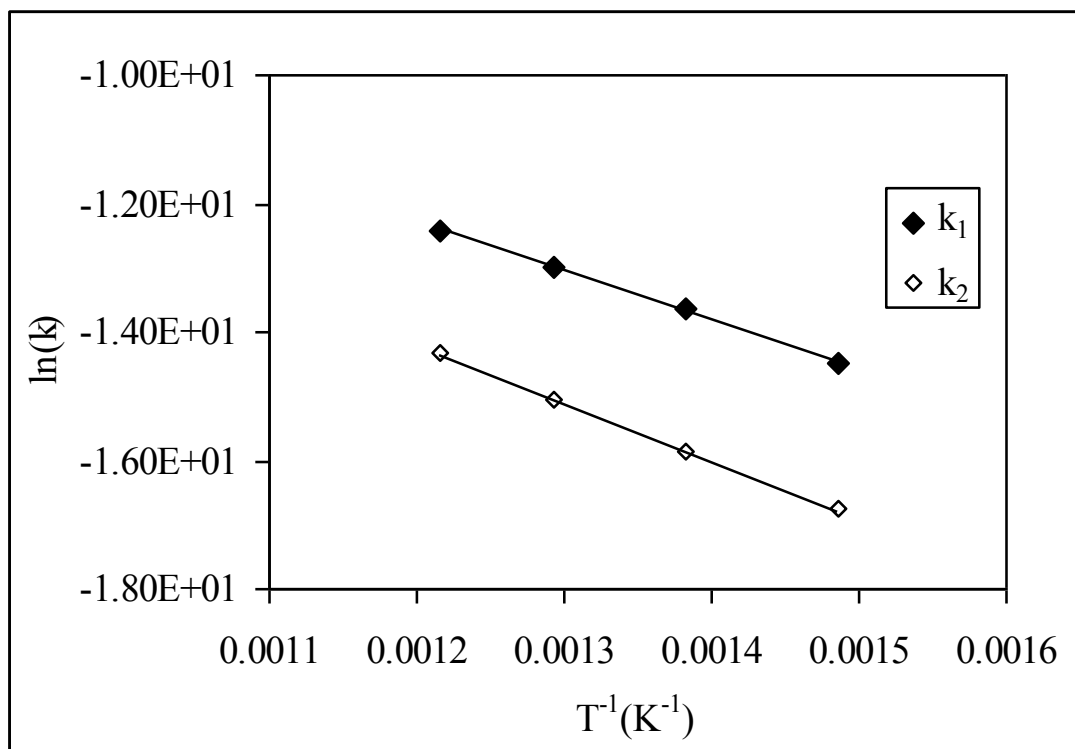


Figure 7.5 Arrhenius plots for the methane combustion over NiO/Ce_{0.75}Zr_{0.25}O₂ catalyst.

CHAPTER VIII

CONCLUSIONS AND RECOMMENDATIONS

8.1 Conclusions

In this thesis, the use of Ni/CeO₂-ZrO₂ for the steam reforming of oxygenated hydrocarbons was systematically investigated on which the various functional-group representatives for the oxygenated hydrocarbons were acetone, acetic acid, and ethanol. The findings can be summarized as follows:

1. Since the CeO₂-ZrO₂ mixed oxides demonstrated a relatively high catalytic activity for methane oxidation, this suggests that they be appropriate as oxidation catalysts required for the reduction of carbon deposition on the catalyst surface. In addition, such mixed oxides can only be active for the breakage of weak C-C bonding compounds like acetone. The presence of Ni over CeO₂-ZrO₂ mixed oxides can immensely improve the catalytic activity for both the oxidation and steam reforming reactions.

2. The catalytic activity and deposited carbon reduction on the Ni/Ce_{0.75}Zr_{0.25}O₂ catalyst can be further improved for steam reforming by the addition of potassium (K). The presence of K species results in the modification of Ni active sites to be unfavorable for the methane activation but favorable for the coke gasification. Moreover, the potassium promoted Ni/Ce_{0.75}Zr_{0.25}O₂ catalyst does not only reduce carbon deposited but also modify the Ni surface which, consequently, improves the catalytic properties of the Ni/Ce_{0.75}Zr_{0.25}O₂ catalyst.

3. At a given s/c ratio, acetic acid causes the most coke deposition onto the Ni/Ce_{0.75}Zr_{0.25}O₂ catalyst as compared to the other compounds. This suggests that the carbon formation can be generated by a few routes initiated with acetone intermediates as well as ketene and ethylene intermediates.

4. For steam reforming of acetone, the Co/Ce_{0.75}Zr_{0.25}O₂ is more active than the Ni/Ce_{0.75}Zr_{0.25}O₂ in terms of less amount of coke deposition present.

8.2 Recommendations

The mechanisms of steam reforming of the oxygenated compounds are very complex in nature depending upon the catalysts used. Therefore, further studies on the reaction mechanisms along with the routes for alleviating carbon formation should be investigated in order to comprehend the particular catalytic system. Moreover, the contents of oxygenated hydrocarbons in natural bio-oils are inevitably varied by different sources, and hence, the effect of the content distribution should also be investigated prior to the real applications.

REFERENCES

- Adjaye, J.D., Bakhshi, N.N. (1995) Production of hydrocarbons by catalytic upgrading of a fast pyrolysis bio-oil. Part 1: conversion over various catalysts. Fuel Process technol, 45(3), 161-183.
- Al-Ubaid, A., Wolf, E.E. (1988) Steam reforming of methane on reduced non-stoichiometric nickel aluminate catalysts. Applied Catalysis, 40, 73-85.
- Anderson, J.A., Fernandez, G. M., Supported Metals in Catalysis, Imperial College Press, London, 2005.
- Arai, H., Yamada, T., Eguchi K., Seiyama, T. (1986) Catalytic combustion of methane over various perovskite-type oxides, Applied Catalysis, 26, 265-276.
- Bahlawane, N. (2006) Kinetics of methane combustion over CVD-made cobalt oxide catalysts, Applied Catalysis B: Environmental, 67, 168-176.
- Balat M, (2009) New biofuel production technologies. Energy Education Science and Technology, 22, 147-61.
- Bartholomew, C.H. (1982) Carbon deposition in steam reforming and methanation. Catalysis Reviews: Science and Engineering, 24, 67-112.
- Basagiannis, A.C., Verykios, X. E. (2007) Steam reforming of the aqueous fraction of bio-oil over structured Ru/MgO/Al₂O₃ catalysts. Catalysis Today, 127, 256–264.
- Basagiannis, A.C., Verykios, X.E. (2006) Reforming reactions of acetic acid on nickel catalysts over a wide temperature range, Applied Catalysis A: General, 308, 182-193.
- Basagiannis, A.C., Verykios, X.E. (2006) Reforming reactions of acetic acid on nickel catalysts over a wide temperature range. Applied Catalysis A: General, 308, 182–193.
- Batista, MS, Santos, RKS, Assaf, EM., Assaf, JM. (2004) Ticianelli EA. High efficiency steam reforming of ethanol by cobalt-based catalysts. Journal of Power Sources, 134, 27–32.

- Breen, J.P., Burch, R., Coleman, H.M., (2002) Metal-catalysed steam reforming of ethanol in the production of hydrogen for fuel cell applications. Applied Catalysis B: Environmental, 39, 65–74.
- Bridgwater, A.V., Peacock, G.V.C. (2000) Fast pyrolysis processes for biomass. renewable & sustainable energy reviews 4(1), 1-37.
- Cadenas, A., Cabezudo, S. (1998) Biofuels as sustainable technologies: perspectives for less developed countries. Technology Forecast Social Change, 58, 83-103.
- Cai, W., Wanga, F., Zhan E., Van Veen, A.C., Mirodatos, C., Shen, W., (2008) Hydrogen production from ethanol over Ir/CeO₂ catalysts: A comparative study of steam reforming, partial oxidation and oxidative steam reforming. Journal of Catalysis, 257, 96-107.
- Chang-Feng Yan, Fei-Fei Cheng, Rong-Rong Hu (2010) Hydrogen production from catalytic steam reforming of bio-oil aqueous fraction over Ni/CeO₂eZrO₂ catalysts, International Journal of Hydrogen energy, 35, 11693-11699.
- Chiaromonti, D., Bonini, M., Fratini, E. (2003) Development of emulsions from biomass pyrolysis liquid and Diesel and their use in engines-Part 1: Emulsion production. Biomass Bioenergy, 25, 85-99.
- Dias, J.A.C., Assaf, J.M., (2008) Autothermal reforming of methane over Ni/ γ -Al₂O₃ promoted with Pd: The effect of the Pd source in activity, temperature profile of reactor and in ignition. Applied Catalysis A: General, 334, 243–250.
- Elliott, D.C., Neuenschwander, G.G. (1996) Liquid fuel by low-severity hydrotreativn of biocrude. Developments in thermochemical biomass conversion. London: Blackie Academic and Professional; 611-612.
- Fatsikostas, A.N., Verykios, X.E., (2004) Reaction network of steam reforming of ethanol over Ni-based catalysts. Journal of Catalysis, 225, 439-452.
- Frusteri, F., Freni, S., Chiodo V., Donato, S., Bonura, S., Cavallaro, S. (2006) Steam and auto-thermal reforming of bio-ethanol over MgO and CeO₂ Ni supported catalysts. International Journal of hydrogen energy, 31, 2193-2199.

- Frusteri, F., Freni, S., Chiodo, V., Spadaro, L., Blasi, O.D., Bonura, G., Cavallaro, S. (2004) Steam reforming of bio-ethanol on alkali-doped Ni/MgO catalysts: hydrogen production for MC fuel cell. Applied Catalysis A: General, 270, 1-7.
- Galda'mez, J.R., Garcí'a, L., Bilbao, R. (2005) Hydrogen Production by Steam Reforming of Bio-Oil Using Coprecipitated Ni-Al Catalysts. Acetic Acid as a Model Compound. Energy Fuels, 19(3), 1133-1142.
- Garcia, L., French, R., Czernik, S., Chornet, E. (2000) Catalytic steam reforming of bio-oils for the production of hydrogen: effects of catalyst composition, Applied Catalysis A: General 201, 225-239.
- Gou, X.Y., Yan, Y.J., Ren, Z.W. (2003) The using and forecast of catalyst in biooil upgrading. Acta Energiæ Solaris Sin. 124(12), 206-212.
- Gust, S. (1997) Combustion of pyrolysis liquid. In: Kaltschmitt M, Bridgwater A.V., editors. Biomass gasification and pyrolysis. Newbury, UK: CPL Press; p. 498-503.
- Hegarty, M.E.S., O'Connor, A.M., and Ross, J.R.H. (1998) Syngas production from natural gas using ZrO₂-supported metals. Catalysis Today, 42, 225-232.
- Hew, K.L., Tamidi, A.M., Yusup, S., Lee, K.T., Ahmad, M.M. (2010) Catalytic cracking of bio-oil to organic liquid product (OLP), Bioresource Technology, 101, 8855-8858.
- Hua Song, Umit, S., Ozkan, Ethanol steam reforming over Co-based catalysts: Role of oxygen mobility. (2009) Journal of Catalysis, 261, 66-74.
- Inache, ID., Auberger, MR., Revel, R. (2004) Differences in the characteristics and catalytic properties of cobalt-based Fischer-Tropsch catalysts supported on zirconia and alumina. Applied Catalysis A: General, 268, 51-60.
- Inguanzo, M., Domnguez, A., Menendez, J.A., Blanco, C.G., Pis, J.J. (2002) On the pyrolysis of sewage sludge: the influence of pyrolysis conditions on solid, liquid and gas fractions. Journal of Analytical and Applied Pyrolysis, 63, 209-222.

- Jacobs, G., Das, TK., Patterson, PM., Li, J., Sanchez, L., Davis, BH. (2003) Fischer–Tropsch synthesis XAFS: XAFS studies of the effect of water on a Pt-promoted Co/Al₂O₃ catalyst. Applied Catalysis A: General, 247, 335–43.
- Jacobs, G., Keogh, R.A., Davis, B.H., (2007) Steam reforming of ethanol over Pt/ceria with co-fed hydrogen. Journal of Catalysis, 245, 326-337.
- Jefferson, M. (2006) Sustainable energy development: performance and prospects. Renew Energy. 31, 571-582.
- Jens, R. Rostrup-Nielsen (1997) Industrial relevance of coking, Catalysis Today 37, 225-232.
- Jindarom, C., Meeyoo, V., Rirksomboon, T., Rangsunvigit, P. (2007) Thermochemical decomposition of sewage sludge in CO₂ and N₂ atmosphere, Chemosphere. 67, 1477-1484.
- Kaiser (1997) Upgrading of fast pyrolysis liquids by DMT. In: Kaltschmitt M, Bridgwater A.V., editors. Biomass gasification and pyrolysis. Newbury, UK: CPL Press; 399-406.
- Klvana, D., Vaillancourt, J., Kirchnerova, J. and Chaouki, J. (1994) Combustion of methane over La_{0.66}Sr_{0.34}Ni_{0.3}Co_{0.7}O₃ and La_{0.4}Sr_{0.6}Fe_{0.4}Co_{0.6}O₃ prepared by freeze-drying, Applied Catalysis A: General, 109, 181-193.
- Laosiripojana, N., Assabumrungrat, S. (2005) Methane steam reforming over Ni/Ce-ZrO₂ catalyst: Influences of Ce-ZrO₂ support on reactivity, resistance toward carbon formation, and intrinsic reaction kinetics, Applied Catalysis A: General, 290, 200-211.
- Leech, J. (1997) Running a dual fuel engine on pyrolysis oil. In: Kaltschmitt M, Bridgwater A.V., editors. Biomass gasification and pyrolysis. Newbury, UK: CPL Press; 495-497.
- Liberatori, J.W.C., Ribeiro, R.U., Zanche, D., Noronha, F.B., Bueno, J.M.C., (2007) Steam reforming of ethanol on supported nickel catalysts. Applied Catalysis A: General, 327, 197–204.
- Liguras, D.K., Kondarides, D.I., Verykios, X.E., (2003) Production of hydrogen for fuel cells by steam reforming of ethanol over supported noble metal catalysts. Applied Catalysis B: Environmental, 43, 345–354.

- Lima, S.M. de, Cruz, I.O. da, Jacobs, G., B.H. Davis, L.V. Mattos, F.B. Noronha, (2008) Steam reforming, partial oxidation, and oxidative steam reforming of ethanol over Pt/CeZrO₂ catalyst. Journal of Catalysis, 257, 356-368.
- Llorca, J., Homs, N., Sales, J., Piscina, P.R. de la (2002) Efficient Production of Hydrogen over Supported Cobalt Catalysts from Ethanol Steam Reforming. Journal of Catalysis, 209, 306–317.
- Llorca, J., Piscina, P.R. de la., Sales, J., Homs, N. (2001) Direct production of hydrogen from ethanolic aqueous solutions over oxide catalysts. Chemical Communication, 641-642.
- Llorca, J., Piscina, P.R. de la, Dalmon, J.-A., Sales, J., Homs, N. (2003) CO-free hydrogen from steam-reforming of bioethanol over ZnO-supported cobalt catalysts: Effect of the metallic precursor. Applied Catalysis B: Environmental, 43, 355–369.
- Luciene, P.R., Profeti, Joelmir, A.C., Dias, José, Assaf M., Elisabete, Assaf M. (2009) Hydrogen production by steam reforming of ethanol over Ni-based catalysts promoted with noble metals, Journal of Power Sources, 190, 525–533.
- Malgosia, M., Pakulska, Catherine, M., Grgicak (2007) The effect of metal and support particle size on NiO/CeO₂ and NiO/ZrO₂ catalyst activity in complete methane oxidation, Applied Catalysis A: General, 332, 124-129.
- McCarty, J.G., Wise, H. (1979) Hydrogenation of surface carbon on alumina-supported nickel. Journal of Catalysis, 57, 406-416.
- Montoya, J.A., Romero-Pascual, E., Gimón, C., Del Angle, P., Monzón, A. (2000) Methane reforming with CO₂ over Ni/ZrO₂-CeO₂ catalysts prepared by sol-gel. Catalysis Today, 63, 71-85.
- Morf, P.O., 2001. Secondary Reactions of Tar during Thermochemical Biomass Conversion, Ph.D. Thesis at the Swiss Federal Institute of Technology Zurich. Zurich, Switzerland.
- Nokkosmaki, M.I., Kuoppala, E.T., Leppamäki, E.A. (2000) Catalytic conversion of biomass pyrolysis vapours with zinc oxide. J. Anal. Appl. Pyrol. 55, 119-131.

- Ozcimen, D., Karaosmanoglu, F. (2004) Production and characterization of bio-oil and biochar from rapeseed cake. Renew Energy, 29, 779-787.
- Pataik, P.C. (1997) Industrial gas turbine tests using a biomass derived fuel. In: Kaltschmitt M, Bridgwater A.V., editors. Biomass gasification and pyrolysis. Newbury, UK: CPL Press.
- Pengpanich, S., Meeyoo, V., Rirksomboon, T. (2004) Methane partial oxidation over Ni/CeO₂-ZrO₂ mixed oxide solid solution catalysts. Catalysis Today, 93-95, 95-105.
- Pengpanich, S., Meeyoo, V., Rirksomboon, T., Bunyakiat, K. (2002) Catalytic oxidation of methane over CeO₂-ZrO₂ mixed oxide solid solution catalysts prepared via urea hydrolysis. Applied Catalysis A: General, 234, 221-233.
- Pindoria, R.V., Lim, J.Y., Hawkes, J.E. (1997) Characterization of biomass pyrolysis tars/ oils from eucalyptus wood wastes: effect of H₂ pressure and samples configuration. Fuel, 76(11), 1013-1023.
- Pindoria, R.V., Megaritis A., Herod, A.A. (1998) A two-stage fixed-bed reactor for direct hydrotreatment of volatiles from the hydrolysis of biomass: effect of catalyst temperature, pressure and catalyst ageing time on product characteristics. Fuel, 77(15), 1715-1726.
- Radlein, D. (1997) Production of chemicals from bio-oil. In: Kaltschmitt M, Bridgwater A.V., editors. Biomass gasification and pyrolysis. Newbury, UK: CPL Press; 471-481.
- Rioche, C., Kulkarni, S., Frederic, C. M., John, P. B., Burch, R. (2005) Steam reforming of model compounds and fast pyrolysis bio-oil on supported noble metal catalysts. Applied Catalysis B: Environmental, 61, 130-139.
- Roh, H., Jun, K., Dong, W., Chang, J., Park, S., Joe, Y., Mol, J. (2002) Highly active and stable Ni/Ce-ZrO₂ catalyst for H₂ production from methane. Journal of Molecular Catalysis A: Chemical, 181, 137-142.
- Romero-Sarria, F., Vargas, J.C., Roger, A., Kiennemann, A., (2008) Hydrogen production by steam reforming of ethanol: Study of mixed oxide catalysts Ce₂Zr_{1.5}Me_{0.5}O₈: Comparison of Ni/Co and effect of Rh. Catalysis Today, 133, 149-153.

- Rostrup-Nielsen, J.R., Trimm, D.L. (1977) Mechanisms of carbon formation on nickel-containing catalysts. Journal of Catalysis, 302, 133-139.
- Sahli, N., Petit, C., Roger, A.C., Kiennemann, A., Libs, S., Bettahar, M.M. (2006) Ni catalysts from NiAl₂O₄ spinel for CO₂ reforming of methane. Catalysis Today, 113, 187-193.
- Salge, J.R., Deluga, G.A., Schmidt, L.D. (2005) Catalytic partial oxidation of ethanol over noble metal catalysts. Journal of Catalysis, 235, 69–78.
- Schanke, D., Vada, S., Blekkan EA., Hilmen, AM., Hoff A, Holmen, A. (1995) Study of Pt-promoted cobalt CO hydrogenation catalysts. Journal of Catalysis, 156, 85–95.
- Seyedeyn-Azad, F., Salehi, E., Abedi, J., Harding, T. (2011) Biomass to hydrogen via catalytic steam reforming of bio-oil over Ni-supported alumina catalysts, Fuel Processing Technology, 92, 563-569.
- Shaddix, C.R., and Huey, S.P. (1997) Combustion characteristics of fast pyrolysis oils derived from hybrid poplar in Developments in Thermochemical Biomass Conversion. Bridgwater A.V., and Boocock., Ed.s, Blackie academic & Professional, London, 465-480.
- Solantausta, Y., Diebold, J., Elliott, Bridgwater, A.V., Beckman, D. (1994) Assessment of liquefaction and pyrolysis systems, VTT Research Notes, 1573.
- Soyal-Baltacıoğlu, F., Aksoylu, A.E., Onsan, Z.I. (2008) Steam reforming of ethanol over Pt–Ni Catalysts. Catalysis Today, 138, 183–186.
- Takanabe, K., Nagaoka, K., Nariai, K., Aika, K. (2005) Influence of reduction temperature on the catalytic behavior of Co/TiO₂ catalysts for CH₄/ CO₂ reforming and its relation with titania bulk crystal structure. Journal of Catalysis, 230, 75–85.
- Trimm, D.L. (1977) The formation and removal of coke from nickel catalyst. Catalysis Reviews: Science and Engineering, 16, 155-189.
- Trimm, D.L. (1997) Coke formation and minimization during steam reforming reactions, Catalysis Today, 37, 233-238.

- Trovarelli, A., Leitenburg, C., Boaro, M., Dolcetti, G. (1999) The utilization of ceria in industrial catalysis, Catalysis Today, 50, 353-367.
- Vangiezen, J. C., VandenBerg, F. N., Kleinen, J. L., Vandilen, A. J., Geus, J. W. (1999) The effect of water on the activity of supported palladium catalysts in the catalytic combustion of methane, Catalysis Today, 47, 287-293.
- Víctor A. de la Peña O'Shea, Raquel Nafria, Pilar Ramírez de la Piscina, Narcís Homs, (2008) Development of robust Co-based catalysts for the selective H₂-production by ethanol steam-reforming. The Fe-promoter effect, International Journal of hydrogen energy, 33, 3601 – 3606.
- Wang, HY., Ruckenstein, E. (2001) Conversions of methane to synthesis gas over Co/c-Al₂O₃ by CO₂ and/or O₂. Catalysis Letter, 75, 13–8.
- Wang, S., Lu, G.Q. (1998) CO₂ reforming of methane on Ni catalysts: Effects of the support phase and preparation technique, Applied Catalysis B: Environmental, 16, 269-277.
- Wang, S., Lu, G.Q. (1998) Refoming of methane with carbon dioxide over Ni/Al₂O₃ catalysts: Effect of nickel precursor, Applied Catalysis A: General, 169, 271-280.
- Weiyang, W., Yunquan, Y., Hean, L., Tao, H., Wenying, L. (2011) Amorphous Co-Mo-B catalyst with high activity for the hydrodeoxygenation of bio-oil, Catalysis Communications, 12, 436-440.
- Xun Hu, Gongxuan Lu, (2009) Inhibition of methane formation in steam reforming reactions through modification of Ni catalyst and the reactants. Green Chemistry, 11, 724-732.
- Zhang, S.P., Yan, Y., Li, T., (2005). Upgrading of liquid fuel from the pyrolysis of biomass. Bioresource Technology, 96, 545-550.
- Zhao, H.Y., Li, D., Bui, P., Oyama, S.T. (2011) Hydrodeoxygenation of guaiacol as model compound for pyrolysis oil on transition metal phosphide hydroprocessing catalysts, Applied Catalysis A: General, 391, 305-310.

CURRICULUM VITAE

Name: Mr. Somsak Thaicharoensutcharittham

Date of Birth: January 25, 1982

Nationality: Thai

University Education:

2000–2004 Bachelor Degree of Chemical Engineering, Faculty of Engineering, Mahanakorn University of Technology, Bangkok, Thailand

Publications:

1. Thaicharoensutcharittham, S.; Meeyoo, V.; Kitiyanan, B.; Rangsunvigit, P.; Risksomboon, T. (2009) Catalytic combustion of methane over Ni/Ce_{0.75}Zr_{0.25}O₂ catalyst. Catalysis Communications, 10, 673-677.
2. Thaicharoensutcharittham, S.; Meeyoo, V.; Kitiyanan, B.; Rangsunvigit, P.; Risksomboon, T. (2011) Hydrogen production by steam reforming of acetic acid over Ni-based catalysts. Catalysis Today, 164, 257-261.

Proceedings:

1. Thaicharoensutcharittham, S.; Meeyoo, V.; Kitiyanan, B.; Rangsunvigit, P.; Risksomboon, T. (2009, July 5-10) Catalytic combustion of methane over M/Ce_{0.75}Zr_{0.25}O₂ catalysts with M=Fe, Co, Ni, and Rh. Proceeding of the 6th World Congress on Oxidation Catalysis (6WCOC), Lille, France.
2. Thaicharoensutcharittham, S.; Meeyoo, V.; Kitiyanan, B.; Rangsunvigit, P.; Risksomboon, T. (2011, September 18-21) Steam reforming of ethanol over Ni/Ce_{0.75}Zr_{0.25}O₂ and Ni-K/Ce_{0.75}Zr_{0.25}O₂ catalysts. Proceeding of the CHEMECA 2011, Sydney, Australia.

Presentations:

1. Thaicharoensutcharittham, S.; Meeyoo, V.; Kitiyanan, B.; Rangsunvigit, P.; Risksomboon, T. (2008, April 4-6) Catalytic combustion of methane over Ni/Ce_{0.75}Zr_{0.25}O₂ and Ni-Rh/Ce_{0.75}Zr_{0.25}O₂. Oral presented at RGJ Ph.D. congress, Chonburi, Thailand.

2. Thaicharoensutcharittham, S.; Meeyoo, V.; Kitiyanan, B.; Rangsunvigit, P.; Risksomboon, T. (2008, October 20-21) Catalytic combustion of methane over NiO/Ce_{0.75}Zr_{0.25}O₂ catalysts. Oral presented at TIChE18, Pattaya, Thailand.
3. Thaicharoensutcharittham, S.; Meeyoo, V.; Kitiyanan, B.; Rangsunvigit, P.; Risksomboon, T. (2009, July 5-10) Catalytic combustion of methane over M/Ce_{0.75}Zr_{0.25}O₂ catalysts with M=Fe, Co, Ni, and Rh. Poster presented at 6WCOC, Lille, France.
4. Thaicharoensutcharittham, S.; Meeyoo, V.; Kitiyanan, B.; Rangsunvigit, P.; Risksomboon, T. (2010 July 18-23) Steam reforming of acetic acid over Ni-based catalysts. Poster presented at TOCAT6/APCAT5, Sapporo, Japan.